Geoscience Frontiers xxx (xxxx) xxx

HOSTED BY

ELSEVIER

Contents lists available at ScienceDirect

Geoscience Frontiers

journal homepage: www.elsevier.com/locate/gsf

Research Paper

An overview of geological originated materials as a trend for adsorption in wastewater treatment

Yasmin Vieira [a], Matias Schadeck Netto [b], Éder C. Lima [c], Ioannis Anastopoulos [d], Marcos L.S. Oliveira [e,f], Guilherme L. Dotto [a,b,*]

[a] Chemistry Department, Federal University of Santa Maria - UFSM, 1000, Roraima Avenue, 97105-900 Santa Maria, RS, Brazil
[b] Chemical Engineering Department, Federal University of Santa Maria - UFSM, 1000, Roraima Avenue, 97105-900 Santa Maria, RS, Brazil
[c] Institute of Chemistry, Federal University of Rio Grande do Sul (UFRGS), P.O. Box 15003, 91501-970 Porto Alegre, RS, Brazil
[d] Department of Chemistry, University of Cyprus, P.O. Box 20537, CY-1678 Nicosia, Cyprus
[e] Universidad de Lima, Avenida Javier Prado Este 4600 - Santiago de Surco 1503, Peru
[f] Department of Civil and Environmental, Universidad de la Costa, Calle 58 #55-66, 080002 Barranquilla, Atlántico, Colombia

ARTICLE INFO

Article history:
Received 1 October 2020
Received in revised form 29 December 2020
Accepted 14 January 2021
Available online xxxx

Handling Editor: M. Santosh

Keywords:
Adsorption
Equilibrium
Geological-based adsorbents
Process parameters
Wastewater treatment

ABSTRACT

Adsorption is a unit operation widely used for the tertiary treatment of the most diverse effluents, whose mechanism is based on removing recalcitrant compounds from the organic and inorganic origin. In this process, choosing a suitable adsorbent is a fundamental point. This review article focuses on the adsorbents with natural geological origin: minerals, clays, geopolymers, and even wastes resulted from mining activity. Therefore, over 450 articles and research papers were explored. These materials' main sources are described, and their characteristics, composition, and intrinsic properties are related to adsorption. Herein, we discuss the effects of several process parameters, such as pH, temperature, pollutant, and adsorbent concentration. Furthermore, equilibrium, kinetics, and thermodynamic aspects are also addressed, and relevant regeneration prospects and final disposal. Finally, some suggestions and perspectives on applying these adsorbents in wastewater treatment are presented as future trends.
© 2021 China University of Geosciences (Beijing) and Peking University. Production and hosting by Elsevier B.V. This is an open access article under the CC BY-NC-ND license (http://creativecommons.org/licenses/by-nc-nd/4.0/).

1. Introduction

Around 95% of the Earth's crust is constituted by rock and rock-based composts; therefore, geological materials are abundant and accessible (Banning, 2020; Ronov and Yaroshevsky, 1922; Taylor and McLennan, 1985) Meanwhile, due to our planet's population's growth and need for more significant development, more and more areas are explored, and more cities are built. Because of these anthropogenic actions, geologic materials are dislocated and disposed of as residues, creating an environmental problem (Bettencourt et al., 2007; Folke et al., 2020; Ghernaout et al., 2020). After considering that these materials are mostly made up of silicon, oxygen, and other metal oxides (Folk, 1954), several studies have demonstrated interest in applying and investigating their natural properties towards adsorption, aiming the removal of environmental pollutants as a bright and elegant way of solving two growing problems (Atun et al., 2009; Bundschuh et al., 2011; Dong et al., 2020; Gu et al., 2019; Li and Arai, 2020; Roy and Krapac, 1994; Teymouri et al., 2020b; Tsai et al., 2006).

Adsorption is one of the most effective techniques in advanced wastewater treatment and can be employed to reduce or even remove hazardous organic and inorganic pollutants present in the effluent (Burakov et al., 2018; Crini, 2006; Dabrowski, 2001; De Gisi et al., 2016; Dotto et al., 2016; Dotto and McKay, 2020; Lütke et al., 2019). The process concerns the accumulation of a substance at the interface between two phases, liquid-solid or gas-solid (Liu and Jiang, 2010; Tóth, 1995). The substance that accumulates at the interface is named adsorbate, while the solid on which adsorption occurs is the adsorbent (Fig. 1) (Dotto and Mckay, 2020).

Adsorption can occur by chemical sorption and physical sorption (Di Toro, 1985; Hammond and Conner, 2013). Chemical adsorption, or chemisorption, consists of forming strong chemical associations – or even bonds – between molecules or ions of adsorbate to the adsorbent surface (Breeuwsma and Lyklema, 1973; Fan et al., 2020; Hong et al., 2020). Contrarily, physical adsorption, or physisorption, is described by intermolecular interactions between adsorbate and adsorbent. Nevertheless, the main physical forces controlling adsorption are van der Waals forces, hydrogen bonds, polarity, dipole-dipole, and π-π interactions (Chen et al., 2020; Halsey, 1948; Li et al., 2019a).

* Corresponding author at: Chemistry Department, Federal University of Santa Maria - UFSM, 1000, Roraima Avenue, 97105-900 Santa Maria, RS, Brazil.
E-mail addresses: msilva@cuc.edu.co (M.L.S. Oliveira), guilherme.dotto@ufsm.br (G.L. Dotto).

https://doi.org/10.1016/j.gsf.2021.101150
1674-9871/© 2021 China University of Geosciences (Beijing) and Peking University. Production and hosting by Elsevier B.V. This is an open access article under the CC BY-NC-ND license (http://creativecommons.org/licenses/by-nc-nd/4.0/).

Please cite this article as: Y. Vieira, M.S. Netto, É.C. Lima, et al., An overview of geological originated materials as a trend for adsorption in wastewater treatment, Geoscience Frontiers, https://doi.org/10.1016/j.gsf.2021.101150

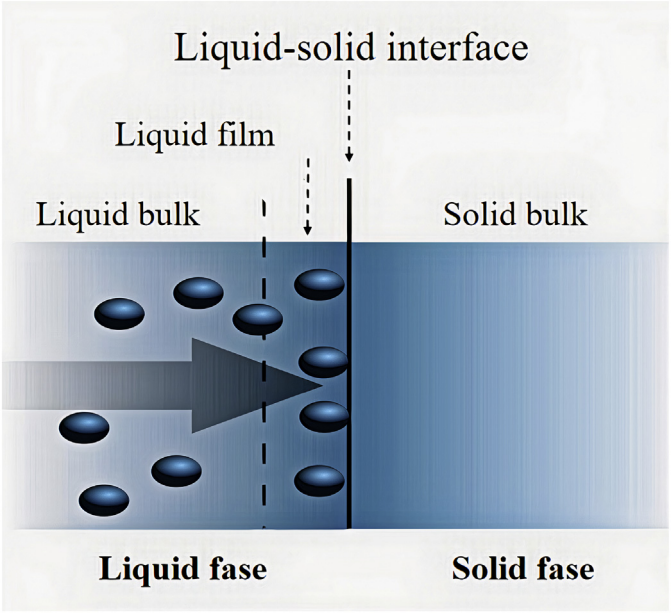

Fig. 1. Representation of the adsorption mechanism in liquid and solid fase.

Overall, adsorption provides an attractive alternative for the treatment of polluted waters, especially if the sorbent is inexpensive, which geological originated materials can be (Asfaram et al., 2014; Ghaedi et al., 2015; Saif Ur Rehman et al., 2013; Shams et al., 2013a; Uddin, 2017). This review article presents how natural, geological originated materials, such as minerals, clays, geopolymers, and even waste resulting from mining activity, can be applied to water treatment and decontamination purposes. The geological materials characteristics, composition, and intrinsic properties related to adsorption are presented. The effects of several process parameters, such as pH, temperature, pollutant, and adsorbent concentration, are discussed. Furthermore, equilibrium, kinetics, and thermodynamic aspects are also addressed mainly, according to each application. Finally, some suggestions and perspectives on applying these adsorbents in wastewater treatment are presented as future trends.

2. Mineral adsorbents

More than 4000 naturally occurring minerals have been found on Earth (Haldar and Tišljar, 2013). To be classified as a mineral, the solid must be inorganic with characteristic chemical composition and specific crystal structure (Haldar and Tišljar, 2013; Mitchell et al., 1994). Due to the abundant presence of oxygen, silicon, and aluminum, silicates and aluminosilicates are quantitatively the most relevant class of minerals. Furthermore, the following classes are recognized: native elements; sulfide, telluride, arsenide, and selenide minerals including sulfosalts of antimony and bismuth; halides; oxides; hydroxides; carbonates; nitrates; borates; chromates; tungstates; molybdates; phosphates; arsenates; vanadates; silicates and aluminosilicates (Mitchell et al., 1994). For adsorption application purposes, the most relevant minerals are silicates, hydrous silicates, oxides, and carbonates (Cornell, 1993; Pehlivan et al., 2009; Rao et al., 1991; Zhang et al., 2019b).

In general, there are several critical parameters for a material to be considered a potentially promising adsorbent, such as its surface area, and porosity, surface charge, mechanical strength, and the surface chemistry of the adsorbent (Dotto et al., 2016; Lütke et al., 2019). In Table 1, it is presented the classifications and the average surface area, connecting geological materials and adsorption (Brantley and Mellott, 2000; Giménez et al., 2007; Hodson, 1998; Meier et al., 1994; Nandi et al., 2009; Reddy and Claassen, 1994; Sorwat et al., 2020; Walker et al., 2003; Wang et al., 2020a; Wang and Zhang, 2020; Yan et al., 2020). Several examples of the application of minerals in adsorption have been reported for various types of contaminants. Talc, chalcopyrite, and barite were tested against the removal of lead ions from liquid wastes (Rashed, 2001), while bisphenol-A adsorption onto andesite, diatomaceous earth, titanium dioxide, and activated bleaching earth were studied. Their results were compared to those of different carbon-based materials (Tsai et al., 2006). Bituminous coal, pumice stone, coconut coal, and volcanic zeolite were evaluated to remove nitrogen, phosphorus, aluminum, iron, cyanobacteria, and saxitoxins (Guimarães Neto and Aguiar, 2020). Furthermore, mineral adsorbents' addition to porous concrete was also investigated to reduce groundwater pollution (Teymouri et al., 2020a,b).

2.1. Silicates

2.1.1. Feldspar

Feldspar is, up to now, little explored when compared to other minerals. In a thorough search, very few related studies were found on its adsorption capacity towards environmental pollutants. However, feldspar is estimated to be the greatest rock-forming mineral in the earth crust (Branlund and Hofmeister, 2012; Horai, 1971; Janecke and Evans, 1988); hence, it is a potentially low-cost industrial material that can be employed in environmental, economic processes (Yazdani et al., 2012). They can also undergo thermal treatment operations to improve its sorption capacity (Pelte et al., 2000).

Table 1
Mineralogical classification of geological originated adsorbents reported in the literature.

Group	Mineral	Molecular formula	Average surface area ($m^2\ g^{-1}$)	Reference
Silicates	Feldspars	$KAlSi_3O_8$ $NaAl_2Si_3O_8$ $CaAl_2Si_2O_8$	0.8	Hodson (1998)
	Micas	$KAl_2(Si_3Al)\cdot O_{10}(OH)_2$ $K_2(MgFe)_6(SiAl)_8O_{20}(OH)_4$	100	Meier et al. (1994)
	Amphiboles	Na, Ca, Mg, Fe, Al silicate	3.1	Brantley and Mellott (2000)
	Pyroxenes	Ca, Mg, Fe, Al silicate	2.3	Reddy and Claassen (1994)
	Olivine	$(MgFe)_2SiO_4$	1.5	Brantley and Mellott (2000)
Hydrous silicate	Kaolinite	$Al_2Si_2O_5(OH)_4$	13.69	Meier et al. (1994)
Oxide	Quartz	SiO_2	0.17	Sorwat et al. (2020)
	Aluminum	Al_2O_3	122	Wang et al. (2020a)
	Iron oxides	Fe_2O_3	0.381	Giménez et al. (2007)
		$(Fe_2O_3)_2(H_2O)_3$	10.26	Yan et al. (2020)
		Fe_3O_4	37.21	Sorwat et al. (2020)
Carbonates	Calcite	$CaCO_3$	0.5	Wang and Zhang et al. (2020)
	Dolomite	$CaMg(CO_3)_2$	0.7	Yan et al. (2020)

The adsorption isotherms, kinetics, and thermodynamics of the cationic dyes Basic red 18 and Basic Blue 41 onto feldspar were investigated, considering both single and binary systems. The optimal adsorbent dosage was 2.5 g L^{-1}, with the dye's concentration ranging from 12.5 to 50 mg L^{-1} (Yazdani et al., 2012). The dye uptake capacity increased as pH increased from 2.5 to 8. This behavior is an exciting point because most effluents' final pH is around 5–8; therefore, no pH adjustment would be necessary (Boczkaj and Fernandes, 2017). Their adsorption behavior followed Langmuir for single and extended Langmuir isotherms for binary systems, respectively. The adsorption kinetics was found to conform to pseudo-second-order kinetic for both systems. Meanwhile, the thermodynamic data showed that dye adsorption onto Feldspar was spontaneous, endothermic, and physisorption was the dominant mechanism (Yazdani et al., 2012).

Besides organic molecules, the adsorption of potentially harmful ions has also been studied in natural and modified feldspar. Ferric ions, uranium (U(VI)), and arsenic (As(V)) are some examples (Al-Anber, 2015; Ding et al., 2014; Yazdani et al., 2016). Natural feldspar was useful for removing Fe^{3+} ions from an aqueous solution. The maximum removal was found at a low-level initial concentration of Fe^{3+} ions (30 mg L^{-1}) on 40 g L^{-1} of adsorbent dosage, 30 °C, and a contact time of 180 min. Finally, it was concluded that the adsorption mechanism was chemisorption (Al-Anber, 2015). In Table 2, a summarization of the technical results on feldspar adsorption is presented.

2.1.2. Micas

Micas are monoclinic pseudohexagonal crystals, similar in chemical composition, with the general molecular formula of $X_2Y_{4-6}Z_8O_{20}(OH, F)_4$ – where X is K, Na, or Ca, Y is Al, Mg, or Fe, and Z is Si or Al but also may include Fe^{3+} or Ti (Frye, 2006). Some examples are biotite, muscovite, lepidolite, phlogopite, zinnwaldite, and margarite (Deer et al., 2013). This mineral was employed in few studies, mostly for the adsorption of metal ions, surfactants, and pharmaceuticals (Alexandre-Franco et al., 2011; Gier and Johns, 2000; Klapyta et al., 2001; Li et al., 2019b, 2019c; Martín et al., 2018, 2019; Orta et al., 2018; Osuna et al., 2019; Pazos et al., 2017).

2.2. Oxides

The oxides include about 40 cationic elements in their composition, such as Si, Ti, Nb, Ta, Mn, Al, Mg, Sn, and Zr combined with oxygen or hydroxyl (Frye, 2006; Marfunin, 1994). The most commonly known and occurring are cuprite (Cu_2O), corundum (Al_2O_3), hematite (Fe_2O_3), cassiterite (SnO_2), magnetite (Fe_3O_4), ilmenite ($FeTiO_3$), perovskite ($CaTiO_3$), brucite ($Mg(OH)_2$) and gibbsite ($Al(OH)_3$) (Frye, 2006; Marfunin, 1994). Among the above-cited minerals, magnetite, hematite, and ilmenite stand out. Because iron is present in their structure, simultaneous degradation reactions can occur, a process known and well established as Fenton reactions (Ghernaout et al., 2020). Moreover, the naturally occurring oxide of titanium, TiO_2, is typically obtained from the minerals ilmenite, rutile, and anatase (Lahiri and Jha, 2007). It is widely used as a pigment in paints and personal care products, and its activity as a photocatalyst is well-established (Diebold, 2003; Weir et al., 2012). Still, these light-interacting properties are mostly used to degrade pollutants, not adsorption per se (Shiraishi et al., 2005).

Magnetic properties are of most interest, considering the difficulty of separating solid catalysts from aqueous solutions (Serpone et al., 2010). Therefore, Fe_3O_4 is the most popular iron oxide: there are about 15 times more studies published on its regard than hematite and ilmenite. Magnetite properties as adsorbent are widely known and accepted (Milonjić et al., 1983; Udovic and Dumesic, 1984), mostly by the adsorption of ions as phosphate, arsenite, and arsenate (Daou et al., 2007; Yean et al., 2005), but its use for adsorption of organic molecules has been reported only with hybrid materials (Cheng et al., 2012b; Qin et al., 2014; Vieira et al., 2020).

Overall, this class of natural geological materials is interesting for adsorption applications because, in their structure, they have metal atoms electrostatically charged or in different oxidation states, which enhances the attraction of the pollutant to the adsorbent surface and, consequently, increases the total removal efficiency (Khaleel et al., 1999; Velazquez-Jimenez et al., 2015; Wang et al., 2020a). Table 3 is presented a portrait of the most relevant studies on adsorption onto oxides.

2.3. Carbonates

In geology and mineralogy, minerals dominated by the carbonate ion, CO_3^{2-}, are designated simply as carbonates, which are incredibly varied and omnipresent in chemically precipitated sedimentary rocks (Lippmann, 1973). The trivial are calcite, dolomite, and siderite (Curtis and Coleman, 1986; Pearce et al., 2013). Calcite, $CaCO_3$, is the primary constituent of limestone and the main component of mollusk shells and coral skeletons (Lorens, 1981; Somasundaran and Agar, 1967; Wray and Daniels, 1957). Dolomite, $CaMg(CO_3)_2$, is used as an ornamental stone, a concrete aggregate, and a source of magnesium oxide (Baker and Kastner, 1981; Sibley and Gregg, 1987; Warren, 2000). Siderite, $FeCO_3$, is the essential iron ore and has been used for steel production (Matthiesen et al., 2003; Mozley, 1989; Zhu et al., 2020). Moreover, some other popular carbonates, such as sodium carbonate and potassium carbonate, have been used since antiquity for cleaning and preservation, as well as for the manufacture of glass (Freilich et al., 2014; Konkol and Rasmussen, 2015; Krumbein et al., 1991; Wood et al., 1984). Carbonates are widely used in industry, e.g., in iron smelting, as a raw material for Portland cement and lime manufacture, in the composition of ceramic glazes, and more (Al-Shalabi and Sepehrnoori, 2016; Boyjoo et al., 2014; Clements, 2003; Dhami et al., 2013).

Table 2
Main feldspar applications in adsorption.

Adsorbent	Dosage ($g\ L^{-1}$)	Adsorbate	C_0 ($mg\ L^{-1}$)	q_{max} ($mg\ g^{-1}$)	Reference
Natural feldspar	2.5	Basic blue 41	25	11.11	Yazdani et al., 2012
		Basic red 18	25	10.75	
Surfactant-modified feldspar	0.5	Acid black 1	10	6.37	Yazdani et al., 2012
		Acid red 14	10	3.98	
Chitosan/Feldspar biohybrid	4	Acid black 1	25	4.16	Yazdani et al., 2014
			50	8.33	
			75	12.5	
			100	16.12	
			125	17.24	
Natural feldspar	40	Fe^{3+}	30	25	Al-Anber, 2015
Raw sodium feldspar	1	U(VI)	0.5	0.314	Ding et al., 2014
Natural feldspar	8		5	235.3	Yazdani et al., 2016

Table 3
Most important aspects of the adsorption studies using oxides for pollutant removal.

N.	Adsorbent		Adsorption test							Reference
	Type	Specific surface area	Pollutant	Adsorbent dosage	Pollutant initial concentration	pH	Amount adsorbed	Isotherm type	R^2	
		(m^2 g^{-1})			C_0		q_{max}			
1	Cuprite	2.15	Diethyldithiocarbamate	20 g L^{-1}	30 g L^{-1}	7	6.08 g g^{-1}	–	–	
2	Perovskite	0.21	Dichlorvos	1 g L^{-1}	100 mg L^{-1}	5	50 mg g^{-1}	Freundlich	0.99	Ghernaout et al., 2020
3		18	Rhodamine B	2 g L^{-1}	100–00 mg L^{-1}	2.5–12	182.2 mg g^{-1}	Langmuir	0.99	Deng et al., 2017
4	Gibbsite	44.1	Nortriptyline	100 m^2 L^{-1}	0.1 mM	3–12	2.4 ± 0.1 μmol m^{-2}	Langmuir	0.99	Sadri et al., 2018
5		5.82	Sb	10 g L^{-1}	1 μmol L^{-1}	5.5	38.66 mmol kg^{-1}	Langmuir	0.98	Essington & Stewart, 2015
6		18	Se	0.8 g L^{-1}	19 μmol L^{-1}	3	9.5 mmol kg^{-1}	Triple-layer model	–	Goldberg, 2014
7	Hematite	19.4	Phenol	5 g L^{-1}	10 mg g^{-1}	2–7	16.17 mg g^{-1}	Langmuir	0.99	Dehghan and Anbia, 2017
8		100.5	Methylene blue and other metal ions - Cr, Co, Ni, Cu, Cd, Hg e Pb	0.62 g L^{-1}	5–40 mg L^{-1}	6.5	44.7 mg g^{-1}	Langmuir	0.99	Sengupta et al., 2017
9		73.9	Congo Red	0.3 g L^{-1}	400–100 mg L^{-1}	–	628.9 mg g^{-1}	Langmuir	0.99	Xu et al., 2012
10	Ilmenite	90.6	Methylene blue	0.03 g L^{-1}	0.5–8 mg L^{-1}	5.5	71.9 mg g^{-1}	Langmuir	0.97	Chen, Jin, et al., 2011
11		152.3	Congo red, Methyl orange, and Methylene blue	0.3 g L^{-1}	50–500 mg L^{-1}	7.2	723.8, 150.7, and 54.5 mg g^{-1}	Sips	0.98	Kang et al., 2018
12	Magnetite	44.82	Acid Red 18	0.75 g L^{-1}	25–100 mg L^{-1}	3	16.259 mg g^{-1}	Freundlich	0.98	Berizi et al., 2016
13		23.35	Pb	10 mg L^{-1}	110 mg L^{-1}	6	41.66 mg g^{-1}	Langmuir	0.99	Singhal et al., 2017
14		98.8	As	2.5 g L^{-1}	45 mmol L^{-1}	4.8	20.8 mg g^{-1}	Langmuir		Daou et al., 2007
15		14.180	Tl	2 g L^{-1}	20–100 mg L^{-1}	6–9	1123 mg g^{-1}	Temkin	0.98	Li and Arai, 2020

The removal of phosphate species from solution by adsorption onto natural-calcite was evaluated alongside the effect of pH, phosphate/mineral ratio, and contact time (Karageorgiou et al., 2007). The results indicated that pH plays an important role, and the adsorption process is more efficient in the basic pH region. The orthophosphate removal is almost complete for concentrations as high as 60 mg L^{-1} of phosphate, which corresponds to 0.1 to 1 mM g^{-1} pollutant to adsorbent ratio (Karageorgiou et al., 2007). Tannic acid, a calcite flotation agent widely used in mineral processing, had its mechanisms and behaviors studied on calcite surfaces, utilizing isothermal, kinetic, and thermodynamic studies. The adsorption capacity of tannic acid increased with initial concentration in the optimal pH 8. Sips isotherm model best predicted equilibrium data, while the adsorption kinetics followed a pseudo-second-order model, indicating that the adsorption process was controlled by chemical reaction. The maximum adsorption capacity was 13.55 mg g^{-1}, considering 10 g L^{-1} of calcite and 100 mg L^{-1} of tannic acid (Karageorgiou et al., 2007). Moreover, other studies were conducted: regarding the dynamic of asphaltene adsorption on calcite packs (Karageorgiou et al., 2007); L-malic, D-malic, and succinic acid adsorption (Li et al., 2019a); determination of Ni isotope fractionation its adsorption processes (Castillo Alvarez et al., 2020); arsenate (Markovski et al., 2014a) and Cd(II) (Song et al., 2011) on modified calcite; as well as a molecular simulation study on the adsorption of hydrogen sulfide in calcite pores (Cai et al., 2020).

Even though calcite is the most commonly found mineral, dolomite is the most studied carbonate towards adsorption. The adsorption of several potentially toxic ions was tested on dolomite, such as those of the elements strontium and barium (Ghaemi et al., 2011), copper and lead (Pehlivan et al., 2009; Şenol and Şimşek, 2020), arsenate (Ayoub and Mehawej, 2007), chromium (Albadarin et al., 2012; Stefaniak et al., 2000), cadmium and nickel (Mohammadi et al., 2015), and fluoride (Wongrueng et al., 2016). As an outcome, all studies warranted dolomite as a cheap and useful solid material, with good adsorption properties towards hazardous inorganic compounds (Stefaniak et al., 2000).

Siderite has been applied as a pristine mineral (Erdem and Özverdi, 2005; Hajji et al., 2019; Wang and Reardon, 2001), as well as the principal constituent in iron-rich sludge adsorbents (Qu et al., 2020; Sharma et al., 2013b; Zhu et al., 2018, 2019). By using stirred flow-through reactor experiments, siderite (90 m^2 g^{-1}) adsorption of As(III), Cr(VI), and competitive As(III)/Cr(VI) was reinvestigated. As and Cr sorption isotherms fit the Langmuir model. Its competitive sorption responded to a sigmoidal Hill model. The maximum uptake for each pollutant was around 60 mg g^{-1} (Hajji et al., 2019). Conversely, by submitting the wasted iron mud to hydrothermal treatment, a magnetic adsorbent removed other metals from smelting wastewater. The modification acted upon ferrihydrite's reductive dissolution to recompose the natural siderite, which was then re-oxidized to maghemite. As a result, at the dosage of 12.5 g L^{-1}, a removal efficiency around 99% of Cu^{2+}, Zn^{2+}, Pb^{2+}, and Cd^{2+} was attained (Zhu et al., 2018).

Moreover, magnesite, smithsonite, aragonite, and bastnasite have all been applied to the wastewater treatment to some extent. Magnesite was employed in phosphate from municipal effluents (Masindi et al., 2016; Mavhungu et al., 2019) and as an adsorbent for cationic and anionic dyes (Ngulube et al., 2018). Lead (Zhang et al., 2019a), iron (Deng et al., 2017), and 8-hydroxyquinoline onto smithsonite have been studied (Cristina et al., 2011). As for aragonite, cadmium (Van et al., 2019; Yang et al., 2018), phosphate (Millero et al., 2001), and methanoic acid adsorption have been reported (Cooper and De Leeuw, 2002)(). Finally, alkyl hydroxamic acid's adsorption mechanism onto bastnasite was explored (Millero et al., 2001).

3. Clays

Clays are phyllosilicate minerals with layered structural units, constituted of one or two tetrahedral silica sheets around an octahedral aluminum sheet (Brigatti et al., 2006; Velde, 1995). They present small particle sizes, typically of less than 2 μm, and high specific surface areas, as a result of their complex porous structures, which facilitates physical and chemical interactions with dissolved species (Bertagnolli et al., 2011; Djomgoue and Njopwouo, 2013; Luo and Daniel, 2003). Moreover, some specific factors determine how the adsorption process will occur onto clay minerals. Besides some of its specific properties, the contact time, clay dosage, and pH, play important roles (Otunola and Ololade, 2020).

Two essential topics on clay adsorption are its cation exchange capacity (Chapman, 2016) and specific surface area (Carter et al., 2018), because in this case, it is understood that they rule its adsorption capability (Dabrowski, 2001). Both properties are related: while cation exchange capacity translates as the total negative charge (Ammann et al., 2005; Lipson and Stotzky, 1983), the specific surface area is the total surface area with available adsorption sites (Kuila and Prasad, 2013; Macht et al., 2011). The larger the surface area, the greater is the cation exchange capacity (Ersahin et al., 2006; Kuila and Prasad, 2013). Besides, it is attractive to the point that variations found in these properties determinations can be attributed to the fact that some clay minerals have only external layers, such as kaolinite and illite, and others have internal and external layers, such as smectites and attapulgite (Hepper et al., 2006).

Another critical variable in adsorption studies is the contact time, which is how long the adsorbent needs to be in the same medium as the pollutant to achieve maximal removal efficiency (McKay, 1982; Suliestyah Hartami and Tuheteru, 2020; Yang et al., 2009). The adsorption rate of clays tends to increase with the increased contact time, remaining constant until equilibrium is reached (Yin and Zhu, 2016). Moreover, the contact time varies according to clay dosage (Otunola and Ololade, 2020). There are no specific guidelines determining clay dosage for wastewater treatment; therefore, previous studies and literature search is needed before application. It has been discussed that a small dosage, around 1 to 3 g L^{-1}, of clay minerals, is enough to adsorb reasonable concentration pollutants from contaminated effluents (Kausar et al., 2018; Lazaratou et al., 2020).

Moreover, observations on the influence of the pH of the system demonstrated that, as pH increases, there is an immediate increase in the rate of adsorption (Akpomie and Dawodu, 2016; Chen et al., 2011b; Es-Sahbany et al., 2019; Otunola and Ololade, 2020; Potgieter et al., 2006). However, it must be emphasized that pH also regulates other processes, such as the chemical equilibrium of the target pollutant molecule with the clay (Beattie, 1956; Hackling and Garnett, 1985). Therefore, even though generally basic pH enhances the clays' adsorption capacity, this is not a rule (Győrfi et al., 2020; Hamza et al., 2020; Maleki and Karimi-Jashni, 2020; Obayomi et al., 2020; Romdhane et al., 2020).

3.1. Kaolinite

One of the most currently applied geological materials for adsorption belongs to the hydrous silicates class: kaolinite (Velde, 1995). Its general molecular formula is $Al_2Si_2O_5(OH)_4$. Kaolinite is a layered silicate mineral, with one tetrahedral sheet of silica linked through oxygen atoms to one octahedral sheet of alumina octahedral (Essington and Stewart, 2015; Kuila and Prasad, 2013; Sadri et al., 2018).

Ghorbanzadeh et al. (2015) reported on the removal of arsenate and arsenite from aqueous solution. Kaolinite surface area was determined as 10.1 m^2 g^{-1}. Adsorption isotherms were conducted with initial arsenic concentrations of 0.05, 0.06, 0.1, 0.15, and 0.2 mmol L^{-1}, with 27 g L^{-1} of the adsorbent. The equilibrium was studied for 24 h. Optimal adsorption pH for As^{5+} was found to be around 5 (99.9%), with the efficiency rates decreasing as pH increased. For As^{3+} adsorption, at pH 7, the maximum adsorption capacity reached was 380 μg g^{-1}. Both As (V) and As(III) adsorption isotherms fit the Langmuir model (R^2 = 0.968 and 0.979, respectively), and q_{max} values of 0.203 and 0.241 mg g^{-1} (Ghorbanzadeh et al., 2015). Mohapatra et al. (2007) observed similar responses while studying pH for As(V) adsorption onto kaolinite, and maximum adsorption was also achieved at pH 5.0. Equilibrium was reached within 3 h, and q_{max} value of 0.86 mg g^{-1} was found by fitting the Langmuir equation to the adsorption isotherms (R^2 = 0.98). The authors also observed an adverse effect of an increase in temperature on As(V) adsorption; therefore, interactions are exothermic. The electrokinetic behavior of kaolinite was modified in the pollutant's presence, which can be concluded as inner-sphere surface complexation and strong specific ion adsorption (Mohapatra et al., 2007).

Chantawong et al. (2003) investigated the adsorption of Cd^{2+}, Cr^{3+}, Cu^{2+}, Ni^{2+}, Pb^{2+}, and Zn^{2+} by thai kaolinite. Except for Ni^{2+}, adsorption increased as pH increased. Isotherms fit the Freundlich model, with R^2 ranging from 0.93 to 0.99, for each ion. Adsorption followed the order: Cr > Zn > Cu ≈ Cd ≈ Pb > Ni, with maximum removal capacity of 1.13×10^{-3}, 1.07×10^{-3}, 4.20×10^{-4}, 6.22×10^{-4}, 7.73×10^{-5}, and 5.11×10^{-5} mmol g^{-1}, respectively (Chantawong et al., 2003). Liu et al., 2016a focused on a wide range of individual Pb, Zn, and Cu concentrations, varying from 0.1 to 100 mM, at different pH conditions. Again, the best results were obtained in basic pH. Also, the isotherms fit the Freundlich and Langmuir models for kaolinite. The maximum removal capacity for Cu was 1.82 mg g^{-1}, for Zn was 6.19 mg g^{-1}, and Pb was 14.47 mg g^{-1} (Liu et al., 2015). Also, Coles and Yong (2002) conducted batch equilibrium tests on kaolinite suspensions adjusted to pH 4 and pH 6, aiming to remove $PbCl_2$ and $CdCl_2$. Better results were obtained at pH 6. Interestingly, by studying the equilibrium curves of both metal retention versus suspension pH, combined with an analysis of the speciation of the metals, it was evidenced that both divalent (Pb^{2+} and Cd^{2+}) and monovalent ($PbCl^+$ and $CdCl^+$) species were adsorbed (Coles and Yong, 2002).

Ghosh and Bhattacharyya (2002) employed raw kaolinite obtained from a local deposit focusing on methylene blue adsorption. The raw adsorbent showed considerable adsorption, superior to the calcinated version of the material. Experiments were conducted considering contact time of 3 h, pH 10, initial methylene blue concentration of 15 mg L^{-1}, and adsorbent dosage of 0.8 g L^{-1}. In this condition, raw kaolinite uptake reached 13.99 mg g^{-1}, and the isotherms fit well the Langmuir model (Ghosh and Bhattacharyya, 2002). Doğan et al. (2009) addressed Maxilon Yellow 4GL and Maxilon Red GRL dyes kinetic adsorption. The equilibrium was set after 150 min. The adsorption kinetics followed pseudo-second-order for both dyes, with k_2 values up to 107.87×10^4 g mol^{-1} min^{-1} for Maxilon Yellow and 72.09×10^4 g mol^{-1} min^{-1} for Maxilon Red (Doğan et al., 2009). Despite kaolinite usual small surface area, several studies have been published on its efficiency towards dyes adsorption: aniline blue (Unuabonah et al., 2008a), basic fuchsin (Khan et al., 2015), crystal violet (Çiftçi et al., 2017; Dobrogowska et al., 1991; Khan et al., 2015; Sarma et al., 2019; Yariv et al., 1991), solophenyl yellow GFL (Kamel et al., 1991), solophenyl red 6BL (Kamel et al., 1991), diphenyl pink BF (Kamel et al., 1991), 9-aminoacridine (Harris et al., 2001, 2006a–c), 3,6-diaminoacridine (Harris et al., 2001, 2006a, 2006b, 2006c), azure A (Harris et al., 2001, 2006a, 2006b, 2006c), safranin O (Harris et al., 2001, 2006a, 2006b, 2006c), reactive blue 221 (Karaoğlu et al., 2010), basic red 5 (Alom et al., 2014), rhodamine B (Batista et al., 2014; Khan et al., 2012; Rosales et al., 2018), methylene blue (Ghosh and Bhattacharyya, 2002; Greathouse et al., 2015; Hang and Brindley, 1970; Mukherjee et al., 2015), malachite green (Castellini et al., 2008; Sarma et al., 2019), reactive red 120 (Abidi et al., 2017), congo red (Bhattacharyya et al., 2015; Shaban et al., 2018), and many others.

Moving on further than dyes, one study investigated their adsorption alongside to other 23 organic pollutants, such as acridine, 8-amino quinoline, quinoline, and pyridine (Harris et al., 2001). Organic pollutants are of great concern due to their ubiquitous occurrence,

even in remote ecosystems (Lu and Astruc, 2020; Sun et al., 2020; Zhang et al., 2003). Among them, pesticides are of great concern (Bache et al., 1964; Sharma et al., 2020). Clausen et al. (2001) investigated atrazine (6-chloro-N2-ethyl-N4-isopropyl-1,3,5-triazine-2,4-diamine), isoproturon ([3-(4-isopropyl phenyl)-(1,1-dimethylurea)]), mecoprop ((*RS*)-2-(4-chloro-2-methyl phenoxy)propionic acid), 2,4-D (2,4-dichloro-phenoxy-acetic acid), and bentazone (3-isopropyl-1H-2,1,3-benzothiadiazin-4-(3H)-one 2,2-dioxide) adsorption towards kaolin. Specific surface area and mineral surface charge proved important factors: detectable adsorption of anionic pesticides was only measured when positive sites were present on the mineral surface. When an electrolyte was added, detectable adsorption of mecoprop and 2,4-D was also measured on kaolinite, probably due to the formation of surface complexes. However, the adsorption of the uncharged pesticides, atrazine, and isoproturon, did not suffer interferences. Despite their efforts, pesticides adsorb weakly to pure kaolin in aqueous solutions (Clausen et al., 2001).

3.2. Montmorillonite

Montmorillonite is a clay mineral, whose molecular formula can be described as $(Na, Ca)_{0.33}(Al, Mg)_2(Si_4O_{10})(OH)_2(H_2O)_n$, with substantial isomorphic substitution. On behalf of adsorption, this mineral presents peculiar characteristics, such as fast cationic exchange and interlaying swelling (Bhattacharyya and Gupta, 2008). Cations such as Na^+ and Ca^{2+} tend to form surface complexes; therefore, they are easily exchanged with solute ions (Dähn et al., 2002). In its structure, interlayer swelling occurs in aqueous media. This process depends on valences and the atomic radius of the exchangeable cations (Hennig et al., 2002), which leads to additional inner-sphere complexation and adsorption (Elzinga and Sparks, 1999). Although there is a conflict in the literature about whether bentonites are a sub-group of montmorillonites or simply the same thing, this review article will approach both subjects together. When it comes to writing reports on different knowledge areas, there is a deficiency sometimes in standardizing terms, which can result in less visibility for several relevant and well-performed studies, just because the authors know a specific material by a name other than the usual one, but that still is scientifically accepted (Malamis and Katsou, 2013).

Several studies report on montmorillonite adsorption towards metals (Álvarez-Ayuso and García-Sánchez, 2003; Andini et al., 2006; Angove et al., 1998; Bhattacharyya and Gupta, 2007a; Donat et al., 2005; Gupta et al., 2003; Gupta and Bhattacharyya, 2006; Jain and Sharma, 2002; Jobstmann and Singh, 2001; Kandah, 2004; Karapinar and Donat, 2009; Liu and Jiang, 2010; López et al., 1998; Mathialagan and Viraraghavan, 2002; Putro et al., 2017; Ulmanu et al., 2003; Wasewar et al., 2010). Gupta and Bhattacharyya (2006) reported the adsorption of Cd^{2+} onto raw and modified montmorillonite. The removal efficiency reached 94.5% for raw montmorillonite, compared to 64.8%, 81.0%, and 99.3% for ZrO/montmorillonite, tetrabutylammonium/montmorillonite and acid-activated montmorillonite, respectively. This removal efficiency can be translated as an adsorption capacity of 32.7 mg g^{-1}. Again, the adsorption of Co^{2+} was only slightly superior onto acid activatated montmorillonite in comparison to the raw material, reaching 29.7 and 28.6 mg g^{-1} of adsorption capacity (Bhattacharyya and Gupta, 2007b). Considering the time, effort, and cost, modified montmorillonite is not offset by raw montmorillonite efficiency (Gupta and Bhattacharyya, 2006). In Table 4, several studies on montmorillonite adsorption towards metals are summarized.

The adsorption of several dyes onto both natural and modified montmorillonites has been studied over the years, such as methylene blue (Benhouria et al., 2015; Feddal et al., 2014; Hong et al., 2009; Kahr and Madsen, 1995; Wei et al., 2018; Zhang et al., 2019a), methyl violet (Fabryanty et al., 2017; Guiza et al., 2012; Puri and Sumana, 2018; Zhang et al., 2019b), methyl orange (Chen et al., 2011a; Leodopoulos et al., 2012; Zhang et al., 2019c), naphthol green (Zhang et al., 2019e), direct red 23 (Mahvi and Dalvand, 2020), diamond fast brown KE (El-Defrawy et al., 2019), reactive red 120 (Mahmoodi et al., 2019; Tabak et al., 2010) and acid fuchsin (Cao et al., 2017; Gong et al., 2018). Data on dye adsorption can be summarized in results obtained by Fil et al. (2014), who studied Red Violet 3RN color removal in simulated wastewater using montmorillonite clay. They concluded that the process efficiency rate increased with increasing pH, temperature, dye concentration, and agitation speed but decreased with increased ionic strength and adsorbent dosage. Langmuir model better represented the equilibrium data. Also, kinetics fit the pseudo-second-order model (Fil et al., 2014).

Chang et al. (2015) investigated tetracycline adsorption, an antibiotic onto high-charge Ca-montmorillonite and low-charge Na-montmorillonite. The adsorption data obeyed Langmuir isotherm, with maximum pollutant adsorption of 468 and 404 mg g^{-1} on Ca and Na montmorillonites, respectively. The adsorption was endothermic, suggesting strong physical adsorption, which is expected for organic molecules adsorbents with high surface area and a small pore size ratio (Chang et al., 2015). Also, concerning natural montmorillonite, Thiebault and Boussafir (2019) explored the adsorption of the psychoactive drugs codeine, diazepam, and oxazepam onto Na-montmorillonite. At pH = 7.5, codeine cation exchange resulted in the highest amount adsorbed among the tests (q_{max} = 0.381 mmol g^{-1}). Therefore, their significant contribution was proving that variation in pH strongly impacts the pollutant and sorbent affinity (Thiebault and Boussafir, 2019). Also, studies report atenolol (Chang et al., 2019) and nortriptyline (Sadri et al., 2018) in raw Ca-montmorillonite, while 4-acetaminophenol (Chu et al., 2019), amoxicillin, and diclofenac (Khan et al., 2020) removal were reported for modified montmorillonite.

At last, pesticides adsorption onto montmorillonite was reported and verified as well, demonstrating that it acts as a natural scavenger of pesticides due to the abundant availability, large specific surface area, and high adsorptive and ion exchange properties (Bhardwaj et al., 2014; Cabrera et al., 2008; Kovacevic et al., 2011; Ozcan et al., 2012; Park et al., 2014; Suciu and Capri, 2009). Carbaryl, aldrin, malathion, 2,4-D, and dimethoate adsorption capacity onto raw montmorillonite were 3.70, 14.96, 7.95 mg g^{-1} and 0.90, 0.96 μg kg^{-1}, respectively (Al Kuisi, 2002; Chen et al., 2009; Ozcan et al., 2012; Pal and Vanjara, 2001; Park et al., 2019); 8-quinoline carboxylic acid adsorption capacity onto Na-, acidic- and organo-montmorillonite was 65.4. 67.6 and 75.9 mg g^{-1} (Mekhloufi et al., 2013); Na- and Ca-montmorillonite adsorption capacity towards phosmet reached 1.04×10^{-3} and 1.648×10^{-3} mg g^{-1} (Sánchez Camazano and Sánchez Martín, 1983), while K-, Na- and Ca-montmorillonite towards phosdrin reached 1.882×10^{-3}, 3.548×10^{-3} and 2.150×10^{-3} mg g^{-1} (Sánchez Camazano and Sánchez Martín, 1983).

3.3. Illite

The term illite was proposed by (Grim et al., 1937) as a general term, not as a specific clay mineral name, to designate mica-like clay minerals of Illinois. Since then, the illite definition was progressively improved (Meunier and Velde, 2010). Thus, Illite is understood as a group of closely related non-expanding phyllosilicate. Its chemical formula is given as $(K,H_3O)(Al,Mg,Fe)_2(Si,Al)_4O_{10}[(OH)_2,(H_2O)]$, with considerable ion substitution (Meunier et al., 2004; Meunier and Velde, 2010). In addition to the surface hydrogen bonds, illite cleavage releases potassium ions, which results in the surface of high-density ionic bonds. Thus, cleaved illite surfaces are moderately hydrophilic (Park et al., 2019; Zhang et al., 2018).

Picloram, a herbicide adsorbed on illite, was studied under pH variation. Batch tests were performed with an adsorbent dosage of 16 g L^{-1} and pollutant concentrations ranging from 0.2 to 5.0 mmolL^{-1}. The adsorption isotherms well-fit both Langmuir and Freundlich models, with q_{max} values of 14 ± 2, 12 ± 3, and 11 ± 1 μmol g^{-1} at pH 3, 5, and 7, respectively (Marco-Brown et al., 2019). The picloram molecule interactions with illite surfaces exhibited anionic profile adsorption, with a decrease in adsorption when the pH increases,

Table 4
Different montmorillonites adsorption response on metal ions removal efficiency.

Type	Dosage ($g\ L^{-1}$)	Pollutant – C_0	q_{max} ($mg\ g^{-1}$)	Reference
Acid-activated	2	Cu^{2+} 10–250 $mg\ L^{-1}$	32.3	Bhattacharyya and Gupta, 2011
	2	Ni^{2+} 10–250 $mg\ L^{-1}$	29.5	Bhattacharyya & Gupta, 2008
Calcareous	1	Cu^{2+} 10–100 $mg\ L^{-1}$	12.97	Sdiri et al., 2012
Calcium	20	Cu^{2+} 13–160 $mg\ L^{-1}$	12.633	Wu et al., 2011
Ilite system	3	Pb^{2+} 100 $mg\ L^{-1}$	54.12	Oubagaranadin et al., 2010
	17	Cu^{2+} 10–150 $mg\ L^{-1}$	30.99	Oubagaranadin and Murthy, 2010
K10	16	Ni^{2+} 10–2000 $mg\ L^{-1}$	2.10	Carvalho et al., 2008
Raw	2	Cu^{2+} 10–250 $mg\ L^{-1}$	31.8	Bhattacharyya and Gupta, 2011
	1	Cu^{2+} 10–100 $mg\ L^{-1}$	17.89	Sdiri et al., 2011
	2	Fe^{3+} 10–250 $mg\ L^{-1}$	28.9	Bhattacharyya and Gupta, 2008
	2.5	Pb^{2+} 150 $mg\ L^{-1}$	57.0	Zhang and Hou, 2008
	2	Ni^{2+} 10–250 $mg\ L^{-1}$	28.4	Bhattacharyya and Gupta, 2008
Tetrabutylammonium	1	Fe^{3+}, Co^{2+}, Ni^{2+} 50 $mg\ L^{-1}$	22.6	Bhattacharyya and Sen Gupta, 2009
	2	Fe^{3+} 10–250 $mg\ L^{-1}$	19.7	Bhattacharyya and Gupta, 2008b
ZrO	2	Fe^{3+}, Co^{2+}, Ni^{2+} 50 $mg\ L^{-1}$	23.8	Bhattacharyya and Gupta, 2008c

which is very interesting, considering that the illite point of zero-charge is around 2.8 (Marco-Brown et al., 2019; Park et al., 2019). Tetracycline is a semi-synthetic antibiotic commonly detected in soils due to animal-produced slurry applications as fertilizer (Agersø et al., 2006). Chang et al. (2012) reported illite adsorption capacity towards tetracycline adsorption at 32 $mg\ g^{-1}$, at pH 5–6. Adsorption equilibrium data obeyed the Freundlich isotherm model. Therefore, considering the q_{max} value reported in this study, illite may act as an essential environmental deposit on fate, routes, and transportation of antibiotics in soils (Chang et al., 2012). Although the studies discussed above, as well as the study carried out by (Fil et al., 2016) regarding methyl violet dye, point to non-linear adsorption models, it has also been reported that for larger molecules, such as microcystin-LR, the application of linear isotherms might be proven more suitable (Liu et al., 2019).

Ionic adsorption onto illite has been inspected as well. For example, uranium sorption characteristics tend to be dominated by chemical ion-exchange, an endothermic and spontaneous process that increases entropy (Liao et al., 2020). Fernandes and Baeyens (2019) modeled lead adsorption considering two sites protolysis non-electrostatic surface complexation and cation exchange, and reported maximal uptake values 4.0×10^{-2} to 2.0×10^{-3} $mol\ kg^{-1}$ (Fernandes and Baeyens, 2019). Moreover, investigations on copper and nickel adsorption on illite/smectite systems were reported by (Du et al., 1997), Rosskopfová's et al. (2016), and Viglašová et al. (2017). In addition to illite ionic adsorption, thallium and strontium adsorption have been investigated as well, but will not be explored in this review for our scope is environmental remediation, and such metals are not yet considered environmental relevant contaminants (Galamboš et al., 2013; Wick et al., 2018; Zhang et al., 2016).

4. Zeolites

Zeolites of natural origin are formed due to volcanic activity, either by water or deposition of volcanic dust in saline deposits (Delkash et al., 2015; Malamis and Katsou, 2013). They are complex, microporous inorganic polymers formed by an infinitely extensive three-dimensional structure of silicon and aluminum tetrahedrons linked together by sharing oxygen (Hong et al., 2019; Niu et al., 2020). The most commonly found natural types are mordenite, chabazite, and clinoptilolite (Dehghan and Anbia, 2017; Flanigen, 1991). The zeolite crystal structure's inner cavities are generally in the range of 0.5–1.2 nm, a factor determined by formation route and different Si/Al ratios. This Si/Al ratio acts directly on the thermal resistance of zeolites and cation exchange properties: low-silica zeolites with Si/Al ratio below 2 have excellent ion exchange capacity; however, the higher the aluminum content, the less stable tends to be the zeolite (Jiang et al., 2018; Wen et al., 2018). Unlike geopolymers, zeolites, despite having the same constitution, are highly crystalline materials with higher thermal and chemical resistance. Another difference is that zeolites need a higher amount of water present in their formation reaction medium. The synthesis reactions take longer than that of the geopolymers, much due to the crystallization stage (Fernández-Jiménez et al., 2005).

Jafari-zare and Habibi-yangjeh (2010) studied the adsorption of rhodamine B and methylene blue in both single and binary component systems, using natural zeolite formed predominantly by clinoptilolite. The experiments were carried out at pH 12, with an adsorbent dosage of 0.2 $g\ L^{-1}$ and initial dye concentration of 6×10^{-6} $mol\ L^{-1}$. Results showed that the maximum capacity of clinoptilolite for the dyes methylene blue and rhodamine B in a single system was 7.95×10^{-5} and 1.26×10^{-5}, respectively, with both isotherms being better described by the Langmuir model, with determination coefficients (R^2) greater than 0.991. A reduction in the adsorption capacity of both dyes was verified in the binary system due to the competition of the molecules for the active sites available in the adsorbent; thus, the q_{max} value for rhodamine B was 2.2×10^{-6} $mol\ g^{-1}$, while for methylene blue was 7.44×10^{-5} $mol\ g^{-1}$, fitted again by Langmuir model (R^2 of 0.984 for the rhodamine B and 0.997 for the methylene blue) (Jafari-zare and Habibi-yangjeh, 2010).

Natural zeolites can also be used as adsorbents to remove pharmaceuticals in an aqueous solution. de Sousa et al. (2018) removed azithromycin, ofloxacin, and sulfamethoxazole using faujasite zeolites

with different Si/Al ratios. The zeolite FAU-1 had a Si/Al ratio of 30 and a surface area of 914 $m^2\ g^{-1,}$ while the FAU-2 had a Si/Al ratio of 82 and a surface area of 899 $m^2\ g^{-1}$. The adsorption tests were carried out with initial concentrations of antibiotics ranging from 10 to 400 μg L^{-1}, for 360 min, with a solution volume of 30 mL. The results showed that the FAU-1 zeolite, with greater surface area, showed greater adsorption capacity for both antibiotics, within the range of 8.5 mg g^{-1} for azithromycin to 31.32 mg g^{-1} for ofloxacin. A study simulating an effluent containing the three antibiotics, under conditions of pH 7.25, an adsorbent dosage of 10 mg L^{-1}, a contact time of 2 h, initial concentration of azithromycin, ofloxacin, and sulfamethoxazole of 391, 378, and 78.6 ng L^{-1}, respectively, showed that zeolite FAU-1 responds well against the treatment of effluents contaminated with pharmaceuticals, removing up to 60% of azithromycin, 76% ofloxacin and 44% of sulfamethoxazole (de Sousa et al., 2018).

Due to zeolite's tetrahedral aluminum structure, a negative surface charge is created in the mineral network structure. The presence of cations can counterbalance this charge, usually, Ca^{2+}, Na^{+} and K^{+}, located in the cavities; therefore, these cations are exchangeable with other cations, including environmental pollutant metals ions (Malamis and Katsou, 2013; Sprynskyy et al., 2006). For further understanding, the works on Ag^{+}, Cd^{2+}, Co^{2+}, Cr^{3+}, Cr^{6+}, Cu^{2+}, Fe^{3+}, Mn^{2+}, Ni^{2+}, Pb^{2+}, and Zn^{2+} adsorption are summarized in Table 5, displaying the most important topics and specifications of each research (Akgül et al., 2006; Álvarez-Ayuso et al., 2003; Álvarez-Ayuso and García-Sánchez, 2003; Baker et al., 2009; Bhattacharyya and Gupta, 2007a; Erdem et al., 2004; Ijagbemi et al., 2009; Malamis and Katsou, 2013; Minceva et al., 2008; Motsi et al., 2009; Ören and Kaya, 2006; Ren et al., 2016a; Sari and Tüzen, 2013; Sen Gupta and Bhattacharyya, 2008; Sheta et al., 2003; Sprynskyy et al., 2006; Yakout and Borai, 2014).

5. Geopolymers

Geopolymers are amorphous or semi-crystalline materials formed from polymerization reactions between geological originated materials containing aluminum and silicon, such as clays and fly ash, and an activating agent, usually strong bases as sodium or potassium hydroxide (Alouani et al., 2018; Bagci et al., 2017). Initially, geopolymers were used as additives to Portland cement because they improved their mechanical properties and durability since geopolymers are highly resistant to acid attacks and are resistant to frost/defrost cycles and fire-resistant (Atiş et al., 2015; Komnitsas, 2011).

The large OH^{-} ion concentration in the reaction medium of geopolymer preparation is responsible for the amorphous three-dimensional network's dissolution, commonly found in the starting materials (Khale and Chaudhary, 2007). In more detail, the activating agent breakdown the solid aluminosilicate by repulsion caused by the strong base cations (Na^{+} or K^{+}). In monomers, Al is tetrahedrally coordinated, and polycondensation reactions follow, forming a network composed of SiO_4 and AlO_4 tetrahedrons linked together by oxygen atoms. In this network, the alkali agent cation acts as a charge compensator in the geopolymer structure, enhancing adsorption possibilities (Duxson et al., 2007; Rahier et al., 2007). Studies involving the use of geopolymers as adsorbents for environmental remediation purposes, despite recent, are widely disseminated in literature, as presented in Table 6, and mainly focus on the removal of dyes molecules of aqueous solutions (Acisli et al., 2020; Alouani et al., 2018; Barbosa et al., 2018; Hua et al., 2020; Li et al., 2006; Rossatto et al., 2020; Schadeck Netto et al., 2019; Siyal et al., 2018) and towards metal ions (Al-Zboon et al., 2011; Chen et al., 2019; Cheng et al., 2012a; Kara et al., 2017; Liu et al., 2016c; Naghsh and Shams, 2017).

Barbosa et al. (2018) prepared a geopolymer using calcined kaolinite and rice husk ash as precursor materials and tested it versus methyl violet dye adsorption from aqueous solutions. The 62 $m^2\ g^{-1}$ surface area as-synthesized geopolymer showed a q_{max} capacity of 277 mg g^{-1}, at pH 4.5, at a temperature of 328 K, and an adsorbent dosage of 1.5 g L^{-1}. Isotherms were better described by the Sips model, with R^2 of 0.995, 0.989, 0.993, and 0.996 for the respective temperatures of 298, 308, 318, and 328 K (Barbosa et al., 2018). The endothermic character, which guarantees an improvement in the adsorption capacity by greater exposure of the geopolymer's active sites, was also reported by Alouani et al. (2018). They synthesized a geopolymer from fly ash from a thermoelectric plant for the adsorption of crystal violet dye. After 120 min, pH 5, and adsorbent dosage of 1 g L^{-1}, the maximum adsorption capacity of 37 mg g^{-1} was found, with the Langmuir model best describing the adsorption isotherms, with $R^2 = 0.999$, much higher

Table 5
Specifications of studies on Ag^{+}, Cd^{2+}, Co^{2+}, Cr^{3+}, Cr^{6+}, Cu^{2+}, Fe^{3+}, Mn^{2+}, Ni^{2+}, Pb^{2+}, and Zn^{2+} adsorption by different zeolites.

Material	Surface area ($m^2\ g^{-1}$)	Metal	Adsorbent dosage ($g\ L^{-1}$)	Initial concentration ($mg\ L^{-1}$)	pH	Temperature (K)	Adsorption capacity ($mg\ g^{-1}$)	Reference
Chabazite	1100	Zn^{2+}	20		6.0	293	7.98	Sheta et al. (2003)
	73.61	Cd^{2+}	2	50	5.5	298	120	Yakout and Borai (2014)
	–	Co^{2+}	5	30	5.0	298	1.50	Ouki and Kavannagh (1997)
		Cu^{2+}					3.80	
	17.83	Pb^{2+}	10	500	6.0	318	22.88	Minceva et al. (2008)
		Zn^{2+}					4.17	
		Cd^{2+}			7.0		5.46	
	–	Mn^{2+}	20	400	7.0	303	4.22	Erdem et al. (2004)
	20.3	Cd^{2+}	10	200	6.0	295	4.60	Álvarez-Ayuso et al. (2003)
		Cu^{2+}			5.0		5.91	
		Cr^{3+}			4.0		4.12	
	15.88	Fe^{3+}	37	400	3.5	295	6.61	Motsi et al. (2009)
		Cu^{2+}			3.5		3.37	
	16.76	Ag^{+}	2	150	4.0	298	33.23	Akgül et al. (2006)
Clinoptilolite/quartz	15.78	Pb^{2+}	12	80	4.0	308	10.00	Ren et al. (2016a)
		Cr(VI)	25				0.34	
Gordes zeolite	–	Zn^{2+}	1	20	4.0	298	6.00	Ören and Kaya (2006)
		Cd^{2+}			5.5		30.7	
		Ni^{2+}			5.7		21.1	
Philipsite	961	Zn^{2+}	20	500	6.0	293	1.70	Sheta et al. (2003)
Vermiculite	14.6	Ni^{2+}	2.5	100	6.0	295	19.3	Álvarez-Ayuso and García-Sánchez (2003)
	0.84	Ag^{+}	20	400	4.0	293	46.2	Sari and Tüzen (2013)
Zeolite	–	Zn^{2+}	5	20	6.0	300	62.9	Baker et al. (2009)
	–	Pb^{2+}					56.82	

Table 6
Summarization of recent studies involving geopolymers as adsorbents for environmental remediation purposes.

Adsorbent	Adsorbate	Surface area ($m^2\ g^{-1}$)	q_{max} ($mg\ g^{-1}$)	Reference
Fly ash	Methylene blue	–	37.04	Alouani et al., 2018
	Pb^{2+}	20.48	118.6	Liu, Huang, et al., 2016
	Cd^{2+}	130.45	26.246	Javadian et al., 2015
	Cs^{+}	114.16	15.24	Lee et al., 2016
Linz Donawitz converted slag	Ni^{2+}	30.84	85.29	
Mesoporous	Methyl violet	62	276.9	Barbosa et al., 2018
Metakaolin	Methyl Orange	35.66	0.339	Fumba et al., 2014
	NH_4^+	22.4	21.07	Luukkonen et al., 2016
	NH_4^+	19.3	19.7	
	Zn^{2+}	39.24	74.53	Kara et al., 2017
	Ni^{2+}	39.24	42.61	Kara et al., 2017
	Cd^{2+}	65.7	75.74	Cheng et al., 2012
	Co^{2+}	39.24	69.23	
	Mn^{2+}	39.24	72.34	
Metakaolin spheres	Cu^{2+}	53.95	52.63	
	Pb^{2+}	100.99	629.21	
Mn-CuO/Graphene bottom ash	Direct sky blue	18.45	0.497	
Modified metakaolin	Cu^{2+}	216	40	Singhal et al., 2017

if compared to the fit of Freundlich ($R^2 = 0.694$), Temkin ($R^2 = 0.866$) and Dubinin-Radushkevich ($R^2 = 0.555$) models (Alouani et al., 2018).

The addition and impregnation of magnetic agents, such as magnetite or zero-valent iron, was presented as a viable and innovative alternative to facilitate the separation of the adsorbent from the aqueous medium (Schadeck Netto et al., 2019; Hua et al., 2020); Rossatto et al. (2020) synthesized a magnetic geopolymer using silica, calcined kaolinite, sodium hydroxide, and magnetite to adsorb acid green 16 dye. The 53 $m^2\ g^{-1}$ surface area magnetic geopolymer presented a maximum adsorption capacity of 400 $mg\ g^{-1}$ of dye at 328 K, at pH 2.3, and an adsorbent dosage of 0.75 $g\ L^{-1}$, with best adsorption isotherms described by the BET model with values of R^2 from 0.96 to 298 K and 0.97 to 328 K (Rossatto et al., 2020).

El-eswed et al. (2012) studied the adsorption of Cu^{2+}, Ni^{2+}, Zn^{2+}, Cd^{2+}, and Pb^{2+} ions in kaolinite/zeolite-based-geopolymers; under pH 4, adsorbent dosage of 1 $g\ L^{-1}$, 298 K, and contact time of 24 h. It was concluded that the adsorption is preferred against small metal ions, such as Cu^{2+}, Ni^{2+}, Zn^{2+}, concerning the larger ones, such as Cd^{2+} and Pb^{2+}. The values of the maximum adsorption capacities found by the Langmuir model's application varied from 0.6 $mmol\ g^{-1}$ for Cu^{2+} to 0.1 $mmol\ g^{-1}$ of Cd^{2+}. Besides, in ionic competition systems, the adsorption of Cu^{2+} and Pb^{2+} in geopolymers did not decrease, indicating cooperative adsorption, which is very interesting from possible interferences in the adsorption of the targeted pollutants (El-eswed et al., 2012).

6. Modified materials and composites

This final section presents an overview of the most relevant topics on modified geological originated materials. This straightforward approach was chosen to illuminate future perspectives while still focusing on natural and raw forms of application. Nevertheless, there are many ways of modifying geological originated materials aspiring to increase in adsorption capacity compared to the raw mineral.

Although in several studies previously discussed, the q_{max} values reported were adequate for untreated materials, many other comparative studies have shown that modifications, such as metal impregnation, or treatments, such as thermal or acid-base activation, can critically enhance adsorption capacity (Bhattacharyya et al., 2015; Bhattacharyya and Gupta, 2008; Bhattacharyya and Sen Gupta, 2009; Carvalho et al., 2008; Kausar et al., 2018; Martín et al., 2019; Obayomi et al., 2020; Park et al., 2014; Sen Gupta and Bhattacharyya, 2014; Singhal et al., 2017; Suciu and Capri, 2009; Unuabonah et al., 2008a,b; Wu et al., 2011). Even simple pre-treatments can extract soluble organic compounds and enhance chelating efficiency (Gaballah et al., 1997). Modifications methods comprise various kinds of modifying agents: bases, such as sodium hydroxide, calcium hydroxide, and sodium carbonate; mineral and organic acid solutions, such as hydrochloric acid, nitric acid, sulfuric acid, tartaric acid, citric acid, and thioglycolic acid, organic compounds, such as ethylenediamine, formaldehyde, epichlorohydrin, and methanol, and even oxidizing agents, such as hydrogen peroxide (Wan Ngah and Hanafiah, 2008).

6.1. Metal ions

Aiming U(VI) adsorption, Li et al. (2014) prepared thermally activated sodium by calcinating micron Na-feldspar at 450 °C for 45 min, which resulted in a material with a larger specific surface area and larger porosity than the original. The prepared material presented maximum adsorption efficiency of 0.5 $mg\ L^{-1}$ of U^{6+}, the equivalent to 95.49%, at pH 5.0, 318 K, and contact time of 600 min. The relationship between q_{max} and equilibrium concentration, *Ce*, was well described by the Freundlich model (Li et al., 2014). Ahmad and Mirza (2017) synthesized a novel ecofriendly alginate/Au/mica bio nanocomposite with remarkable environmental remediation capacity of Pb^{2+} and Cu^{2+} in a single and binary system. The bionanocomposite adsorption experiments data best fit the Freundlich isotherm model for Pb^{2+}, whereas for Cu^{2+} Langmuir isotherm model was more suitable, both single and binary systems, with a maximum adsorption capacity of 224.97 and 169.817 $mg\ g^{-1}$, respectively. Adsorption process was found to be endothermic and spontaneous, thus, the nanocomposite can be applied successfully to industrial wastewaters.

Hematite and ilmenite modified composites have been studied and proposed by several authors (Chen et al., 2017; Kang et al., 2018; Lee et al., 2013a; Ma et al., 2018; Sengupta et al., 2017; Shu et al., 2019; Waanders et al., 2016; Wang et al., 2019a; Xu et al., 2017, 2018; Yousef, 2017). Sengupta et al. (2017) prepared a mesoporous composite consisting of hematite micro sheets modified and decorated with tetragonal zirconia nanocrystallites, useful for adsorbing cationic pollutants from water, by a simple hydrothermal method. It exhibited improved adsorption behavior of various metal ions, with about 99% removal efficiency reached for Cu^{2+}, Cd^{2+}, and Pb^{2+} at an initial concentration ranging from 5 to 20 $mg\ L^{-1}$, in comparison to unmodified zirconia and hematite. Wang et al., 2019b synthesized using ilmenite

and NaOH as starting materials a nanosized titanate composite by the solid-state route. After calcination at 900 °C, the final molecular formula of the composite was reached: $Na_{0.79–0.82}Fe_{0.96–0.98}Mg_{0.07–0.08}TiO_{3.85–3.88}$. The adsorption of Cu^{2+}, Cd^{2+}, and Pb^{2+} ions fit pseudo-second-order adsorption kinetics and the Langmuir adsorption model. At 20 °C, the maximum adsorption capacities of the as-synthesized nanocomposite for Cu^{2+}, Cd^{2+}, and Pb^{2+} were 13.8, 8.8, and 20.3 mg g^{-1}, respectively. The thermodynamic parameters also revealed that these ions' adsorption was spontaneous and endothermic (Wang et al., 2019b). Interestingly, on the contrary to hematite and ilmenite, magnetite is usually used to cover other adsorbents to increase their magnetization capacity and adsorption (Amaria et al., 2017; Chiou et al., 2017; Çiftçi et al., 2017; Malik et al., 2020; Tahergorabi et al., 2016; Talebzadeh et al., 2017). It has also been applied as the lead material for adsorption purposes, as by Mahdavian and Mirrahimi (2010). They proposed anchoring polyacrylic acid on superparamagnetic magnetite nanoparticles through surface modification for efficient separation of heavy metal cations from aqueous solutions. Four cations were studied: Cu^{2+}, Pb^{2+}, Ni^{2+}, and Cd^{2+}. For the prepared cation solutions at the constant thermal, time, and pH conditions, the maximum adsorption capacity was found to be for Pb^{2+} (40 ± 0.55 mg g^{-1}), and the minimum was for Cd^{2+} (7 ± 0.6 mg g^{-1}) (Mahdavian and Mirrahimi, 2010).

Adsorption of As(V) onto activated siderite was reported by Zhao and Guo (2014), with q_{max} values reaching 2.19 mg g^{-1} estimated from Langmuir isotherm at 25 °C (Zhao and Guo, 2014). Calcite modifications resulted in novel porous bentonite and calcite-biochar composite, used for lead adsorption, among other studies (Markovski et al., 2014b; Mohammadi and Sedighi, 2013; Ramola et al., 2020). Under optimized conditions, 0.07 g of the adsorbent composite effectively removed 97.06% of 232 mg L^{-1} after 3.5 h at pH of 5.5, and the maximum adsorption capacity reported was 500 mg g^{-1} (Ramola et al., 2020). Suzuki et al. (2004) investigated the construction of a uniform three-dimensional network porous structure of $CaZrO_3$/MgO composites, synthesized using reactive sintering of highly pure mixtures of natural dolomite ($CaMg(CO_3)_2$) and synthesized zirconia powders, with $LiF_{(aq)}$ additive. The pore-size distribution was set at around 1 μm, and the porosity was controllable (about 30% to 50%) through different sintering temperatures (Suzuki et al., 2004). Porosity is a critical factor, and Stefaniak et al. (2002) reported as well on the influence of preparation conditions on adsorption properties and porosity of dolomite-based sorbents. The thermal decomposition of carbonates has a dominant role in creating a new solid phase: as temperature increases over 800 °C, the porosity decreases (Stefaniak et al., 2002). This controlled tailoring form has been investigated towards phosphate adsorption on Al/dolomite/montmorillonite composite (Gao et al., 2013) and dolomite–alginate composite beads (Huang et al., 2019), towards Cr^{6+} onto thermally treated dolomite and Pb^{2+} onto chitosan-dolomite composite beads (Şenol and Şimşek, 2020).

Without a doubt, modified clays are the most explored geological materials, according to how much data on the subject has been published compared to previously presented minerals (Uddin, 2017). The modified forms of kaolinite provided excellent results in reported studies. The adsorption of Pb^{2+} onto tripolyphosphate-modified kaolinite clay (Unuabonah and Adebowale, 2009) and 25% (*w*/w) aluminum sulfate modified kaolinite clay (Jiang et al., 2009) were investigated. In the first study, the mechanism suggested that adsorption possibly took place at the negatively charged sites. Thus, the presence of Penta sodium tripolyphosphate adsorbed onto the kaolinite clay may contribute to enhancing the adsorption capacity of the proposed adsorbent (Unuabonah and Adebowale, 2009). In the second report, the maximum adsorption capacity of Pb^{2+} adsorption onto the modified kaolinite was 20 mg g^{-1}, about 4.5 times higher than the amount adsorbed onto unmodified kaolin, of 4.2 mg g^{-1}, under the optimized conditions (Jiang et al., 2009). Moreover, aiming to remove Pb^{2+}, Zn^{2+}, and Cd^{2+}, sodium polyphosphate (SPP) modified kaolinite clay was synthesized and evaluated, indicating that increase in temperature was the dominant parameter for increasing adsorption capacity (Amer et al., 2010). Nano-magnetite/kaolinite composite with kaolinite were produced and tested against Cu, Pb, Cd, Cr and Ni ions adsorption. The magnetic composite capacity increased over time and over increased pH (Lasheen et al., 2016).

Modified forms of montmorillonite clays have been studied and applied to the adsorption of Cu, Pb, Hg, Cd, Cs, Zn, Fe, Co, Ni, Sr, As, Cr, Fe, and even Pu (Abou-El-Sherbini and Hassanien, 2010; Begg et al., 2013; Bhattacharyya and Sen Gupta, 2009; Cruz-Guzmán et al., 2006; Goncharuk et al., 2010; Karamanis and Assimakopoulos, 2007; Liu et al., 2016a; Ma et al., 2015; Na et al., 2010; Oubagaranadin et al., 2010; Park et al., 2012; Sen Gupta and Bhattacharyya, 2009; Soltermann et al., 2013; Vinuth et al., 2015; Xu et al., 2008; Yu et al., 2008, 2009; Pereira et al., 2013). Organically modified montmorillonite clay was used to remove Cu^{2+}, $q_{max} = 62.5$ μg g^{-1} (Abou-El-Sherbini and Hassanien, 2010). Montmorillonites modified with natural organic cations were synthesized and tested for the adsorption of Pb^{2+} and Hg^{2+} by Cruz-Guzmán et al. (2006). Carbon modified aluminum-pillared montmorillonite has shown good uptake of Cd^{2+} from an aqueous system, $q_{max} = 161.75$ g g^{-1} (Yu et al., 2008). Al-13 pillared montmorillonites were also prepared with different Al to clay ratios to remove Cd^{2+} and PO_4^{3-} from aqueous solution (Ma et al., 2015). Aluminum-pillared-layered montmorillonites also proved their potential as a sorbent in removing Cu^{2+} and Cs^{+} from aqueous solutions (Karamanis and Assimakopoulos, 2007). Acid-activated montmorillonite-illite was examined for removing Cu^{2+} and Zn^{2+} from industrial wastewater containing Pb^{2+} at low concentration (Oubagaranadin et al., 2010). Calcined tetrabutylammonium bromide modified montmorillonite was prepared and used for the adsorption of Fe^{3+}, Co^{2+}, and Ni^{2+} from aqueous solution (Bhattacharyya and Sen Gupta, 2009).

The reports on montmorillonites modifications also include thermal (Aytas et al., 2009; Zuo et al., 2017), acid/base chemical treatment (Akpomie and Dawodu, 2016; Shawabkeh et al., 2007), polycyclic-aromatic hydrocarbon (Biswas et al., 2016), phosphate (Park et al., 2012), polyethyleneimine (Goncharuk et al., 2010), Ti-pillared (Na et al., 2010), chitosan-beads (Arvand and Pakseresht, 2013; Liu et al., 2015; Pereira et al., 2013), cyestein (El Adraa et al., 2017; Stathi et al., 2007), goethite (Olu-Owolabi et al., 2010), alkyl benzene sulfonate (Sandy Maramis et al., 2012), 3-aminopropyltrietoxisilane (Guerra et al., 2013) and 3,2-aminoethylamino-propyl-trimetoxisilane (Guerra et al., 2013), manganese oxide (Eren and Afsin, 2008), amine and carboxylate (Anirudhan et al., 2012), aluminum pillaring (Arfaoui et al., 2008), thermal-hydro-mechanical (Lee et al., 2013b), magnesium ferrite nanoparticles (Kaur et al., 2015) and humic acid (Wu et al., 2011).

Zeolites modifications can be separated into two larger groups: organic and inorganic treatments. For the first group, reports include hexadecyltrimethylammonium bromide-modified NaY zeolite for both cationic and oxyanionic metal ions (Chao and Chen, 2012), amine-modified zeolite for Pb and Cd ions adsorption (Wingenfelder et al., 2005), surfactant-modified natural zeolites for As^{5+} adsorption (Chutia et al., 2009), thiourea modified synthetic zeolite X and its adsorption of Cd^{2+} (Zhang et al., 2019a), cetylpyridinium bromide modified zeolite for Hg ion adsorption (Liu et al., 2016b), ethylenediamine and monoethanolamine modified synthesized β-zeolite for adsorption of Pb^{2+} (Motlagh Bahadory Esfahani and Faghihian, 2014), hexadecylpyridinium bromide modified zeolite for Cr^{6+} adsorption (Zeng et al., 2010), surfactant modified zeolite for the selective adsorption of Pb^{2+} and Cr^{6+} (Ren et al., 2016b) and Cu^{2+} (Zhan et al., 2013), dithizone-immobilized zeolite for Hg^{2+} adsorption (Mudasir et al., 2016), poly(methacrylic acid)/iron-oxide-coated zeolite for removal of Mn^{2+}, Fe^{2+} and As^{3+} (Pak et al., 2018), humic acid-immobilized surfactant-modified zeolite for the adsorption of Cu^{2+} (Lin et al., 2011), and polyacrylamide-zeolite composite modified by phytic acid for the adsorption of UO_2^{2+}, Tl^{+}, Pb^{2+}, Ra^{2+}, Bi^{3+} and Ac^{3+} (Şimşek and Ulusoy, 2004). The inorganic modifications comprehend mostly changes and procedures of coating, layering, or supporting metals on

zeolites, aiming to improve some specific adsorption sites towards contaminants removal (Alswat et al., 2016; Jiménez-Cedillo et al., 2011; Kazansky and Pidko, 2005; Luo et al., 2019; Medina-Ramirez et al., 2019; Onyango et al., 2003; Pahlavanzadeh and Motamedi, 2020; Qiu et al., 2018; Salam et al., 2020; Simsek et al., 2013; Venkata Ramana et al., 2013; Zhang et al., 2019f).

6.2. Organic molecules

6.2.1. Dyes

Yazdani et al. (2014) synthesized chitosan/feldspar bio-based beads and tested for the removal of Acid Black 1 dye from aquatic phases in 31 different batch experiments. The results showed uptake of 19.85 mg g^{-1} under the optimum conditions of pH 3, the temperature at 15 °C, initial dye concentration of 125 mg L^{-1}, and an adsorbent dosage of 2 g L^{-1}, which was very close to the predicted maximum adsorption amount by the statistical model of 21.63 mg g^{-1}. The mathematical modeling on the dyes' adsorption behavior illustrated that the process followed Langmuir isotherm, as well as pseudo-second-order kinetics. Langmuir's maximum sorption capacity was found to be 17.86 mg g^{-1}. The thermodynamic parameters were evaluated and revealed that the adsorption process was exothermic and favorable (Yazdani et al., 2014).

Saiphaneendra et al. (2017) used hematite and magnetite nanoparticles to functionalize reduced graphene oxide sheets via a facile one-step co-precipitation technique. It has been postulated that both minerals' co-existence on the graphene sheet causes synergistic effects to enhance adsorption. For comparison purposes, the authors studied the adsorption behavior of pure graphene oxide, reduced graphene oxide, reduced graphene oxide/hematite composite (surface area = 230 m^2 g^{-1}), reduced graphene oxide/magnetite composite (surface area = 231 m^2 g^{-1}), and reduced graphene oxide/magnetite/hematite composite (surface area = 216 m^2 g^{-1}) against methylene blue adsorption. The adsorption kinetics was well described by the pseudo-second-order model, and Langmuir adsorption isotherm for the equilibrium adsorption behavior of rGO-Fe_2O_3-Fe_3O_4. The maximum adsorption capacity was determined to be 72.8 ± 2.7 mg g^{-1} (Saiphaneendra et al., 2017). Kang et al. (2018) provided a novel approach to "waste eliminates waste" by employing ilmenite's acid leachate as the precursor in its structure tailoring. They reported that the final product's morphology and structure could be controlled, originating from nanoparticles, microcubes, rhombohedrons to the microsphere, by merely varying synthetic parameters. Due to its large surface area (152.3 m^2 g^{-1}) and large functional groups, Fe_2O_3 microspheres efficiently removed organic dyes from aqueous solutions. The maximum adsorption capacities obtained by Sips model (R^2 = 0.9820) fit were 723.8, 150.7, and 54.5 mg g^{-1} for Congo red, Methyl orange, and Methylene blue, respectively, with 0.3 g L^{-1} of adsorbent, at pH of 7.2 ± 0.1 and at 25 °C (Kang et al., 2018).

Thermally treated, modified, and calcined dolomites have been used for dye adsorption. In 2010, Dolomite was thermally treated at 1000 °C, going from a surface area of 1.82 to 11.36 m^2 g^{-1}. The batch adsorption experiments were performed at 25 °C, 0.06 g L^{-1} of adsorbent, and aqueous orange I solution in a concentration range of 20–200 mg L^{-1}. The synthesized material's final uptake was 25 mg g^{-1} (Boucif et al., 2010). In 2018, the adsorption of reactive black 5 and congo red by dolomite treated at 900 °C was investigated in single and binary solutions. At equilibrium, congo red was more strongly coadsorbed than reactive black 5, with maximum adsorption capacities of 229.18 and 72.37 mg g^{-1} at 40 °C, respectively (Ziane et al., 2018). At last, in 2019, low-cost porous calcined dolomite microspheres were prepared by simple spray drying and subsequent calcination. The material was tested against methylene blue removal in the conditions of 20 g L^{-1} of adsorbent and 100 mg L^{-1} of dye. The adsorption kinetics followed the pseudo-second-order, while the isotherm data fit the Langmuir model. In this context, the microspheres' removal efficiency reached 95.6% (Yan et al., 2019).

Mahmoodi and Saffar-Dastgerdi (2019) prepared sodalite zeolite nanoparticles, subsequently modified by different amounts of 3-aminopropyl-triethoxy-silane, resulting in products with 2.3 wt.%, 4.4 wt.%, and 6.5 wt.% of the organic modifier, named 0.5, 1, and 1.5 zeolites, respectively. The surface-modified products were used for adsorption of Direct Red 23 and Direct Red 80 from simulated wastewater. After initial tests, 0.5 zeolite was elected as the best, and it was tested furtherly. Equilibrium data followed Langmuir isotherm and pseudo-second-order kinetic. The adsorption capacity of the 0.5 composite reached expressive 2415 and 4842 mg g^{-1} for Direct Red 80 and Direct Red 23, respectively. Thermodynamics was studied and measured Gibbs free energies at 298, 313, 323, and 333 K were − 12.53, −14.68, −16.12, and − 17.55 kJ mol^{-1} for Direct Red 23, and − 9.27, −11.73, −13.37, and − 15.01 kJ mol^{-1} for Direct Red 80, respectively. The adsorption process was physisorption, exothermic, and spontaneous (Mahmoodi and Saffar-Dastgerdi, 2019).

6.2.2. Pharmaceuticals

Martín et al. (2019) modified natural montmorillonite and a synthetic mica with cationic octadecyl-amine by a cation-exchange reaction and explored its potential use adsorbent for ibuprofen removal. The adsorption equilibrium isotherm was fitted with the Langmuir and Freundlich mathematical models (R^2 > 0.999). The adsorption rate of C_{18}-montmorillonite (removal efficiency = 99.9%) was not dependent on ibuprofen concentration (0.1–80 mg L^{-1}), but C_{18}-mica behaved contrarily (from 99.9% at 0.1 mg L^{-1} to 67% at 80 mg L^{-1}). Variations in pH ranging from 4 to 9, did not affect the process. Pseudo-second-order kinetic model best described the adsorption of ibuprofen (R^2 > 0.993), reaching equilibrium, with outstanding efficiency up to 100%, in less than 5 and 60 min for C18-montmorillonite and C_{18}-mica, respectively (Martín et al., 2019).

Azizi (2020) studied a green preparation method of iron oxide/cellulose nanocomposite, used to remove metronidazole, an antibiotic, from aquatic solutions in the form of an aqueous extract of spent tea waste, regarding its effective and magnetic separation capability. The prepared nanocomposite had spherical particles with an average size of 15.5 nm. At pH 5, the metronidazole concentration of 10 mg L^{-1}, the adsorbent dosage of 25 mg L^{-1}, and contact time of 30 min, the pollutant's removal efficiency was 97.04%. Langmuir isotherm determined the maximum adsorption capacity of 332 mg g^{-1}, pseudo-first-order kinetic constant rate of 1.15 L min^{-1}, with the determination coefficient of 0.97 (Azizi, 2020).

The adsorption and advanced oxidation of diverse pharmaceuticals and personal care products from the water were studied by Masud et al. (2020). Interestingly, they started assuming that their model pollutants are found as a complex mixture in wastewater and the environment and used reduced graphene oxide as a support for nanozerovalent iron against a complex mixture of 12 diverse personal care products (including antibiotic, anti-inflammatory, anti-seizure, and antidepressant pharmaceuticals). This approach is exciting for most studies on removing personal care products results with only one pollutant at a time, typically at high initial concentrations, not environmentally relevant. Considering starting concentration of 200 μg L^{-1}, an adsorbent dosage of 533 mg L^{-1}, pH 3, and after a contact time of 30 min, final removal efficiencies for venlafaxine, citalopram, paroxetine, fluoxetine, diclofenac, ibuprofen, naproxen, acetaminophen, carbamazepine, lamotrigine, sulfamethoxazole, and caffeine reached 88.5%, 98.92%, 99.58%, 98.71%, 97.92%, 88.55%, 99.25%, 82.97%, 85.75%, 95.23%, 74.13% and 93.12%, respectively (Masud et al., 2020).

De Oliveira et al. (2020) investigated micro and mesoporous silica prepared with coal fly ash as starting material and used as an adsorbent to remove parabens. The composite prepared at pH 7 presented higher adsorption capacity, with a surface area of 396 m^2 g^{-1}. Adsorption kinetics were carried out in a batch system with a 40 mL multicomponent

paraben solution at 5 mg L^{-1}, 2 mg adsorbent mass, pH 3, agitation at 300 rpm for 30 min at room temperature (28 ± 2 °C). The same conditions were used in equilibrium tests, but the multicomponent parabens concentrations varied from 1 to 20 mg L^{-1}. The adsorption capacity was determined as 0.01, 0.07, 0.54, and 1.31 mg g^{-1} for methylparaben, ethylparaben, propylparaben, and butylparaben, respectively, by fitting the data obtained to Freundlich isotherm ($R^2 > 0.999$) (De Oliveira et al., 2020).

Differently than the previous minerals, modified clays have been prepared by several different research groups and applied for the adsorption of many pharmaceuticals, such as amoxicillin (Pierucci et al., 2017), atenolol (Seema, 2013), carbamazepine (Dordio et al., 2009; Styszko et al., 2015), chloramphenicol (Lawal and Moodley, 2018), cinnamic acid (Calabrese et al., 2017), ciprofloxacin (Hamilton et al., 2014), diclofenac (Pierucci et al., 2017; Styszko et al., 2015), furosemide (Machado et al., 2017), gemfibrozil (Dordio et al., 2017), ibuprofen (Dordio et al., 2009; Styszko et al., 2015), ketoprofen (Styszko et al., 2015), mefanamic acid (Dordio et al., 2017), metronidazole (Calabrese et al., 2013; Kalhori et al., 2017), nalidixic acid (Lawal and Moodley, 2018), naproxen (Dordio et al., 2017), ofloxacin (Wang et al., 2014), oxytetracycline (Figueroa et al., 2004), promethazine (Gereli et al., 2006; Seki and Yurdakoç, 2009), propranolol (Pierucci et al., 2017), sulfamethoxazole (Lawal and Moodley, 2018), tetracycline (Figueroa et al., 2004; Lawal and Moodley, 2018; Liu et al., 2011), trimethoprim (Bekçi et al., 2006) and venlafaxine (Silva et al., 2018).

7. Conclusion

After exploring the literature, it was stated that unmodified and modified geological materials have yet been poorly explored as adsorbents. The studies performed report generally high adsorption ability against inorganic and organic pollutants, associated with low-cost in retrieving, recycling, and applying these materials for environmental remediation purposes. In general, all minerals presented interesting q_{max} values for metal ions adsorption, while clay composites presented themselves as a more suitable choice for removing dyes and other organic pollutants. Besides, geopolymers rise in the "from waste to waste" approach, re-destining environmental liabilities, such as fly ash, by using polymerization reactions between minerals containing aluminum and silicon and an activating agent. Overall, the geological originated materials represent promising candidates for removing metal ions, antibiotics, phenolic compounds, dyes, pesticides, and herbicides in their modified and unmodified versions, from various industrial wastewater types and aquatic environments.

Declaration of competing interest

The authors declare that they have no known competing financial interests or personal relationships that could have appeared to influence the work reported in this paper.

Acknowledgments

The authors thank the funding agencies CAPES, CNPq, and FAPERGS for financial support.

References

Abidi, N., Duplay, J., Jada, A., Baltenweck, R., Errais, E., Semhi, K., Trabelsi-Ayadi, M., 2017. Toward the understanding of the treatment of textile industries' effluents by clay: adsorption of anionic dye on kaolinite. Arab. J. Geosci. 10, 373. https://doi.org/10.1007/s12517-017-3161-3.

Abou-El-Sherbini, K.S., Hassanien, M.M., 2010. Study of organically-modified montmorillonite clay for the removal of copper (II). J. Hazard. Mater. 184, 654–661. https://doi.org/10.1016/j.jhazmat.2010.08.088.

Acisli, O., Acar, I., Khataee, A., 2020. Preparation of a fly ash-based geopolymer for removal of a cationic dye: Isothermal, kinetic and thermodynamic studies. J. Ind. Eng. Chem. 83, 53–63. https://doi.org/10.1016/j.jiec.2019.11.012.

Agersø, Y., Wulff, G., Vaclavik, E., Halling-Sørensen, B., Jensen, L.B., 2006. Effect of tetracycline residues in pig manure slurry on tetracycline-resistant bacteria and resistance gene tet(M) in soil microcosms. Environ. Int. 32, 876–882. https://doi.org/10.1016/j.envint.2006.05.008.

Ahmad, R., Mirza, A., 2017. Adsorption of Pb(II) and Cu(II) by Alginate-Au-Mica bionanocomposite: Kinetic, isotherm and thermodynamic studies. Process Saf. Environ. Prot. 109, 1–10. https://doi.org/10.1016/j.psep.2017.03.020.

Akgül, M., Karabakan, A., Acar, O., Yürüm, Y., 2006. Removal of silver (I) from aqueous solutions with clinoptilolite. Microporous Mesoporous Mat. 94, 99–104. https://doi.org/10.1016/j.micromeso.2006.02.023.

Akpomie, K.G., Dawodu, F.A., 2016. Acid-modified montmorillonite for sorption of heavy metals from automobile effluent. Beni-Suef Univ. J. Basic Appl. Sci. 5, 1–12. https://doi.org/10.1016/j.bjbas.2016.01.003.

Al Kuisi, M., 2002. Adsorption of dimethoate and 2,4-D on Jordan Valley soils and their environmental impacts. Environ. Geol. 42, 666–671. https://doi.org/10.1007/s00254-002-0575-2.

Al-Anber, M.A., 2015. Adsorption of ferric ions onto natural feldspar: kinetic modeling and adsorption isotherm. Int. J. Environ. Sci. Technol. 12, 139–150. https://doi.org/10.1007/s13762-013-0410-1.

Albadarin, A.B., Mangwandi, C., Al-Muhtaseb, A.H., Walker, G.M., Allen, S.J., Ahmad, M.N.M., 2012. Kinetic and thermodynamics of chromium ions adsorption onto low-cost dolomite adsorbent. Chem. Eng. J. 179, 193–202. https://doi.org/10.1016/j.cej.2011.10.080.

Alexandre-Franco, M., Albarrán-Liso, A., Gómez-Serrano, V., 2011. An identification study of vermiculites and micas: Adsorption of metal ions in aqueous solution. Fuel Process. Technol. 92 (2), 200–205. https://doi.org/10.1016/j.fuproc.2010.03.005.

Alom, S., Amin, N.U., Bangash, F.K., Ali, M., 2014. Removal of basic red 5 on calcined kaolinite - Characterization and adsorption kinetics. Tenside Surfactants Deterg. 51, 59–71. https://doi.org/10.3139/113.110287.

Alouani, M.E.L., Alehyn, S., Achouri, M.E.L., Taibi, M., 2018. Removal of cationic dye – methylene blue- from aqueous solution by adsorption on fly ash-based geopolymer. J. Mater. Environ. Sci. 9, 32–46. https://doi.org/10.26872/jmes.2018.9.1.5.

Al-Shalabi, E.W., Sepehrnoori, K., 2016. A comprehensive review of low salinity/engineered water injections and their applications in sandstone and carbonate rocks. J. Pet. Sci. Eng. 139, 137–161. https://doi.org/10.1016/j.petrol.2015.11.027.

Alswat, A.A., Ahmad, M. Bin, Saleh, T.A., 2016. Zeolite modified with copper oxide and iron oxide for lead and arsenic adsorption from aqueous solutions. Journal of Water Supply: Research and Technology-AQUA 65, 465–479. https://doi.org/10.2166/aqua.2016.014.

Álvarez-Ayuso, E., García-Sánchez, A., 2003. Removal of heavy metals from waste waters by vermiculites. Environ. Technol. (United Kingdom) 24, 615–625. https://doi.org/10.1080/09593330309385596.

Alvarez-Ayuso, E., Garćia-Śanchez, A., 2003. Removal of heavy metals from waste waters by natural and Na-exchanged bentonites. Clay Clay Min. 51, 475–480. https://doi.org/10.1346/CCMN.2003.0510501.

Álvarez-Ayuso, E., García-Sánchez, A., Querol, X., 2003. Purification of metal electroplating waste waters using zeolites. Water Res. 37, 4855–4862. https://doi.org/10.1016/j.watres.2003.08.009.

Al-Zboon, K., Al-Harahsheh, M.S., Hani, F.B., 2011. Fly ash-based geopolymer for Pb removal from aqueous solution. J. Hazard. Mater. 188, 414–421. https://doi.org/10.1016/j.jhazmat.2011.01.133.

Amaria, A., Nuryono, N., Suyanta, S., 2017. Preparation of L-arginine-modified silica-coated magnetite nanoparticles for Au(III) adsorption. Oriental Journal of Chemistry 33, 384–395. https://doi.org/10.13005/ojc/330146.

Amer, M.W., Khalili, F.I., Awwad, A.M., 2010. Adsorption of lead, zinc and cadmium ions on polyphosphate-modified kaolinite clay. J. Environ. Chem. Ecotoxicol. 2, 001–008. https://doi.org/10.5897/JECE.9000005.

Ammann, L., Bergaya, F., Lagaly, G., 2005. Determination of the cation exchange capacity of clays with copper complexes revisited. Clay Miner. 40, 441–453. https://doi.org/10.1180/0009855054040182.

Andini, S., Cioffi, R., Montagnaro, F., Pisciotta, F., Santoro, L., 2006. Simultaneous adsorption of chlorophenol and heavy metal ions on organophilic bentonite. Appl. Clay Sci. 31, 126–133. https://doi.org/10.1016/j.clay.2005.09.004.

Angove, M.J., Johnson, B.B., Wells, J.D., 1998. The influence of temperature on the adsorption of cadmium(II) and cobalt(II) on kaolinite. J. Colloid Interface Sci. 204, 93–103. https://doi.org/10.1006/jcis.1998.5549.

Anirudhan, T.S., Jalajamony, S., Sreekumari, S.S., 2012. Adsorption of heavy metal ions from aqueous solutions by amine and carboxylate functionalised bentonites. Appl. Clay Sci. 65–66, 67–71. https://doi.org/10.1016/j.clay.2012.06.005.

Arfaoui, S., Frini-Srasra, N., Srasra, E., 2008. Modelling of the adsorption of the chromium ion by modified clays. Desalination 222, 474–481. https://doi.org/10.1016/j.desal.2007.03.014.

Arvand, M., Pakseresht, M.A., 2013. Cadmium adsorption on modified chitosan-coated bentonite: batch experimental studies. J. Chem. Technol. Biotechnol. 88, 572–578. https://doi.org/10.1002/jctb.3863.

Asfaram, A., Fathi, M.R., Khodadoust, S., Naraki, M., 2014. Removal of Direct Red 12B by garlic peel as a cheap adsorbent: Kinetics, thermodynamic and equilibrium isotherms study of removal. Spectrochim. Acta - Part A Mol. Biomol. Spectrosc. 127, 415–421. https://doi.org/10.1016/j.saa.2014.02.092.

Atiş, C.D., Görür, E.B., Karahan, O., Bilim, C., Ilkentapar, S., Luga, E., 2015. Very high strength (120 MPa) class F fly ash geopolymer mortar activated at different NaOH amount,

heat curing temperature and heat curing duration. Constr. Build. Mater. 96, 673–678. https://doi.org/10.1016/j.conbuildmat.2015.08.089.

Atun, G., Tunçay, M., Hisarli, G., Talman, R.Y., Hoşgörmez, H., 2009. Adsorption equilibria between dye and surfactant in single and binary systems onto geological materials. Appl. Clay Sci. 45, 254–261. https://doi.org/10.1016/j.clay.2009.06.003.

Ayoub, G.M., Mehawej, M., 2007. Adsorption of arsenate on untreated dolomite powder. J. Hazard. Mater. 148, 259–266. https://doi.org/10.1016/j.jhazmat.2007.02.011.

Aytas, S., Yurtlu, M., Donat, R., 2009. Adsorption characteristic of U(VI) ion onto thermally activated bentonite. J. Hazard. Mater. 172, 667–674. https://doi.org/10.1016/j.jhazmat.2009.07.049.

Azizi, A., 2020. Green Synthesized Fe_3O_4/Cellulose Nanocomposite Suitable Adsorbent for Metronidazole Removal. Polymer Science, Series B https://doi.org/10.1134/S1560090420050012.

Bache, C.A., Lisk, D.J., Wagner, D.G., Warner, R.G., 1964. Elimination of 2-methyl-4-chlorophenoxyacetic acid and 4-(2-methyl-4-chlorophenoxybutyric) acid in the urine from cows. J. Dairy Sci. 47, 93–95. https://doi.org/10.3168/jds.S0022-0302(64)88590-8.

Bagci, C., Kutyla, G.P., Waltraud, M., 2017. Fully reacted high strength geopolymer made with diatomite as a fumed silica alternative. Ceram. Int. 43, 14784–14790. https://doi.org/10.1016/j.ceramint.2017.07.222.

Baker, P.A., Kastner, M., 1981. Constraints on the formation of sedimentary dolomite. Science. 213, 214–216. https://doi.org/10.1126/science.213.4504.214.

Baker, H.M., Massadeh, A.M., Younes, H.A., 2009. Natural Jordanian zeolite: Removal of heavy metal ions from water samples using column and batch methods. Environ. Monit. Assess. 157, 319–330. https://doi.org/10.1007/s10661-008-0537-6.

Banning, E.B., 2020. Soils, Sediments, and Geoarchaeology. Springer, Cham, pp. 293–308 https://doi.org/10.1007/978-3-030-47992-3_17.

Barbosa, T.R., Foletto, E.L., Dotto, G.L., Jahn, S.L., 2018. Preparation of mesoporous geopolymer using metakaolin and rice husk ash as synthesis precursors and its use as potential adsorbent to remove organic dye from aqueous solutions. Ceram. Int. 44, 416–423. https://doi.org/10.1016/j.ceramint.2017.09.193.

Batista, L.C.D., De, S., Dantas, D., De Farias, R.F., 2014. Dye adsorption on inorganic matrices as a new strategy to gas capture: Hydrogen sulfide adsorption on rodhamine B modified kaolinite. Synth. React. Inorganic, Met. Nano-Metal Chem. 44, 1398–1400. https://doi.org/10.1080/15533174.2013.802344.

Beattie, J.A., 1956. The principles of chemical equilibrium, with applications in chemistry and chemical engineering. J. Am. Chem. Soc. 78, 2916. https://doi.org/10.1021/ja01593a082.

Begg, J.D., Zavarin, M., Zhao, P., Tumey, S.J., Powell, B., Kersting, A.B., 2013. Pu(V) and Pu(IV) sorption to montmorillonite. Environ. Sci. Technol. 47, 5146–5153. https://doi.org/10.1021/es305257s.

Bekçi, Z., Seki, Y., Yurdakoç, M.K., 2006. Equilibrium studies for trimethoprim adsorption on montmorillonite KSF. J. Hazard. Mater. 133, 233–242. https://doi.org/10.1016/j.jhazmat.2005.10.029.

Benhouria, A., Islam, M.A., Zaghouane-Boudiaf, H., Boutahala, M., Hameed, B.H., 2015. Calcium alginate-bentonite-activated carbon composite beads as highly effective adsorbent for methylene blue. Chem. Eng. J. 270, 621–630. https://doi.org/10.1016/j.cej.2015.02.030.

Berizi, Z., Hashemi, S.Y., Hadi, M., Azari, A., Mahvi, A.H., 2016. The study of non-linear kinetics and adsorption isotherm models for Acid Red 18 from aqueous solutions by magnetite nanoparticles and magnetite nanoparticles modified by sodium alginate. Water Sci. Technol. 74 (5), 1235–1242. https://doi.org/10.2166/wst.2016.320.

Bertagnolli, C., Kleinübing, S.J., da Silva, M.G.C., 2011. Preparation and characterization of a Brazilian bentonite clay for removal of copper in porous beds. Appl. Clay Sci. 53, 73–79. https://doi.org/10.1016/j.clay.2011.05.002.

Bettencourt, L.M.A., Lobo, J., Helbing, D., Kühnert, C., West, G.B., 2007. Growth, innovation, scaling, and the pace of life in cities. Proc. Natl. Acad. Sci. U. S. A. 104, 7301–7306. https://doi.org/10.1073/pnas.0610172104.

Bhardwaj, D., Sharma, P., Sharma, M., Tomar, R., 2014. Surfactant modified tectosilicates and phyllosilicates for 2,4-D removal and slow release formulation. RSC Adv. 4, 4504–4514. https://doi.org/10.1039/c3ra44121k.

Bhattacharyya, K.G., Gupta, S. Sen, 2007a. Influence of acid activation of kaolinite and montmorillonite on adsorptive removal of Cd(II) from water. Industrial and Engineering Chemistry Research 46, 3734–3742. https://doi.org/10.1021/ie061475n.

Bhattacharyya, K.G., Gupta, S. Sen, 2007b. Adsorption of Co(II) from Aqueous Medium on Natural and Acid Activated Kaolinite and Montmorillonite. Separation Science and Technology 42, 3391–3418. https://doi.org/10.1080/01496390701515136.

Bhattacharyya, K.G., Gupta, S. Sen, 2008. Adsorption of a few heavy metals on natural and modified kaolinite and montmorillonite: a review. Adv. Colloid Interface Sci. 140 (2), 114–131. https://doi.org/10.1016/j.cis.2007.12.008.

Bhattacharyya, K.G., Gupta, S.S., 2011. Removal of Cu(II) by natural and acid-activated clays: An insight of adsorption isotherm, kinetic and thermodynamics. Desalination 272 (1–3), 66–75. https://doi.org/10.1016/j.desal.2011.01.001.

Bhattacharyya, K.G., Gupta, S. Sen, Sarma, G.K., 2015. Kinetics, equilibrium isotherms and thermodynamics of adsorption of Congo red onto natural and acid-treated kaolinite and montmorillonite. Desalin. Water Treat. 53, 530–542. https://doi.org/10.1080/19443994.2013.839405.

Bhattacharyya, K.G., Sen Gupta, S., 2009. Calcined tetrabutylammonium kaolinite and montmorillonite and adsorption of Fe(II), Co(II) and Ni(II) from solution. Appl. Clay Sci. 46, 216–221. https://doi.org/10.1016/j.clay.2009.08.006.

Biswas, B., Sarkar, B., Mandal, A., Naidu, R., 2016. Specific adsorption of cadmium on surface-engineered biocompatible organoclay under metal-phenanthrene mixed-contamination. Water Res. 104, 119–127. https://doi.org/10.1016/j.watres.2016.08.009.

Boczkaj, G., Fernandes, A., 2017. Wastewater treatment by means of advanced oxidation processes at basic pH conditions: a review. Chem. Eng. J. 320, 608–633. https://doi.org/10.1016/j.cej.2017.03.084.

Boucif, F., Marouf-Khelifa, K., Batonneau-Gener, I., Schott, J., Khelifa, A., 2010. Preparation, characterisation of thermally treated Algerian dolomite powders and application to azo-dye adsorption. Powder Technol. 201, 277–282. https://doi.org/10.1016/j.powtec.2010.04.013.

Boyjoo, Y., Pareek, V.K., Liu, J., 2014. Synthesis of micro and nano-sized calcium carbonate particles and their applications. J. Mater. Chem. A https://doi.org/10.1039/c4ta02070g.

Branlund, J.M., Hofmeister, A.M., 2012. Heat transfer in plagioclase feldspars. Am. Mineral. 97, 1145–1154. https://doi.org/10.2138/am.2012.3986.

Brantley, S.L., Mellott, N.P., 2000. Surface area and porosity of primary silicate minerals. Am. Mineral. 85, 1767–1783. https://doi.org/10.2138/am-2000-11-1220.

Breeuwsma, A., Lyklema, J., 1973. Physical and chemical adsorption of ions in the electrical double layer on hematite (α-Fe_2O_3). J. Colloid Interface Sci. 43, 437–448. https://doi.org/10.1016/0021-9797(73)90389-5.

Brigatti, M.F., Galan, E., Theng, B.K.G., 2006. Chapter 2 Structures and Mineralogy of Clay Minerals. Dev. Clay Sci. 1, 19–86. https://doi.org/10.1016/S1572-4352(05)01002-0.

Bundschuh, J., Bhattacharya, P., Sracek, O., Mellano, M.F., Ramírez, A.E., Storniolo, A., del Martín, R.A., Cortés, J., Litter, M.I., Jean, J.-S., 2011. Arsenic removal from groundwater of the Chaco-Pampean Plain (Argentina) using natural geological materials as adsorbents. J. Environ. Sci. Heal. Part A 46, 1297–1310. https://doi.org/10.1080/10934529.2011.598838.

Burakov, A.E., Galunin, E.V., Burakova, I.V., Kucherova, A.E., Agarwal, S., Tkachev, A.G., Gupta, V.K., 2018. Adsorption of heavy metals on conventional and nanostructured materials for wastewater treatment purposes: a review. Ecotox. Environ. Safe. 148, 702–712. https://doi.org/10.1016/j.ecoenv.2017.11.034.

Cabrera, A., Trigo, C., Cox, L., Celis, R., Cornejo, J., 2008. A comparative study of the use of organoclay-based formulations and organic amendment to reduce the leaching of the herbicide MCPA in soil. Clean-Soil Air Water 36, 990–995. https://doi.org/10.1002/clen.200800159.

Cai, S., Li, Q., Liu, C., Liu, X., 2020. The adsorption of hydrogen sulfide in calcite pores: a molecular simulation study. J. Mol. Liq. 299, 112253. https://doi.org/10.1016/j.molliq.2019.112253.

Calabrese, I., Cavallaro, G., Scialabba, C., Licciardi, M., Merli, M., Sciascia, L., Turco Liveri, M.L., 2013. Montmorillonite nanodevices for the colon metronidazole delivery. Int. J. Pharm. 457, 224–236. https://doi.org/10.1016/j.ijpharm.2013.09.017.

Calabrese, I., Gelardi, G., Merli, M., Liveri, M.L.T., Sciascia, L., 2017. Clay-biosurfactant materials as functional drug delivery systems: slowing down effect in the in vitro release of cinnamic acid. Appl. Clay Sci. 135, 567–574. https://doi.org/10.1016/j.clay.2016.10.039.

Cao, C.Y., Zhang, T., Cong, Q., 2017. Adsorption of acid fuchsin onto the chitosan–montmorillonite composite. Mar. Geores. Geotechnol. 35, 799–805. https://doi.org/10.1080/1064119X.2016.1240277.

Carter, D.L., Mortland, M.M., Kemper, W.D., 2018. Specific Surface. John Wiley & Sons, Ltd, pp. 413–423 https://doi.org/10.2136/sssabookser5.1.2ed.c16.

Carvalho, W.A., Vignado, C., Fontana, J., 2008. Ni(II) removal from aqueous effluents by silylated clays. J. Hazard. Mater. 153, 1240–1247. https://doi.org/10.1016/j.jhazmat.2007.09.083.

Castellini, E., Andreoli, R., Malavasi, G., Pedone, A., 2008. Deflocculant effects on the surface properties of kaolinite investigated through malachite green adsorption. Colloids and Surfaces A: Physicochemical and Engineering Aspects 329, 31–37. https://doi.org/10.1016/j.colsurfa.2008.06.045.

Castillo Alvarez, C., Quitté, G., Schott, J., Oelkers, E.H., 2020. Experimental determination of Ni isotope fractionation during Ni adsorption from an aqueous fluid onto calcite surfaces. Geochim. Cosmochim. Acta 273, 26–36. https://doi.org/10.1016/j.gca.2020.01.010.

Chang, P.H., Jiang, W.T., Sarkar, B., Wang, W., Li, Z., 2019. The triple mechanisms of atenolol adsorption on Ca-montmorillonite: implication in pharmaceutical wastewater treatment. Materials (Basel) 12, 2858. https://doi.org/10.3390/ma12182858.

Chang, P.H., Li, Z., Jean, J.S., Jiang, W.T., Wang, C.J., Lin, K.H., 2012. Adsorption of tetracycline on 2:1 layered non-swelling clay mineral illite. Appl. Clay Sci. 67–68, 158–163. https://doi.org/10.1016/j.clay.2011.11.004.

Chang, P.H., Li, Z., Jiang, W.T., Kuo, C.Y., Jean, J.S., 2015. Adsorption of tetracycline on montmorillonite: influence of solution pH, temperature, and ionic strength. Desalin. Water Treat. 55, 1380–1392. https://doi.org/10.1080/19443994.2014.924881.

Chantawong, V., Harvey, N.W., Bashkin, V.N., 2003. Comparison of heavy metal adsorptions by Thai kaolin and ballclay. Water Air Soil Pollut. 148, 111–125. https://doi.org/10.1023/A:1025401927023.

Chao, H.P., Chen, S.H., 2012. Adsorption characteristics of both cationic and oxyanionic metal ions on hexadecyltrimethylammonium bromide-modified NaY zeolite. Chem. Eng. J. 193–194, 283–289. https://doi.org/10.1016/j.cej.2012.04.059.

Chapman, H.D., 2016. Cation-Exchange Capacity. John Wiley & Sons, Ltd, pp. 891–901.

Chen, X., Guo, Y., Ding, S., Zhang, H., Xia, F., Wang, J., Zhou, M., 2019. Utilization of red mud in geopolymer-based pervious concrete with function of adsorption of heavy metal ions. J. Clean Prod. 207, 789–800. https://doi.org/10.1016/j.jclepro.2018.09.263.

Chen, H., He, X., Rong, X., Chen, W., Cai, P., Liang, W., Li, S., Huang, Q., 2009. Adsorption and biodegradation of carbaryl on montmorillonite, kaolinite and goethite. Appl. Clay Sci. 46, 102–108. https://doi.org/10.1016/j.clay.2009.07.006.

Chen, Z.X., Jin, X.Y., Chen, Z., Megharaj, M., Naidu, R., 2011a. Removal of methyl orange from aqueous solution using bentonite-supported nanoscale zero-valent iron. J. Colloid Interface Sci. 363, 601–607. https://doi.org/10.1016/j.jcis.2011.07.057.

Chen, Y., Xiang, Z., Wang, D., Kang, J., Qi, H., 2020. Effective photocatalytic degradation and physical adsorption of methylene blue using cellulose/GO/TiO_2 hydrogels. RSC Adv. 10, 23936–23943. https://doi.org/10.1039/d0ra04509h.

Chen, Y.G., Ye, W.M., Yang, X.M., Deng, F.Y., He, Y., 2011b. Effect of contact time, pH, and ionic strength on Cd(II) adsorption from aqueous solution onto bentonite from Gaomiaozi. China. Environ. Earth Sci. 64, 329–336. https://doi.org/10.1007/s12665-010-0850-6.

Chen, P., Zhai, J., Sun, W., Hu, Y., Yin, Z., Lai, X., 2017. Adsorption mechanism of lead ions at ilmenite/water interface and its influence on ilmenite flotability. J. Ind. Eng. Chem. 53, 285–293. https://doi.org/10.1016/j.jiec.2017.04.037.

Cheng, T.W., Lee, M.L., Ko, M.S., Ueng, T.H., Yang, S.F., 2012a. The heavy metal adsorption characteristics on metakaolin-based geopolymer. Appl. Clay Sci. 56, 90–96. https://doi.org/10.1016/j.clay.2011.11.027.

Cheng, J.P., Ma, R., Li, M., Wu, J.S., Liu, F., Zhang, X.B., 2012b. Anatase nanocrystals coating on silica-coated magnetite: Role of polyacrylic acid treatment and its photocatalytic properties. Chem. Eng. J. 210, 80–86. https://doi.org/10.1016/J.CEJ.2012.08.059.

Chiou, C.S., Hong, G.B., Chen, H.W., 2017. Adsorption behavior of recyclable magnetites with N-components for adsorption of copper ion. J. Nanosci. Nanotechnol. 18, 2241–2248. https://doi.org/10.1166/jnn.2018.14266.

Chu, Y., Khan, M.A., Xia, M., Lei, W., Wang, F., Zhu, S., 2019. Synthesis and mechanism of adsorption capacity of modified montmorillonite with amino acids for 4-acetaminophenol removal from wastewaters. J. Chem. Eng. Data 64, 5900–5909. https://doi.org/10.1021/acs.jced.9b00795.

Chutia, P., Kato, S., Kojima, T., Satokawa, S., 2009. Adsorption of as(V) on surfactant-modified natural zeolites. J. Hazard. Mater. 162, 204–211. https://doi.org/10.1016/j.jhazmat.2008.05.024.

Çiftçi, H., Ersoy, B., Evcin, A., 2017. Synthesis, characterization and Cr(VI) adsorption properties of modified magnetite nanoparticles. Acta Phys. Pol. A 132, 564–569. https://doi.org/10.12693/APhysPolA.132.564.

Clausen, L., Fabricius, I., Madsen, L., 2001. Adsorption of pesticides onto quartz, calcite, kaolinite, and α-alumina. J. Environ. Qual. 30, 846–857. https://doi.org/10.2134/jeq2001.303846x.

Clements, J.H., 2003. Reactive applications of cyclic alkylene carbonates. Ind. Eng. Chem. Res. 42 (4), 663–674. https://doi.org/10.1021/ie020678i.

Coles, C.A., Yong, R.N., 2002. Aspects of kaolinite characterization and retention of Pb and Cd. Appl. Clay Sci. 22, 39–45. https://doi.org/10.1016/S0169-1317(02)00110-2.

Cooper, T.G., De Leeuw, N.H., 2002. Adsorption of methanoic acid onto the low-index surfaces of calcite and aragonite. Mol. Simul. 28 (6–7), 539–556. https://doi.org/10.1080/08927020290030125.

Cornell, R.M., 1993. Adsorption of cesium on minerals: a review. J. Radioanal. Nucl. Chem. 171, 483–500. https://doi.org/10.1007/BF02219872.

Crini, G., 2006. Non-conventional low-cost adsorbents for dye removal: a review. Bioresour. Technol. 97 (9), 1061–1085. https://doi.org/10.1016/j.biortech.2005.05.001.

Cristina, M., Oprea, G.M., Michnea, A.M., Mihali, C., 2011. Adsorption kinetics of 8-hydroxyquinoline on smithsonite. Revue Roumaine de Chimie 56, 1021–1027.

Cruz-Guzmán, M., Celis, R., Hermosín, M.C., Koskinen, W.C., Nater, E.A., Cornejo, J., 2006. Heavy metal adsorption by montmorillonites modified with natural organic cations. Soil Sci. Soc. Am. J. 70, 215–221. https://doi.org/10.2136/sssaj2005.0131.

Curtis, C.D., Coleman, M.L., 1986. Controls on the Precipitation of Early Diagenetic Calcite, Dolomite and Siderite Concretions in Complex Depositional Sequences. Roles of Organic Matter in Sediment Diagenesis 38. SEPM Society for Sedimentary Geology.

Dabrowski, A., 2001. Adsorption - From theory to practice. Adv. Colloid Interface Sci. 93, 135–224. https://doi.org/10.1016/S0001-8686(00)00082-8.

Dähn, R., Scheidegger, A.M., Manceau, A., Curti, E., Baeyens, B., Bradbury, M.H., Chateigner, D., 2002. Th uptake on montmorillonite: a powder and polarized extended X-ray absorption fine structure (EXAFS) study. J. Colloid Interface Sci. 249, 8–21. https://doi.org/10.1006/jcis.2002.8236.

Daou, T.J., Begin-Colin, S., Greneche, J.M., Thomas, F., Derory, A., Bernhardt, P., Legare, P., Pourroy, G., 2007. Phosphate adsorption properties of magnetite-based nanoparticles. Chem. Mat. 19, 4494–4505. https://doi.org/10.1021/CM071046V.

De Gisi, S., Lofrano, G., Grassi, M., Notarnicola, M., 2016. Characteristics and adsorption capacities of low-cost sorbents for wastewater treatment: A review. Sustainable Materials and Technologies 9, 10–40. https://doi.org/10.1016/j.susmat.2016.06.002.

De Oliveira, F.F., Moura, K.O., Costa, L.S., Vidal, C.B., Loiola, A.R., Do Nascimento, R.F., 2020. Reactive adsorption of parabens on synthesized micro- and mesoporous silica from coal fly ash: PH effect on the modification process. ACS Omega 5, 3346–3357. https://doi.org/10.1021/acsomega.9b03537.

de Sousa, D.N.R., Insa, S., Mozeto, A.A., Petrovic, M., Chaves, T.F., Fadini, P.S., 2018. Equilibrium and kinetic studies of the adsorption of antibiotics from aqueous solutions onto powdered zeolites. Chemosphere 205, 137–146. https://doi.org/10.1016/j.chemosphere.2018.04.085.

Deer, W.A., Howie, R.A., Zussman, J., 2013. An Introduction to the Rock-Forming Minerals. Mineralogical Society of Great Britain and Ireland https://doi.org/10.1180/dhz.

Dehghan, R., Anbia, M., 2017. Zeolites for adsorptive desulfurization from fuels: a review. Fuel Process. Technol. 167, 99–116. https://doi.org/10.1016/j.fuproc.2017.06.015.

Delkash, M., Ebrazi Bakhshayesh, B., Kazemian, H., 2015. Using zeolitic adsorbents to cleanup special wastewater streams: a review. Microporous Mesoporous Mat. 214, 224–241. https://doi.org/10.1016/j.micromeso.2015.04.039.

Deng, R., Hu, Y., Ku, J., Zuo, W., Yang, Z., 2017. Adsorption of Fe(III) on smithsonite surfaces and implications for flotation. Colloids and Surfaces A: Physicochemical and Engineering Aspects 533, 308–315. https://doi.org/10.1016/j.colsurfa.2017.09.004.

Dhami, N.K., Reddy, M.S., Mukherjee, M.S., 2013. Biomineralization of calcium carbonates and their engineered applications: a review. Front. Microbiol. 4, 314. https://doi.org/10.3389/fmicb.2013.00314.

Di Toro, D.M., 1985. A particle interaction model of reversible organic chemical sorption. Chemosphere 14, 1503–1538. https://doi.org/10.1016/0045-6535(85)90008-6.

Diebold, U., 2003. The surface science of titanium dioxide. Surf. Sci. Rep. 48 (5–8), 53–229. https://doi.org/10.1016/s0167-5729(02)00100-0.

Ding, D., Fu, P., Li, L., Xin, X., Hu, N., Li, G., 2014. U(VI) ion adsorption thermodynamics and kinetics from aqueous solution onto raw sodium feldspar and acid-activated sodium feldspar. J. Radioanal. Nucl. Chem. 299, 1903–1909. https://doi.org/10.1007/s10967-013-2903-2.

Djomgoue, P., Njopwouo, D., 2013. FT-IR spectroscopy applied for surface clays characterization. J. Surf. Eng. Mater. Adv. Technol. 3, 275–282. https://doi.org/10.4236/jsemat.2013.34037.

Dobrogowska, C., Hepler, L.G., Ghosh, D.K., Yariv, S., 1991. Metachromasy in clay mineral systems. Journal of Thermal Analysis 37, 1347–1356. https://doi.org/10.1007/BF01913866.

Doğan, M., Karaoğlu, M.H., Alkan, M., 2009. Adsorption kinetics of maxilon yellow 4GL and maxilon red GRL dyes on kaolinite. J. Hazard. Mater. 165, 1142–1151. https://doi.org/10.1016/j.jhazmat.2008.10.101.

Donat, R., Akdogan, A., Erdem, E., Cetisli, H., 2005. Thermodynamics of Pb^{2+} and Ni^{2+} adsorption onto natural bentonite from aqueous solutions. J. Colloid Interface Sci. 286, 43–52. https://doi.org/10.1016/j.jcis.2005.01.045.

Dong, W., Ding, J., Wang, W., Zong, L., Xu, J., Wang, A., 2020. Magnetic nano-hybrids adsorbents formulated from acidic leachates of clay minerals. J. Clean Prod. 256, 120383. https://doi.org/10.1016/j.jclepro.2020.120383.

Dordio, A.V., Estêvão Candeias, A.J., Pinto, A.P., Teixeira da Costa, C., Palace Carvalho, A.J., 2009. Preliminary media screening for application in the removal of clofibric acid, carbamazepine and ibuprofen by SSF-constructed wetlands. Ecol. Eng. 35, 290–302. https://doi.org/10.1016/j.ecoleng.2008.02.014.

Dordio, A.V., Miranda, S., Prates Ramalho, J.P., Carvalho, A.J.P., 2017. Mechanisms of removal of three widespread pharmaceuticals by two clay materials. J. Hazard. Mater. 323, 575–583. https://doi.org/10.1016/j.jhazmat.2016.05.091.

Dotto, G.L., McKay, G., 2020. Current scenario and challenges in adsorption for water treatment. Journal of Environmental Chemical Engineering 8 (4), 103988.

Dotto, G.L., Ocampo-Pérez, R., Moura, J.M., Cadaval, T.R.S., Pinto, L.A.A., 2016. Adsorption rate of Reactive Black 5 on chitosan based materials: geometry and swelling effects. Adsorption 22, 973–983. https://doi.org/10.1007/s10450-016-9804-y.

Du, Q., Sun, Z., Forsling, W., Tang, H., 1997. Adsorption of copper at aqueous illite surfaces. J. Colloid Interface Sci. 187, 232–242. https://doi.org/10.1006/jcis.1996.4676.

Duxson, P., Fernández-Jiménez, A., Provis, J.L., Lukey, G.C., Palomo, A., Van Deventer, J.S.J., 2007. Geopolymer technology: the current state of the art. J. Mater. Sci. 42, 2917–2933. https://doi.org/10.1007/s10853-006-0637-z.

El Adraa, K., Georgelin, T., Lambert, J.F., Jaber, F., Tielens, F., Jaber, M., 2017. Cysteine-montmorillonite composites for heavy metal cation complexation: A combined experimental and theoretical study. Chem. Eng. J. 314, 406–417. https://doi.org/10.1016/j.cej.2016.11.160.

El-Defrawy, M.M., Kenawy, I.M.M., Zaki, E.G., Eltabey, R.M., 2019. Adsorption of the anionic dye (diamond fast brown Ke) from textile wastewater onto chitosan/montmorillonite nanocomposites. Egyptian Journal of Chemistry 62, 2183–2193. https://doi.org/10.21608/EJCHEM.2019.12467.1775.

El-eswed, B., Alshaaer, M., Yousef, R.I., Hamadneh, I., 2012. Adsorption of Cu (II), Ni (II), Zn (II), Cd (II) and Pb (II) onto kaolin/zeolite based- geopolymers. Adv. Mater. Phys. Chem. 2, 119–125. https://doi.org/10.4236/ampc.2012.24B032.

Elzinga, E.J., Sparks, D.L., 1999. Nickel sorption mechanisms in a pyrophyllite-montmorillonite mixture. J. Colloid Interface Sci. 213 (2), 506–512.

Erdem, E., Karapinar, N., Donat, R., 2004. The removal of heavy metal cations by natural zeolites. J. Colloid Interface Sci. 280, 309–314. https://doi.org/10.1016/j.jcis.2004.08.028.

Erdem, M., Özverdi, A., 2005. Lead adsorption from aqueous solution onto siderite. Sep. Purif. Technol. 42, 259–264. https://doi.org/10.1016/j.seppur.2004.08.004.

Eren, E., Afsin, B., 2008. An investigation of Cu(II) adsorption by raw and acid-activated bentonite: a combined potentiometric, thermodynamic, XRD, IR, DTA study. J. Hazard. Mater. 151, 682–691. https://doi.org/10.1016/j.jhazmat.2007.06.040.

Ersahin, S., Gunal, H., Kutlu, T., Yetgin, B., Coban, S., 2006. Estimating specific surface area and cation exchange capacity in soils using fractal dimension of particle-size distribution. Geoderma 136, 588–597. https://doi.org/10.1016/j.geoderma.2006.04.014.

Es-Sahbany, H., Berradi, M., Nkhili, S., Hsissou, R., Allaoui, M., Loutfi, M., Bassir, D., Belfaquir, M., El Youbi, M.S., 2019. Removal of heavy metals (nickel) contained in wastewater-models by the adsorption technique. Elsevier Ltd, pp. 866–875 https://doi.org/10.1006/jcis.1996.4676.

Essington, M.E., Stewart, M.A., 2015. Influence of temperature and pH on antimonate adsorption by gibbsite, goethite, and kaolinite. Soil Sci. 180, 54–66. https://doi.org/10.1097/SS.0000000000000112.

Fabryanty, R., Valencia, C., Soetaredjo, F.E., Putro, J.N., Santoso, S.P., Kurniawan, A., Ju, Y.H., Ismadji, S., 2017. Removal of crystal violet dye by adsorption using bentonite – alginate composite. J. Environ. Chem. Eng. 5 (6), 5677–5687. https://doi.org/10.1016/j.jece.2017.10.057.

Fan, G., Zhang, C., Wang, T., Deng, J., Cao, Y., Chang, L., Zhou, G., Wu, Y., Li, P., 2020. New insight into surface adsorption thermodynamic, kinetic properties and adsorption mechanisms of sodium oleate on ilmenite and titanaugite. Adv. Powder Technol. 31 (8), 3628–3639. https://doi.org/10.1016/j.apt.2020.07.011.

Feddal, I., Ramdani, A., Taleb, S., Gaigneaux, E.M., Batis, N., Ghaffour, N., 2014. Adsorption capacity of methylene blue, an organic pollutant, by montmorillonite clay. Desalin. Water Treat. 52, 2654–2661. https://doi.org/10.1080/19443994.2013.865566.

Fernandes, M.M., Baeyens, B., 2019. Cation exchange and surface complexation of lead on montmorillonite and illite including competitive adsorption effects. Appl. Geochem. 100, 190–202. https://doi.org/10.1016/j.apgeochem.2018.11.005.

Fernández-Jiménez, A., Palomo, A., Criado, M., 2005. Microstructure development of alkali-activated fly ash cement : a descriptive model. Cem. Concr. Res. 35, 1204–1209. https://doi.org/10.1016/j.cemconres.2004.08.021.

Figueroa, R.A., Leonard, A., Mackay, A.A., 2004. Modeling tetracycline antibiotic sorption to clays. Environ. Sci. Technol. 38, 476–483. https://doi.org/10.1021/es0342087.

Fil, B.A., Korkmaz, M., Özmetin, C., 2016. Application of nonlinear regression analysis for methyl violet (MV) dye adsorption from solutions onto illite clay. J. Dispersion Sci. Technol. 37, 991–1001. https://doi.org/10.1080/01932691.2015.1077455.

Fil, B.A., Yilmaz, M.T., Bayar, S., Elkoca, M.T., 2014. Investigation of adsorption of the dyestuff astrazon red violet 3rn (basic violet 16) on montmorillonite clay. Brazilian Journal of Chemical Engineering 31, 171–182. https://doi.org/10.1590/S0104-66322014000100016.

Flanigen, E.M., 1991. Chapter 2 Zeolites and Molecular Sieves an Historical Perspective. In: van Bekkum, H., FlanigenJansen, E.MJ.C. (Eds.), Introduction to Zeolite Science and Practice. 58. Elsevier, pp. 13–34.

Folk, R.L., 1954. The distinction between grain size and mineral composition in sedimentary-rock nomenclature. J. Geol. 62, 344–359. https://doi.org/10.1086/626171.

Folke, C., Vetenskapsakademien, K., Carpenter, S.R., Gaffney, O., 2020. Our Future in the Anthropocene Biosphere: Global Sustainability and Resilient Societies. In: Nobel Prize Summit - Our Planet, Our Future. Stockholm, Sweden, Beijer Discussion Paper Series, p. No. 272.

Freilich, M.B., Petersen, R.L., by Staff, U, 2014. Potassium compounds. Kirk-Othmer Encyclopedia of Chemical Technology. John Wiley & Sons, Inc., Hoboken, NJ, USA, pp. 1–35 https://doi.org/10.1002/0471238961.1615200106180509.a01.pub3.

Frye, K., 2006. Rock-forming minerals. Mineralogy. Kluwer Academic Publishers, pp. 447–449 https://doi.org/10.1007/0-387-30720-6_124.

Fumba, G., Essomba, J.S., Tagne, G.M., Nsami, N.J., Désiré, P., Bélibi Bélibi, P.D., Mbadcam, J.K., 2014. Equilibrium and kinetic adsorption studies of methyl orange from aqueous solutions using kaolinite, metakaolinite and activated geopolymer as low cost adsorbents. Journal of Academia and Industrial Research 3 (4), 156–163.

Gaballah, I., Goy, D., Allain, E., Kilbertus, G., Thauront, J., 1997. Recovery of copper through decontamination of synthetic solutions using modified barks. Metall Mater Trans B 28, 13–23. https://doi.org/10.1007/s11663-997-0122-3.

Galamboš, M., Krajňák, A., Rosskopfová, O., Viglašová, E., Adamcová, R., Rajec, P., 2013. Adsorption equilibrium and kinetic studies of strontium on Mg-bentonite, Fe-bentonite and illite/smectite. J. Radioanal. Nucl. Chem. 298, 1031–1040. https://doi.org/10.1007/s10967-013-2511-1.

Gao, Y., Chen, N., Hu, W., Feng, C., Zhang, B., Ning, Q., Xu, B., 2013. Phosphate removal from aqueous solution by an effective clay composite material. J. Solut. Chem. 42, 691–704. https://doi.org/10.1007/s10953-013-9985-x.

Gereli, G., Seki, Y., Murat Kuşoğlu, I., Yurdakoç, K., 2006. Equilibrium and kinetics for the sorption of promethazine hydrochloride onto K10 montmorillonite. J. Colloid Interface Sci. 299, 155–162. https://doi.org/10.1016/j.jcis.2006.02.012.

Ghaedi, M., Nasab, A.G., Khodadoust, S., Sahraei, R., Daneshfar, A., 2015. Characterization of zinc oxide nanorods loaded on activated carbon as cheap and efficient adsorbent for removal of methylene blue. J. Ind. Eng. Chem. 21, 986–993. https://doi.org/10.1016/j.jiec.2014.05.006.

Ghaemi, A., Torab-Mostaedi, M., Ghannadi-Maragheh, M., 2011. Characterizations of strontium(II) and barium(II) adsorption from aqueous solutions using dolomite powder. J. Hazard. Mater. 190, 916–921. https://doi.org/10.1016/j.jhazmat.2011.04.006.

Ghernaout, D., Elboughdiri, N., Ghareba, S., 2020. Fenton Technology for Wastewater Treatment: Dares and Trends. OALib Journal 7, 1–26. https://doi.org/10.4236/oalib.1106045.

Ghorbanzadeh, N., Jung, W., Halajnia, A., Lakzian, A., Kabra, A.N., Jeon, B.H., 2015. Removal of arsenate and arsenite from aqueous solution by adsorption on clay minerals. Geosystem Eng. 18, 302–311. https://doi.org/10.1080/12269328.2015.1062436.

Ghosh, D., Bhattacharyya, K.G., 2002. Adsorption of methylene blue on kaolinite. Appl. Clay Sci. 20, 295–300. https://doi.org/10.1016/S0169-1317(01)00081-3.

Gier, S., Johns, W.D., 2000. Heavy metal-adsorption on micas and clay minerals studied by X-ray photoelectron spectroscopy. Appl. Clay Sci. 16, 289–299. https://doi.org/10.1016/S0169-1317(00)00004-1.

Giménez, J., Martínez, M., de Pablo, J., Rovira, M., Duro, L., 2007. Arsenic sorption onto natural hematite, magnetite, and goethite. J. Hazard. Mater. 141, 575–580. https://doi.org/10.1016/j.jhazmat.2006.07.020.

Goldberg, S., 2014. Macroscopic experimental and modeling evaluation of selenite and selenate adsorption mechanisms on gibbsite. Soil Chemistry 78 (2), 473–479. https://doi.org/10.2136/sssaj2013.06.0249.

Goncharuk, V.V., Puzyrnaya, L.N., Pshinko, G.N., Bogolepov, A.A., Demchenko, V.Y., 2010. The removal of heavy metals from aqueous solutions by montmorillonite modified with polyethylenimine. Journal of Water Chemistry and Technology 32, 67–72. https://doi.org/10.3103/S1063455X10020013.

Gong, N., Liu, Y., Huang, R., 2018. Simultaneous adsorption of Cu^{2+} and Acid fuchsin (AF) from aqueous solutions by CMC/bentonite composite. International Journal of Biological Macromolecules 115, 580–589. https://doi.org/10.1016/j.ijbiomac.2018.04.075.

Greathouse, J.A., Geatches, D.L., Pike, D.Q., Greenwell, H.C., Johnston, C.T., Wilcox, J., Cygan, R.T., 2015. Methylene blue adsorption on the basal surfaces of kaolinite: Structure and thermodynamics from quantum and classical molecular simulation. Clays and Clay Minerals 63, 185–198. https://doi.org/10.1346/CCMN.2015.0630303.

Grim, R.E., Bray, R.H., Bradley, W.F., 1937. The Mica in Argillaceous Sediments. American Mineralogist 22, 813–829.

Gu, S., Kang, X., Wang, L., Lichtfouse, E., Wang, C., 2019. Clay mineral adsorbents for heavy metal removal from wastewater: a review. Environmental Chemistry Letters https://doi.org/10.1007/s10311-018-0813-9.

Guerra, D.J.L., Mello, I., Resende, R., Silva, R., 2013. Application as absorbents of natural and functionalized Brazilian bentonite in Pb^{2+} adsorption: Equilibrium, kinetic, pH, and thermodynamic effects. Water Resour. Ind. 4, 32–50. https://doi.org/10.1016/j.wri.2013.11.001.

Guimarães Neto, J.O.A., Aguiar, T.R., 2020. Evaluation of the efficiency of three different mineral adsorbents in the removal of pollutants in samples from a tropical spring in Northeastern Brazil. Water Environment Research 92, 1195–1207. https://doi.org/10.1002/wer.1314.

Guiza, Sami, Bagane, Mohamed, Guiza, S., Bagane, M., 2012. External mass transport process during the adsorption of methyl violet onto sodic bentonite. J Univ Chem Technol Metal 47, 283–288.

Gupta, S. Sen, Bhattacharyya, K.G., 2006. Removal of Cd(II) from aqueous solution by kaolinite, montmorillonite and their poly(oxo zirconium) and tetrabutylammonium derivatives. Journal of Hazardous Materials 128, 247–257. https://doi.org/10.1016/j.jhazmat.2005.08.008.

Gupta, V.K., Jain, C.K., Ali, I., Sharma, M., Saini, V.K., 2003. Removal of cadmium and nickel from wastewater using bagasse fly ash - a sugar industry waste. Water Research 37, 4038–4044. https://doi.org/10.1016/S0043-1354(03)00292-6.

Győrfi, K., Vágvölgyi, V., Zsirka, B., Horváth, E., Szilágyi, R.K., Baán, K., Balogh, S., Kristóf, J., 2020. Kaolins of high iron-content as photocatalysts: challenges of acidic surface modifications and mechanistic insights. Applied Clay Science 195, 105722. https://doi.org/10.1016/j.clay.2020.105722.

Hackling, M., Garnett, P., 1985. Misconceptions of chemical equilibrium. European Journal of Science Education 7, 205–214. https://doi.org/10.1080/0140528850070211.

Hajji, S., Montes-Hernandez, G., Sarret, G., Tordo, A., Morin, G., Ona-Nguema, G., Bureau, S., Turki, T., Mzoughi, N., 2019. Arsenite and chromate sequestration onto ferrihydrite, siderite and goethite nanostructured minerals: Isotherms from flow-through reactor experiments and XAS measurements. Journal of Hazardous Materials 362, 358–367. https://doi.org/10.1016/j.jhazmat.2018.09.031.

Haldar, S.K., Tišljar, J., 2013. Introduction to Mineralogy and Petrology. Introduction to Mineralogy and Petrology. Elsevier Inc. https://doi.org/10.1016/C2012-0-03337-6.

Halsey, G., 1948. Physical adsorption on non-uniform surfaces. The Journal of Chemical Physics 16, 931–937. https://doi.org/10.1063/1.1746689.

Hamilton, A.R., Hutcheon, G.A., Roberts, M., Gaskell, E.E., 2014. Formulation and antibacterial profiles of clay-ciprofloxacin composites. Applied Clay Science 87, 129–135. https://doi.org/10.1016/j.clay.2013.10.020.

Hammond, K.D., Conner, W.C., 2013. Analysis of catalyst surface structure by physical sorption, in: Advances in Catalysis. Academic Press Inc., pp. 1–101. doi.https://doi.org/10.1016/B978-0-12-420173-6.00001-2.

Hamza, W., Fakhfakh, N., Dammak, N., Belhadjltaeif, H., Benzina, M., 2020. Sono-assisted adsorption of organic compounds contained in industrial solution on iron nanoparticles supported on clay: Optimization using central composite design. Ultrasonics Sonochemistry 67, 105134. https://doi.org/10.1016/j.ultsonch.2020.105134.

Hang, P.T., Brindley, G.W., 1970. Methylene blue absorption by clay minerals. Determination of surface areas and cation exchange capacities (clay-organic studies XVIII). Clays and Clay Minerals 18, 203–212. https://doi.org/10.1346/CCMN.1970.0180404.

Harris, R.G., Johnson, B.B., Wells, J.D., 2006a. Competitive adsorption of Cd and dyes to kaolinite. Clays and Clay Minerals 54, 449–455. https://doi.org/10.1346/CCMN.2006.0540405.

Harris, R.G., Johnson, B.B., Wells, J.D., 2006b. Studies on the adsorption of dyes to kaolinite. Clays and Clay Minerals 54, 435–448. https://doi.org/10.1346/CCMN.2006.0540404.

Harris, R.G., Wells, J.D., Angove, M.J., Johnson, B.B., 2006c. Modeling the adsorption of organic dye molecules to kaolinite. Clay Clay Min. 54, 456–465. https://doi.org/10.1346/CCMN.2006.0540406.

Harris, R.G., Wells, J.D., Johnson, B.B., 2001. Selective adsorption of dyes and other organic molecules to kaolinite and oxide surfaces. Colloids and Surfaces A: Physicochemical and Engineering Aspects 180, 131–140. https://doi.org/10.1016/S0927-7757(00)00747-0.

Hennig, C., Reich, T., Dähn, R., Scheidegger, A.M., 2002. Structure of uranium sorption complexes at montmorillonite edge sites. Radiochimica Acta. R. Oldenbourg Verlag GmbH, pp. 653–657 https://doi.org/10.1524/ract.2002.90.9-11_2002.653.

Hepper, E.N., Buschiazzo, D.E., Hevia, G.G., Urioste, A., Antón, L., 2006. Clay mineralogy, cation exchange capacity and specific surface area of loess soils with different volcanic ash contents. Geoderma 135, 216–223. https://doi.org/10.1016/j.geoderma.2005.12.005.

Hodson, M.E., 1998. Micropore surface area variation with grain size in unweathered alkali feldspars: Implications for surface roughness and dissolution studies. Geochimica et Cosmochimica Acta 62, 3429–3435. https://doi.org/10.1016/s0016-7037(98)00244-0.

Hong, X., Wang, R., Liu, Y., Fu, J., Liang, J., Dou, S., 2020. Recent advances in chemical adsorption and catalytic conversion materials for Li–S batteries. Journal of Energy Chemistry https://doi.org/10.1016/j.jechem.2019.07.001.

Hong, S., Wen, C., He, J., Gan, F., Ho, Y.S., 2009. Adsorption thermodynamics of Methylene Blue onto bentonite. Journal of Hazardous Materials 167, 630–633. https://doi.org/10.1016/j.jhazmat.2009.01.014.

Hong, M., Yu, L., Wang, Y., Zhang, J., Chen, Z., Dong, L., Zan, Q., Li, R., 2019. Heavy metal adsorption with zeolites: the role of hierarchical pore architecture. Chemical Engineering Journal https://doi.org/10.1016/j.cej.2018.11.087.

Horai, K., 1971. Thermal conductivity of rock-forming minerals. Journal of Geophysical Research 76, 1278–1308. https://doi.org/10.1029/jb076i005p01278.

Hua, P., Sellaoui, L., Franco, D., Netto, M.S., Luiz Dotto, G., Bajahzar, A., Belmabrouk, H., Bonilla-Petriciolet, A., Li, Z., 2020. Adsorption of acid green and procion red on a magnetic geopolymer based adsorbent: experiments, characterization and theoretical treatment. Chemical Engineering Journal 383, 123113. https://doi.org/10.1016/j.cej.2019.123113.

Huang, Y., Liu, M., Chen, S., Jasmi, I.I., Tang, Y., Lin, S., 2019. Enhanced adsorption and slow release of phosphate by dolomite–alginate composite beads as potential fertilizer. Water Environment Research 91, 797–804. https://doi.org/10.1002/wer.1122.

Ijagbemi, C.O., Baek, M.H., Kim, D.S., 2009. Montmorillonite surface properties and sorption characteristics for heavy metal removal from aqueous solutions. Journal of Hazardous Materials 166, 538–546. https://doi.org/10.1016/j.jhazmat.2008.11.085.

Jafari-zare, F., Habibi-yangjeh, A., 2010. Competitive adsorption of methylene blue and rhodamine B on natural zeolite: Thermodynamic and kinetic studies. Chinese J. Chem. 28, 349–356. https://doi.org/10.1002/cjoc.201090078.

Jain, C.K., Sharma, M.K., 2002. Adsorption of cadmium on bed sediments of river Hindon: Adsorption models and kinetics. Water, Air, and Soil Pollution 137, 1–19. https://doi.org/10.1023/A:1015530702297.

Janecke, S.U., Evans, J.P., 1988. Feldspar-influenced rock rheologies. Geology 16, 1064–1067 10.1130/0091-7613(1988)016<1064:FIRR>2.3.CO;2.

Javadian, H., Ghorbani, F., Tayebi, H.-a., Asl, S.M.H., 2015. Study of the adsorption of Cd (II) from aqueous solution using zeolite-based geopolymer, synthesized from coal fly ash; kinetic, isotherm and thermodynamic studies. Arab. J. Chem. 8 (6), 837–849. https://doi.org/10.1016/j.arabjc.2013.02.018.

Jiang, N., Shang, R., Heijman, S.G.J., Rietveld, L.C., 2018. High-silica zeolites for adsorption of organic micro-pollutants in water treatment: a review. Water Research 144, 145–161. https://doi.org/10.1016/j.watres.2018.07.017.

Jiang, M., Wang, Qin, Jin, Q. Ping, Chen, X. Ying, Liang, Z., 2009. Removal of Pb(II) from aqueous solution using modified and unmodified kaolinite clay. Journal of Hazardous Materials 170, 332–339. https://doi.org/10.1016/j.jhazmat.2009.04.092.

Jiménez-Cedillo, M.J., Olguín, M.T., Fall, C., Colín, A., 2011. Adsorption capacity of iron- or iron-manganese-modified zeolite-rich tuffs for as(III) and as(V) water pollutants. Applied Clay Science 54, 206–216. https://doi.org/10.1016/j.clay.2011.09.004.

Jobstmann, H., Singh, B., 2001. Cadmium sorption by hydroxy-aluminium interlayered montmorillonite. Water, Air, and Soil Pollution 131, 203–215. https://doi.org/10.1023/A:1011928829059.

Kahr, G., Madsen, F.T., 1995. Determination of the cation exchange capacity and the surface area of bentonite, illite and kaolinite by methylene blue adsorption. Applied Clay Science 9, 327–336. https://doi.org/10.1016/0169-1317(94)00028-O.

Kalhori, E.M., Al-Musawi, T.J., Ghahramani, E., Kazemian, H., Zarrabi, M., 2017. Enhancement of the adsorption capacity of the light-weight expanded clay aggregate surface for the metronidazole antibiotic by coating with MgO nanoparticles: Studies on the kinetic, isotherm, and effects of environmental parameters. Chemosphere 175, 8–20. https://doi.org/10.1016/j.chemosphere.2017.02.043.

Kamel, M.M., Youssef, B.M., Kamel, Magda M., 1991. Adsorption of anionic dyes by kaolinites. Dyes and Pigments 15, 175–182. https://doi.org/10.1016/0143-7208(91)80002-Q.

Kandah, M.I., 2004. Zinc and cadmium adsorption on low-grade phosphate. Separation and Purification Technology 35, 61–70. https://doi.org/10.1016/S1383-5866(03)00131-X.

Kang, D., Hu, C., Zhu, Q., 2018. Morphology controlled synthesis of hierarchical structured Fe_2O_3 from natural ilmenite and its high performance for dyes adsorption. Applied Surface Science 459, 327–335. https://doi.org/10.1016/j.apsusc.2018.07.220.

Kara, İ., Yilmazer, D., Akar, S.T., 2017. Metakaolin based geopolymer as an effective adsorbent for adsorption of zinc(II) and nickel(II) ions from aqueous solutions. Applied Clay Science 139, 54–63. https://doi.org/10.1016/j.clay.2017.01.008.

Karageorgiou, K., Paschalis, M., Anastassakis, G.N., 2007. Removal of phosphate species from solution by adsorption onto calcite used as natural adsorbent. Journal of Hazardous Materials 139, 447–452. https://doi.org/10.1016/j.jhazmat.2006.02.038.

Karamanis, D., Assimakopoulos, P.A., 2007. Efficiency of aluminum-pillared montmorillonite on the removal of cesium and copper from aqueous solutions. Water Research 41, 1897–1906. https://doi.org/10.1016/j.watres.2007.01.053.

Karaoğlu, M.H., Doğan, M., Alkan, M., 2010. Kinetic analysis of reactive blue 221 adsorption on kaolinite. Desalination 256, 154–165. https://doi.org/10.1016/j.desal.2010.01.021.

Karapinar, N., Donat, R., 2009. Adsorption behaviour of Cu^{2+} and Cd^{2+} onto natural bentonite. Desalination 249, 123–129. https://doi.org/10.1016/j.desal.2008.12.046.

Kaur, M., Singh, M., Mukhopadhyay, S.S., Singh, D., Gupta, M., 2015. Structural, magnetic and adsorptive properties of clay ferrite nanocomposite and its use for effective removal of Cr (VI) from water. Journal of Alloys and Compounds 653, 202–211. https://doi.org/10.1016/j.jallcom.2015.08.265.

Kausar, A., Iqbal, M., Javed, A., Aftab, K., Nazli, Z.i.H., Bhatti, H.N., Nouren, S., 2018. Dyes adsorption using clay and modified clay: A review. Journal of Molecular Liquids 256, 395–407. https://doi.org/10.1016/j.molliq.2018.02.034.

Kazansky, V.B., Pidko, E.A., 2005. A new insight in the unusual adsorption properties of Cu^{+} cations in Cu-ZSM-5 zeolite. Catalysis Today. Elsevier, Pp. 281–293. Doi.10.1016/J.Cattod.2005. vol. 09, p. 037.

Khale, D., Chaudhary, R., 2007. Mechanism of geopolymerization and factors influencing its development: a review. Journal of Materials Science 42, 729–746. https://doi.org/10.1007/s10853-006-0401-4.

Khaleel, A., Kapoor, P.N., Klabunde, K.J., 1999. Nanocrystalline metal oxides as new adsorbents for air purification. Nanostructured Materials 11, 459–468. https://doi.org/10.1016/S0965-9773(99)00329-3.

Khan, T.A., Dahiya, S., Ali, I., 2012. Use of kaolinite as adsorbent: Equilibrium, dynamics and thermodynamic studies on the adsorption of Rhodamine B from aqueous solution. Applied Clay Science 69, 58–66. https://doi.org/10.1016/j.clay.2012.09.001.

Khan, T.A., Khan, E.A., Shahjahan, 2015. Removal of basic dyes from aqueous solution by adsorption onto binary iron-manganese oxide coated kaolinite: Non-linear isotherm and kinetics modeling. Applied Clay Science 107, 70–77. https://doi.org/10.1016/j.clay.2015.01.005.

Khan, S.A., Siddiqui, M.F., Khan, T.A., 2020. Synthesis of Poly(methacrylic acid)/Montmorillonite Hydrogel Nanocomposite for Efficient Adsorption of Amoxicillin and Diclofenac from Aqueous Environment: Kinetic, Isotherm, Reusability, and Thermodynamic Investigations. ACS Omega https://doi.org/10.1021/acsomega.9b03617.

Klapyta, Z., Fujita, T., Iyi, N., 2001. Adsorption of dodecyl- and octadecyltrimethylammonium ions on a smectite and synthetic micas. Applied Clay Science 19, 5–10. https://doi.org/10.1016/S0169-1317(01)00059-X.

Komnitsas, K.A., 2011. Potential of geopolymer technology towards green buildings and sustainable cities. Procedia Eng. 21, 1023–1032. https://doi.org/10.1016/j.proeng.2011. 11.2108.

Konkol, K.L., Rasmussen, S.C., 2015. An ancient cleanser: Soap production and use in antiquity. ACS Symposium Series. American Chemical Society, pp. 245–266 https://doi.org/10.1021/bk-2015-1211.ch009.

Kovacevic, D., Lemic, J., Damjanovic, M., Petronijevic, R., Janackovic, D., Stanic, T., 2011. Fe-nitrothion adsorption - desorption on organo - minerals. Applied Clay Science 52, 109–114. https://doi.org/10.1016/j.clay.2011.02.006.

Krumbein, W.E., Urzì, C.E., Gehrmann, C., 1991. Biocorrosion and biodeterioration of antique and medieval glass. Geomicrobiology Journal 9, 139–160. https://doi.org/10.1080/01490459109385995.

Kuila, U., Prasad, M., 2013. Specific surface area and pore-size distribution in clays and shales. Geophysical Prospecting 61, 341–362. https://doi.org/10.1111/1365-2478.12028.

Lahiri, A., Jha, A., 2007. Kinetics and reaction mechanism of soda ash roasting of ilmenite ore for the extraction of titanium dioxide. Metallurgical and Materials Transactions B: Process Metallurgy and Materials Processing Science 38, 939–948. https://doi.org/10.1007/s11663-007-9095-5.

Lasheen, M.R., El-Sherif, I.Y., Sabry, D.Y., El-Wakeel, S.T., El-Shahat, M.F., 2016. Adsorption of heavy metals from aqueous solution by magnetite nanoparticles and magnetite-kaolinite nanocomposite: equilibrium, isotherm and kinetic study. Desalination and Water Treatment 57, 17421–17429. https://doi.org/10.1080/19443994.2015.1085446.

Lawal, I.A., Moodley, B., 2018. Fixed-Bed and batch Adsorption of Pharmaceuticals from Aqueous Solutions on Ionic Liquid-Modified Montmorillonite. Chemical Engineering and Technology 41, 983–993. https://doi.org/10.1002/ceat.201700107.

Lazaratou, C.V., Vayenas, D.V., Papoulis, D., 2020. The role of clays, clay minerals and clay-based materials for nitrate removal from water systems: a review. Applied Clay Science https://doi.org/10.1016/j.clay.2019.105377.

Lee, J.O., Cho, W.J., Choi, H., 2013a. Sorption of cesium and iodide ions onto KENTEX-bentonite. Environment and Earth Science 70, 2387–2395. https://doi.org/10.1007/s12665-013-2530-9.

Lee, I., Lee, C.G., Park, J.A., Kang, J.K., Yoon, S.Y., Kim, S.B., 2013b. Removal of Cr(VI) from aqueous solution using alginate/polyvinyl alcohol-hematite composite. Desalin. Water Treat. 51, 3438–3444. https://doi.org/10.1080/19443994.2012.749204.

Lee, S., van Riessen, A., Chon, C.-M., Kang, N.-H., Jou, H.-T., Kim, Y.-J., 2016. Impact of activator type on the immobilisation of lead in fly ash-based geopolymer. J. Hazard. Mater. 305, 59–66. https://doi.org/10.1016/j.jhazmat.2015.11.023.

Leodopoulos, C., Doulia, D., Gimouhopoulos, K., Triantis, T.M., 2012. Single and simultaneous adsorption of methyl orange and humic acid onto bentonite. Applied Clay Science 70, 84–90. https://doi.org/10.1016/j.clay.2012.08.005.

Li, Z., Arai, Y., 2020. Comprehensive evaluation of mineral adsorbents for phosphate removal in agricultural water, in: advances in Agronomy. Academic Press Inc. https://doi.org/10.1016/bs.agron.2020.06.003.

Li, L., Ding, D., Hu, N., Fu, P., Xin, X., Wang, Y., 2014. Adsorption of U(VI) ions from low concentration uranium solution by thermally activated sodium feldspar. Journal of Radioanalytical and Nuclear Chemistry 299, 681–690. https://doi.org/10.1007/s10967-013-2769-3.

Li, H.P., Dou, Z., Chen, S.Q., Hu, M., Li, S., Sun, H.M., Jiang, Y., Zhai, Q.G., 2019a. Design of a multifunctional indium-organic framework: Fluorescent sensing of nitro compounds, physical adsorption, and photocatalytic degradation of organic dyes. Inorg. Chem. 58, 11220–11230. https://doi.org/10.1021/acs.inorgchem.9b01862.

Li, X., Liu, N., Zhang, J., 2019b. Adsorption of cesium at the external surface of TOT type clay mineral: effect of the interlayer cation and the hydrated state. J. Phys. Chem. C 123, 19540–19548. https://doi.org/10.1021/acs.jpcc.9b04035.

Li, L., Wang, S., Zhu, Z., 2006. Geopolymeric adsorbents from fly ash for dye removal from aqueous solution. Journal of Colloid and Interface Science 300, 52–59. https://doi.org/10.1016/j.jcis.2006.03.062.

Li, Z., Xiao, J., Huang, L., Xu, D., Liu, D., Sun, X., Yu, L., Wu, H., 2019c. Comparative study of carboxylic acid adsorption on calcite: l-malic acid, d-malic acid and succinic acid. Carbonates and Evaporites 34, 1131–1139. https://doi.org/10.1007/s13146-017-0416-8.

Liao, R., Shi, Z., Chen, Y., Zhang, J., Wang, X., Hou, Y., Zhang, K., 2020. Characteristics of uranium sorption on illite in a ternary system: effect of phosphate on adsorption. Journal of Radioanalytical and Nuclear Chemistry 323, 159–168. https://doi.org/10.1007/s10967-019-06878-y.

Lin, J., Zhan, Y., Zhu, Z., 2011. Adsorption characteristics of copper (II) ions from aqueous solution onto humic acid-immobilized surfactant-modified zeolite. Colloids and Surfaces A: Physicochemical and Engineering Aspects 384, 9–16. https://doi.org/10.1016/j.colsurfa.2011.02.044.

Lippmann, F., 1973. Sedimentary Carbonate Minerals, Sedimentary Carbonate Minerals. Springer Berlin Heidelberg https://doi.org/10.1007/978-3-642-65474-9.

Lipson, S.M., Stotzky, G., 1983. Adsorption of reovirus to clay minerals: effects of cation-exchange capacity, cation saturation, and surface area. Applied and Environmental Microbiology 46.

Liu, X., Hicher, P., Muresan, B., Saiyouri, N., Hicher, P.Y., 2016a. Heavy metal retention properties of kaolin and bentonite in a wide range of concentration and different pH conditions. Appl. Clay Sci. 119, 365–374. https://doi.org/10.1016/j.clay.2015.09.021.

Liu, J., Huang, H., Huang, R., Zhang, J., Hao, S., Shen, Y., Chen, H., 2016b. Mechanisms of CPB modified zeolite on mercury adsorption in simulated wastewater. Water Environ. Res. 88, 490–499. https://doi.org/10.2175/106143016x14504669767850.

Liu, M., Jiang, L., 2010. Switchable Adhesion on Liquid/Solid Interfaces, in: Advanced Functional Materials. John Wiley & Sons, Ltd, pp. 3753–3764 https://doi.org/10.1002/adfm.201001208.

Liu, Y., Lu, X., Wu, F., Deng, N., 2011. Adsorption and photooxidation of pharmaceuticals and personal care products on clay minerals. Reaction Kinetics, Mechanisms and Catalysis 104, 61–73. https://doi.org/10.1007/s11144-011-0349-5.

Liu, Y.L., Walker, H.W., Lenhart, J.J., 2019. Adsorption of microcystin-LR onto kaolinite, illite and montmorillonite. Chemosphere 220, 696–705. https://doi.org/10.1016/j.chemosphere.2018.12.137.

Liu, C., Wu, P., Zhu, Y., Tran, L., 2016c. Simultaneous adsorption of Cd^{2+} and BPA on amphoteric surfactant activated montmorillonite. Chemosphere 144, 1026–1032. https://doi.org/10.1016/j.chemosphere.2015.09.063.

Liu, Q., Yang, B., Zhang, L., Huang, R., 2015. Adsorptive removal of Cr(VI) from aqueous solutions by cross-linked chitosan/bentonite composite. Korean Journal of Chemical Engineering 32, 1314–1322. https://doi.org/10.1007/s11814-014-0339-1.

López, E., Soto, B., Arias, M., Núñez, A., Rubinos, D., Barral, M.T., 1998. Adsorbent properties of red mud and its use for wastewater treatment. Water Research 32, 1314–1322. https://doi.org/10.1016/S0043-1354(97)00326-6.

Lorens, R.B., 1981. Sr, Cd, Mn and Co distribution coefficients in calcite as a function of calcite precipitation rate. Geochimica et Cosmochimica Acta 45, 553–561. https://doi.org/10.1016/0016-7037(81)90188-5.

Lu, F., Astruc, D., 2020. Nanocatalysts and other nanomaterials for water remediation from organic pollutants. Coordination Chemistry Reviews https://doi.org/10.1016/j.ccr.2020.213180.

Luo, J.J., Daniel, I.M., 2003. Characterization and modeling of mechanical behavior of polymer/clay nanocomposites. Composites Science and Technology 63, 1607–1616. https://doi.org/10.1016/S0266-3538(03)00060-5.

Luo, Q., Jiang, D., Hou, D., Chen, W., Hu, X., He, Y., 2019. Effective adsorption of metal ions by modified clinoptilolite zeolite from simulated radioactive solution. Journal of Radioanalytical and Nuclear Chemistry 319, 1069–1081. https://doi.org/10.1007/s10967-018-6383-2.

Lütke, S.F., Igansi, A.V., Pegoraro, L., Dotto, G.L., Pinto, L.A.A., Cadaval, T.R.S., 2019. Preparation of activated carbon from black wattle bark waste and its application for phenol adsorption. Journal of Environmental Chemical Engineering 7, 103396. https://doi.org/10.1016/j.jece.2019.103396.

Luukkonen, T., Sarkkinen, M., Kemppainen, K., Rämö, J., Lassi, U., 2016. Metakaolin geopolymer characterization and application for ammonium removal from model solutions and landfill leachate. Appl.Clay Sci. 119, 266–276. https://doi.org/10.1016/j.clay.2015.10.027.

Ma, Z., Shan, C., Liang, J., Tong, M., 2018. Efficient adsorption of Selenium(IV) from water by hematite modified magnetic nanoparticles. Chemosphere 193, 134–141. https://doi.org/10.1016/j.chemosphere.2017.11.005.

Ma, L., Zhu, J., Xi, Y., Zhu, R., He, H., Liang, X., Ayoko, G.A., 2015. Simultaneous adsorption of Cd(II) and phosphate on Al13 pillared montmorillonite. RSC Advances 5, 77227–77234. https://doi.org/10.1039/c5ra15744g.

Machado, A.I., Dordio, A., Fragoso, R., Leitão, A.E., Duarte, E., 2017. Furosemide removal in constructed wetlands: Comparative efficiency of LECA and Cork granulates as support matrix. Journal of Environmental Management 203, 422–428. https://doi.org/10.1016/j.jenvman.2017.08.002.

Macht, F., Eusterhues, K., Pronk, G.J., Totsche, K.U., 2011. Specific surface area of clay minerals: Comparison between atomic force microscopy measurements and bulk-gas (N_2) and -liquid (EGME) adsorption methods. Applied Clay Science 53, 20–26. https://doi.org/10.1016/j.clay.2011.04.006.

Mahdavian, A.R., Mirrahimi, M.A.S., 2010. Efficient separation of heavy metal cations by anchoring polyacrylic acid on superparamagnetic magnetite nanoparticles through surface modification. Chemical Engineering Journal 159, 264–271. https://doi.org/10.1016/j.cej.2010.02.041.

Mahmoodi, N.M., Saffar-Dastgerdi, M.H., 2019. Zeolite nanoparticle as a superior adsorbent with high capacity: Synthesis, surface modification and pollutant adsorption ability from wastewater. Microchemical Journal 145, 74–83. https://doi.org/10.1016/j.microc.2018.10.018.

Mahmoodi, N.M., Taghizadeh, A., Taghizadeh, M., Azimi, M., 2019. Surface modified montmorillonite with cationic surfactants: Preparation, characterization, and dye adsorption from aqueous solution. Journal of Environmental Chemical Engineering 7. https://doi.org/10.1016/j.jece.2019.103243.

Mahvi, A.H., Dalvand, A., 2020. Kinetic and equilibrium studies on the adsorption of direct red 23 dye from aqueous solution using montmorillonite nanoclay. Water Quality Research Journal of Canada 55, 132–144. https://doi.org/10.2166/WQRJ.2019.008.

Malamis, S., Katsou, E., 2013. A review on zinc and nickel adsorption on natural and modified zeolite, bentonite and vermiculite: Examination of process parameters, kinetics and isotherms. Journal of Hazardous Materials https://doi.org/10.1016/j.jhazmat.2013.03.024.

Maleki, S., Karimi-Jashni, A., 2020. Optimization of Ni(II) adsorption onto Cloisite Na^+ clay using response surface methodology. Chemosphere 246, 125710. https://doi.org/10.1016/j.chemosphere.2019.125710.

Malik, L.A., Bashir, A., Ahmad, N., Qureashi, A., Pandith, A.H., 2020. Exploring Metal Ion Adsorption and Antifungal Properties of Carbon-Coated Magnetite Composite. ChemistrySelect 5, 3208–3216. https://doi.org/10.1002/slct.201904830.

Marco-Brown, J.L., Gaigneaux, E.M., Torres Sánchez, R.M., dos Santos Afonso, M., 2019. Adsorption of picloram on clays nontronite, illite and kaolinite: equilibrium and herbicide-clays surface complexes. J. Environ. Sci. Heal. - Part B Pestic. Food Contam. Agric. Wastes 54, 281–289. https://doi.org/10.1080/03601234.2018.1561055.

Marfunin, A.S. (Ed.), 1994. Advanced Mineralogy – Volume 1 – composition, structure, and properties of mineral matter: concepts, results, and problems. Springer Berlin Heidelberg https://doi.org/10.1007/978-3-642-78523-8.

Markovski, J.S., Crossed, D., Signokić, V., Milosavljević, M., Mitrić, M., Perić-Grujić, A.A., Onjia, A.E., Marinković, A.D., 2014a. Ultrasonic assisted arsenate adsorption on solvothermally synthesized calcite modified by goethite, α-MnO2 and goethite/α-MnO2. Ultrasonics Sonochemistry 21, 790–801. https://doi.org/10.1016/j.ultsonch.2013.10.006.

Markovski, J.S., Crossed, D., Signokić, V., Milosavljević, M., Mitrić, M., Perić-Grujić, A.A., Onjia, A.E., Marinković, A.D., 2014b. Ultrasonic assisted arsenate adsorption on solvothermally synthesized calcite modified by goethite, α-MnO_2 and goethite/α-MnO_2. Ultrasonics Sonochemistry 21, 790–801. https://doi.org/10.1016/j.ultsonch.2013.10.006.

Martín, J., del Orta, M., Medina-Carrasco, S., Santos, J.L., Aparicio, I., Alonso, E., 2019. Evaluation of a modified mica and montmorillonite for the adsorption of ibuprofen from aqueous media. Applied Clay Science 171, 29–37. https://doi.org/10.1016/j.clay.2019.02.002.

Martín, J., Orta, Del M., Medina-Carrasco, S., Santos, J.L., Aparicio, I., Alonso, E., 2018. Removal of priority and emerging pollutants from aqueous media by adsorption onto synthetic organo-funtionalized high-charge swelling micas. Environmental Research 164, 488–494. https://doi.org/10.1016/j.envres.2018.03.037.

Masindi, V., Gitari, W.M., Pindihama, K.G., 2016. Adsorption of phosphate from municipal effluents using cryptocrystalline magnesite: complementing laboratory results with geochemical modelling. Desalination and Water Treatment 57, 20957–20969. https://doi.org/10.1080/19443994.2015.1110720.

Masud, A., Chavez Soria, N.G., Aga, D.S., Aich, N., 2020. Adsorption and advanced oxidation of diverse pharmaceuticals and personal care products (PPCPs) from water using highly efficient rGO–nZVI nanohybrids. Environmental Science: Water Research & Technology 6, 2223–2238. https://doi.org/10.1039/d0ew00140f.

Mathialagan, T., Viraraghavan, T., 2002. Adsorption of cadmium from aqueous solutions by perlite. Journal of Hazardous Materials 94, 291–303. https://doi.org/10.1016/S0304-3894(02)00084-5.

Matthiesen, H., Hilbert, L.R., Gregory, D.J., 2003. Siderite as a corrosion product on archaeological iron from a waterlogged environment. Studies in Conservation 48, 183–194. https://doi.org/10.1179/sic.2003.48.3.183.

Mavhungu, A., Mbaya, R., Masindi, V., Foteinis, S., Muedi, K.L., Kortidis, I., Chatzisymeon, E., 2019. Wastewater treatment valorisation by simultaneously removing and recovering phosphate and ammonia from municipal effluents using a mechano-thermo activated magnesite technology. Journal of Environmental Management 250. https://doi.org/10.1016/j.jenvman.2019.109493.

McKay, G., 1982. Adsorption of dyestuffs from aqueous solutions with activated carbon I: Equilibrium and batch contact-time studies. Journal of Chemical Technology and Biotechnology 32, 759–772. https://doi.org/10.1002/jctb.5030320712.

Medina-Ramirez, A., Gamero-Melo, P., Ruiz-Camacho, B., Minchaca-Mojica, J.I., Romero-Toledo, R., Gamero-Vega, K.Y., 2019. Adsorption of Aqueous as (III) in Presence of Coexisting Ions by a Green Fe-Modified W Zeolite. Water 11, 281. https://doi.org/10.3390/w11020281.

Meier, L.P., Shelden, R.A., Caseri, W.R., Suter, U.W., 1994. Polymerization of styrene with initiator ionically bound to high surface area mica: Grafting via an unexpected mechanism. Macromolecules 27, 1637–1642.

Mekhloufi, M., Zehhaf, A., Benyoucef, A., Quijada, C., Morallon, E., 2013. Removal of 8-quinolinecarboxylic acid pesticide from aqueous solution by adsorption on activated montmorillonites. Environmental Monitoring and Assessment 185, 10365–10375. https://doi.org/10.1007/s10661-013-3338-5.

Meunier, A., Velde, B., 2010. Illite: Origins. Evolution and Metamorphism. Springer. https://doi.org/10.1007/978-3-662-07850-1.

Meunier, A., Velde, B., Meunier, A., Velde, B., 2004. The Mineralogy of Illite — What Is Illite?, in: Illite. Springer, Berlin Heidelberg, pp. 3–62 https://doi.org/10.1007/978-3-662-07850-1_2.

Millero, F., Huang, F., Zhu, X., Liu, X., Zhang, J.Z., 2001. Adsorption and desorption of phosphate on calcite and aragonite in seawater. Aquatic Geochemistry 7, 33–56. https://doi.org/10.1023/A:1011344117092.

Milonjić, S.K., Kopečni, M.M., Ilić, Z.E., 1983. The point of zero charge and adsorption properties of natural magnetite. Journal of Radioanalytical Chemistry 78, 15–24. https://doi.org/10.1007/BF02519745.

Minceva, M., Fajgar, R., Markovska, L., Meshko, V., 2008. Comparative study of Zn^{2+}, Cd^{2+}, and Pb^{2+} removal from water solution using natural clinoptilolitic zeolite and commercial granulated activated carbon. Equilibrium of adsorption. Sep. Sci. Technol. 43, 2117–2143. https://doi.org/10.1080/01496390801941174.

Mitchell, R.H., Novgorodova, M.I., Semenov, E.I., 1994. Chemical Composition of Minerals, Crystallochemical Constraints and the Nature of Impurities, in: Advanced Mineralogy. Springer, Berlin Heidelberg, pp. 2–12 https://doi.org/10.1007/978-3-642-78523-8_1.

Mohammadi, M., Ghaemi, A., Torab-Mostaedi, M., Asadollahzadeh, M., Hemmati, A., 2015. Adsorption of cadmium (II) and nickel (II) on dolomite powder. Desalination and Water Treatment 53, 149–157. https://doi.org/10.1080/19443994.2013.836990.

Mohammadi, M., Sedighi, M., 2013. Modification of Langmuir isotherm for the adsorption of asphaltene or resin onto calcite mineral surface: Comparison of linear and nonlinear methods. Protection of Metals and Physical Chemistry of Surfaces 49, 460–470. https://doi.org/10.1134/S2070205113040205.

Mohapatra, D., Mishra, D., Chaudhury, G.R., Das, R.P., 2007. Arsenic adsorption mechanism on clay minerals and its dependence on temperature. Korean Journal of Chemical Engineering 24, 426–430. https://doi.org/10.1007/s11814-007-0073-z.

Motlagh Bahadory Esfahani, S., Faghihian, H., 2014. Modification of synthesized β-zeolite by ethylenediamine and monoethanolamine for adsorption of Pb2+. J. Water Process Eng. 3, 62–66. https://doi.org/10.1016/j.jwpe.2014.05.007.

Motsi, T., Rowson, N.A., Simmons, M.J.H., 2009. Adsorption of heavy metals from acid mine drainage by natural zeolite. International Journal of Mineral Processing 92, 42–48. https://doi.org/10.1016/j.minpro.2009.02.005.

Mozley, P.S., 1989. Relation between depositional environment and the elemental composition of early diagenetic siderite. Geology 17, 704–706. https://doi.org/10.1130/0091-7613(1989)017<0704:RBDEAT>2.3.CO;2.

Mudasir, M., Karelius, K., Aprilita, N.H., Wahyuni, E.T., 2016. Adsorption of mercury(II) on dithizone-immobilized natural zeolite. Journal of Environmental Chemical Engineering 4, 1839–1849. https://doi.org/10.1016/j.jece.2016.03.016.

Mukherjee, K., Kedia, A., Jagajjanani Rao, K., Dhir, S., Paria, S., 2015. Adsorption enhancement of methylene blue dye at kaolinite clay-water interface influenced by electrolyte solutions. RSC Advances 5, 30654–30659. https://doi.org/10.1039/c5ra03534a.

Na, P., Jia, X., Yuan, B., Li, Y., Na, J., Chen, Y., Wang, L., 2010. Arsenic adsorption on Ti-pillared montmorillonite. Journal of Chemical Technology and Biotechnology 85, 708–714. https://doi.org/10.1002/jctb.2360.

Naghsh, M., Shams, K., 2017. Synthesis of a kaolin-based geopolymer using a novel fusion method and its application in effective water softening. Applied Clay Science 146, 238–245. https://doi.org/10.1016/j.clay.2017.06.008.

Nandi, B.K., Goswami, A., Purkait, M.K., 2009. Adsorption characteristics of brilliant green dye on kaolin. Journal of Hazardous Materials 161, 387–395. https://doi.org/10.1016/j.jhazmat.2008.03.110.

Ngulube, T., Gumbo, J.R., Masindi, V., Maity, A., 2018. Calcined magnesite as an adsorbent for cationic and anionic dyes: characterization, adsorption parameters, isotherms and kinetics study. Heliyon 4. https://doi.org/10.1016/j.heliyon.2018.e00838.

Niu, X., Sun, Y., Lei, Z., Qin, G., Yang, C., 2020. Facile synthesis of hierarchical hollow Mn-ZSM-5 zeolite for enhanced cyclohexane catalytic oxidation. Progress in Natural Science: Materials International 30, 35–40. https://doi.org/10.1016/j.pnsc.2019.09.006.

Obayomi, K.S., Auta, M., Kovo, A.S., 2020. Isotherm, Kinetic and Thermodynamic Studies for Adsorption of Lead(II) onto Modified Aloji Clay. https://doi.org/10.5004/dwt.2020.25142.

Olu-Owolabi, B.I., Popoola, D.B., Unuabonah, E.I., 2010. Removal of Cu^{2+} and Cd^{2+} from aqueous solution by bentonite clay modified with binary mixture of goethite and humic acid. Water, Air, and Soil Pollution 211, 459–474. https://doi.org/10.1007/s11270-009-0315-2.

Onyango, M.S., Kojima, Y., Matsuda, H., Ochieng, A., 2003. Adsorption Kinetics of Arsenic Removal from Groundwater by Iron-Modified Zeolite. J. Chem. Eng. JAPAN 36, 1516–1522. https://doi.org/10.1252/jcej.36.1516.

Ören, A.H., Kaya, A., 2006. Factors affecting adsorption characteristics of Zn^{2+} on two natural zeolites. Journal of Hazardous Materials 131, 59–65. https://doi.org/10.1016/j.jhazmat.2005.09.027.

Orta, Del M., Martín, J., Medina-Carrasco, S., Santos, J.L., Aparicio, I., Alonso, E., 2018. Novel synthetic clays for the adsorption of surfactants from aqueous media. Journal of Environmental Management 206, 357–363. https://doi.org/10.1016/j.jenvman.2017.10.053.

Osuna, F.J., Pavón, E., Alba, M.D., 2019. Design swelling micas: Insights on heavy metals cation exchange reaction. Applied Clay Science 182, 105298. https://doi.org/10.1016/j.clay.2019.105298.

Otunola, B.O., Ololade, O.O., 2020. A review on the application of clay minerals as heavy metal adsorbents for remediation purposes. Environmental Technology and Innovation https://doi.org/10.1016/j.eti.2020.100692.

Oubagaranadin, J.U.K., Murthy, Z.V.P., Mallapur, V.P., 2010. Removal of Cu(II) and Zn(II) from industrial wastewater by acid-activated montmorillonite-illite type of clay. Comptes Rendus Chimie 13, 1359–1363. https://doi.org/10.1016/j.crci.2010.05.024.

Ozcan, S., Tor, A., Aydin, M.E., 2012. An investigation on the sorption behaviour of montmorillonite for selected organochlorine pesticides from water. Environmental Technology 33, 1239–1245. https://doi.org/10.1080/09593330.2011.618936.

Pahlavanzadeh, H., Motamedi, M., 2020. Adsorption of nickel, Ni(ii), in aqueous solution by modified zeolite as a cation-exchange adsorbent. Journal of Chemical & Engineering Data 65, 185–197. https://doi.org/10.1021/acs.jced.9b00868.

Pak, S.-H., Park, S.-M., An, J., Park, C.-G., 2018. Adsorption Behavior of Poly(Methacrylic Acid)/Iron-Oxide-Coated Zeolite for the Removal of Mn(II), Fe(II), and as(III) from Aqueous Solution. https://doi.org/10.5004/dwt.2018.22649.

Pal, O.R., Vanjara, A.K., 2001. Removal of malathion and butachlor from aqueous solution by clays and organoclays. Separation and Purification Technology 24, 167–172. https://doi.org/10.1016/S1383-5866(00)00226-4.

Park, S.M., Alessi, D.S., Baek, K., 2019. Selective adsorption and irreversible fixation behavior of cesium onto 2:1 layered clay mineral: a mini review. Journal of Hazardous Materials 369, 569–576. https://doi.org/10.1016/j.jhazmat.2019.02.061.

Park, Y., Shin, W.S., Choi, S.J., 2012. Removal of Co, Sr and Cs from aqueous solution using self-assembled monolayers on mesoporous supports. Korean Journal of Chemical Engineering 29, 1556–1566. https://doi.org/10.1007/s11814-012-0035-y.

Park, Y., Sun, Z., Ayoko, G.A., Frost, R.L., 2014. Removal of herbicides from aqueous solutions by modified forms of montmorillonite. Journal of Colloid and Interface Science 415, 127–132. https://doi.org/10.1016/j.jcis.2013.10.024.

Pazos, M.C., Castro, M.A., Cota, A., Osuna, F.J., Pavón, E., Alba, M.D., 2017. New insights into surface-functionalized swelling high charged micas: their adsorption performance for non-ionic organic pollutants. Journal of Industrial and Engineering Chemistry 52, 179–186. https://doi.org/10.1016/j.jiec.2017.03.042.

Pearce, M.A., Timms, N.E., Hough, R.M., Cleverley, J.S., 2013. Reaction mechanism for the replacement of calcite by dolomite and siderite: Implications for geochemistry, microstructure and porosity evolution during hydrothermal mineralisation. Contributions to Mineralogy and Petrology 166, 995–1009. https://doi.org/10.1007/s00410-013-0905-2.

Pehlivan, E., Özkan, A.M., Dinç, S., Parlayici, Ş., 2009. Adsorption of Cu^{2+} and Pb^{2+} ion on dolomite powder. Journal of Hazardous Materials 167, 1044–1049. https://doi.org/10.1016/j.jhazmat.2009.01.096.

Pelte, S., Flamant, G., Flamand, R., Gauthier, D., Beche, E., Berjoan, R., 2000. Effects of thermal treatment on feldspar sorptive properties: Identification of uptake mechanisms. Minerals Engineering 13, 609–622. https://doi.org/10.1016/S0892-6875(00)00044-3.

Pereira, F.A.R., Sousa, K.S., Cavalcanti, G.R.S., Fonseca, M.G., de Souza, A.Ô.G., Alves, A.P.M., 2013. Chitosan-montmorillonite biocomposite as an adsorbent for copper (II) cations from aqueous solutions. International Journal of Biological Macromolecules doi. https://doi.org/10.1016/j.ijbiomac.2013.08.017.

Pierucci, S., Klemeš, J.J., Piazza, L., Bakalis, S., Maia, G.S., Andrade, J.R., Oliveira, M.F., Vieira, M.G.A., Da Silva, G.C., 2017. Affinity studies between drugs and clays as adsorbent material, in: CHEMICAL ENGINEERING TRANSACTIONS. doi.https://doi.org/10.3303/CET1757098.

Potgieter, J.H., Potgieter-Vermaak, S.S., Kalibantonga, P.D., 2006. Heavy metals removal from solution by palygorskite clay. Minerals Engineering 19, 463–470. https://doi.org/10.1016/j.mineng.2005.07.004.

Puri, C., Sumana, G., 2018. Highly effective adsorption of crystal violet dye from contaminated water using graphene oxide intercalated montmorillonite nanocomposite. Applied Clay Science 166, 102–112. https://doi.org/10.1016/j.clay.2018.09.012.

Putro, J.N., Santoso, S.P., Ismadji, S., Ju, Y.H., 2017. Investigation of heavy metal adsorption in binary system by nanocrystalline cellulose – Bentonite nanocomposite: Improvement on extended Langmuir isotherm model. Microporous and Mesoporous Materials 246, 166–177. https://doi.org/10.1016/j.micromeso.2017.03.032.

Qin, Y., Long, M., Tan, B., Zhou, B., 2014. RhB Adsorption Performance of magnetic Adsorbent Fe_3O_4/RGO Composite and its Regeneration through a Fenton-like Reaction. Nano-Micro Lett. 6, 125–135. https://doi.org/10.1007/BF03353776.

Qiu, Q., Jiang, X., Lv, G., Chen, Z., Lu, S., Ni, M., Yan, J., Deng, X., 2018. Adsorption of heavy metal ions using zeolite materials of municipal solid waste incineration fly ash modified by microwave-assisted hydrothermal treatment. Powder Technology 335, 156–163. https://doi.org/10.1016/j.powtec.2018.05.003.

Qu, Z., Dong, W., Chen, Y., Dong, G., Zhu, S., Yu, Y., Bian, D., 2020. Upcycling of groundwater treatment sludge to magnetic Fe/Mn-bearing nanorod for chromate adsorption from wastewater treatment. PLoS One 15, e0234136. https://doi.org/10.1371/journal.pone.0234136.

Rahier, H., Wastiels, J., Biesemans, M., Willlem, R., Van Assche, G., Van Mele, B., 2007. Reaction mechanism, kinetics and high temperature transformations of geopolymers. Journal of Materials Science 42, 2982–2996. doi.https://doi.org/10.1007/s10853-006-0568-8.

Ramola, S., Belwal, T., Li, C.J., Wang, Y.Y., Lu, H.H., Yang, S.M., Zhou, C.H., 2020. Improved lead removal from aqueous solution using novel porous bentonite - and calcite-biochar composite. Sci. Total Environ. 709, 136171. https://doi.org/10.1016/j.scitotenv.2019.136171.

Rao, K.H., Cases, J.M., Forssberg, K.S.E., 1991. Mechanism of oleate interaction on salt-type minerals. V. Adsorption and precipitation reactions in relation to the solid/liquid ratio in the synthetic fluorite-sodium oleate system. Journal of Colloid and Interface Science 145, 330–348. https://doi.org/10.1016/0021-9797(91)90365-F.

Rashed, M.N., 2001. Lead removal from contaminated water using mineral adsorbents. Environmentalist 21, 187–195. https://doi.org/10.1023/A:1017931404249.

Reddy, M.M., Claassen, H.C., 1994. Specific surface area of a crushed welded tuff before and after aqueous dissolution. Applied Geochemistry 9, 223–233. https://doi.org/10.1016/0883-2927(94)90008-6.

Ren, H., Jiang, J., Wu, D., Gao, Z., Sun, Y., Luo, C., 2016a. Selective Adsorption of Pb(II) and Cr(VI) by Surfactant-Modified and Unmodified Natural Zeolites: a Comparative Study on Kinetics, Equilibrium, and Mechanism. Water, Air, and Soil Pollution 227, 1–11. https://doi.org/10.1007/s11270-016-2790-6.

Ren, H., Jiang, J., Wu, D., Gao, Z., Sun, Y., Luo, C., 2016b. Selective Adsorption of Pb(II) and Cr(VI) by Surfactant-Modified and Unmodified Natural Zeolites: a Comparative Study on Kinetics, Equilibrium, and Mechanism. Water, Air, and Soil Pollution 227, 1–11. https://doi.org/10.1007/s11270-016-2790-6.

Romdhane, D.F., Satlaoui, Y., Nasraoui, R., Charef, A., Azouzi, R., 2020. And Kinetic Studies of Methyl Red Removal from Textile-Polluted Water Using Natural and Purified Organic Matter Rich Clays as Low-Cost Adsorbent. Res. Artic, Adsorpt https://doi.org/10.1155/2020/4376173.

Ronov, A.B., Yaroshevsky, A.A., 1922. Chemical composition of the earth's crust. Nature. https://doi.org/10.1029/gm013p0037.

Rosales, E., Anasie, D., Pazos, M., Lazar, I., Sanromán, M.A., 2018. Kaolinite adsorption-regeneration system for dyestuff treatment by Fenton based processes. Sci. Total Environ. 622–623, 556–562. https://doi.org/10.1016/j.scitotenv.2017.11.301.

Rossatto, D.L., Netto, M.S., Jahn, S.L., Mallmann, E.S., Dotto, G.L., Foletto, E.L., 2020. Highly efficient adsorption performance of a novel magnetic geopolymer/Fe_3O_4 composite towards removal of aqueous acid green 16 dye. Journal of Environmental Chemical Engineering https://doi.org/10.1016/j.jece.2020.103804.

Rosskopfová's, O., Pivarčiová's, L., Krajňák's, A., Galamboš's, M., Rajec's, P., 2016. Adsorption of nickel on illite/smectite Dolná Ves. Journal of Radioanalytical and Nuclear Chemistry 307, 179–185. https://doi.org/10.1007/s10967-015-4110-9.

Roy, W.R., Krapac, I.G., 1994. Adsorption and Desorption of Atrazine and Deethylatrazine by Low Organic Carbon Geologic Materials. Journal of Environmental Quality 23, 549–556. https://doi.org/10.2134/jeq1994.00472425002300030021x.

Sadri, S., Johnson, B.B., Ruyter-Hooley, M., Angove, M.J., 2018. The adsorption of nortriptyline on montmorillonite, kaolinite and gibbsite. Applied Clay Science 165, 64–70. https://doi.org/10.1016/j.clay.2018.08.005.

Saif Ur Rehman, M., Munir, M., Ashfaq, M., Rashid, N., Nazar, M.F., Danish, M., Han, J.I., 2013. Adsorption of Brilliant Green dye from aqueous solution onto red clay. Chemical Engineering Journal 228, 54–62. https://doi.org/10.1016/j.cej.2013.04.094.

Saiphaneendra, B., Saxena, T., Singh, S.A., Madras, G., Srivastava, C., 2017. Synergistic effect of co-existence of hematite (α-Fe_2O_3) and magnetite (Fe_3O_4) nanoparticles on graphene sheet for dye adsorption. Journal of Environmental Chemical Engineering 5, 26–37. https://doi.org/10.1016/j.jece.2016.11.017.

Salam, M.A., Abukhadra, M.R., Mostafa, M., 2020. Effective decontamination of as(V), Hg (II), and U(VI) toxic ions from water using novel muscovite/zeolite aluminosilicate composite: adsorption behavior and mechanism. Environmental Science and Pollution Research 27, 13247–13260. https://doi.org/10.1007/s11356-020-07945-8.

Sánchez Camazano, M., Sánchez Martín, M.J., 1983. Factors influencing interactions of organophosphorus pesticides with montmorillonite. Geoderma 29, 107–118. https://doi.org/10.1016/0016-7061(83)90035-6.

Sandy Maramis, V., Kurniawan, A., Ayucitra, A., Sunarso, J., Ismadji, S., 2012. Removal of copper ions from aqueous solution by adsorption using LABORATORIES-modified bentonite (organo-bentonite). Frontiers of Chemical Science and Engineering 6, 58–66. https://doi.org/10.1007/s11705-011-1160-6.

Sari, A., Tüzen, M., 2013. Adsorption of silver from aqueous solution onto raw vermiculite and manganese oxide-modified vermiculite. Microporous and Mesoporous Materials 170, 155–163. https://doi.org/10.1016/j.micromeso.2012.12.004.

Sarma, G.K., Sen Gupta, S., Bhattacharyya, K.G., 2019. Removal of hazardous basic dyes from aqueous solution by adsorption onto kaolinite and acid-treated kaolinite: kinetics, isotherm and mechanistic study. SN Appl. Sci. 1. https://doi.org/10.1007/s42452-019-0216-y.

Schadeck Netto, M., Leindcker Rossatto, D., Jahn, S.L., Stoffels Mallmann, E., Luiz Dotto, G., Luiz Foletto, E., 2019. Preparation of a novel magnetic geopolymer/zero–valent iron composite with remarkable adsorption performance towards aqueous Acid Red 97. Chemical Engineering Communications https://doi.org/10.1080/00986445.2019.1635467.

Sdiri, A., Higashi, T., Chaabouni, R., Jamoussi, F., 2012. Competitive removal of heavy metals from aqueous solutions by montmorillonitic and calcareous clays. Water Air Soil Pollut 223, 1191–1204. https://doi.org/10.1007/s11270-011-0937-z.

Seema, M.D., 2013. In vitro sustained delivery of atenolol, an antihypertensive drug using naturally occurring clay mineral montmorillonite as a carrier. Eur. Chem. Bull. 2, 942–951. https://doi.org/10.17628/ECB.2013.2.942-951.

Seki, Y., Yurdakoç, K., 2009. Equilibrium, kinetics and thermodynamic aspects of Promethazine hydrochloride sorption by iron rich smectite. Colloids and Surfaces A: Physicochemical and Engineering Aspects 340, 143–148. https://doi.org/10.1016/j.colsurfa.2009.03.020.

Sen Gupta, S., Bhattacharyya, K.G., 2008. Immobilization of Pb(II), Cd(II) and Ni(II) ions on kaolinite and montmorillonite surfaces from aqueous medium. Journal of Environmental Management 87, 46–58. https://doi.org/10.1016/j.jenvman.2007.01.048.

Sen Gupta, S., Bhattacharyya, K.G., 2009. Treatment of water contaminated with Pb(II) and Cd(II) by adsorption on kaolinite, montmorillonite and their acid-activated forms. Indian Journal of Chemical Technology.

Sen Gupta, S., Bhattacharyya, K.G., 2014. Adsorption of metal ions by clays and inorganic solids. RSC Advances https://doi.org/10.1039/c4ra03673e.

Sengupta, A., Mallick, S., Bahadur, D., 2017. Tetragonal nanostructured zirconia modified hematite mesoporous composite for efficient adsorption of toxic cations from wastewater. Journal of Environmental Chemical Engineering 5, 5285–5292. https://doi.org/10.1016/j.jece.2017.10.002.

Şenol, Z.M., Şimşek, S., 2020. Equilibrium, kinetics and thermodynamics of Pb(II) ions from aqueous solution by adsorption onto chitosan-dolomite composite beads. International Journal of Environmental Analytical Chemistry 1–15. https://doi.org/10.1080/03067319.2020.1790546.

Serpone, N., Horikoshi, S., Emeline, A.V., 2010. Microwaves in advanced oxidation processes for environmental applications. A brief review. J. Photochem. Photobiol. C Photochem. Rev. 11, 114–131. https://doi.org/10.1016/j.jphotochemrev.2010.07.003.

Shaban, M., Sayed, M.I., Shahien, M.G., Abukhadra, M.R., Ahmed, Z.M., 2018. Adsorption behavior of inorganic- and organic-modified kaolinite for Congo red dye from water, kinetic modeling, and equilibrium studies. Journal of Sol-Gel Science and Technology 87, 427–441. https://doi.org/10.1007/s10971-018-4719-6.

Shams, M., Nabipour, I., Dobaradaran, S., Ramavandi, B., Qasemi, M., Afsharnia, M., 2013a. An environmental friendly and cheao adsorbent (municipal solid waste compost ash) with high efficiency in removal of phosphorus from aqueous solution. Fresenius Environ. Bull. 22, 722–726.

Sharma, A., Shukla, A., Attri, K., Kumar, M., Kumar, P., Suttee, A., Singh, G., Barnwal, R.P., Singla, N., 2020. Global trends in pesticides: a looming threat and viable alternatives. Ecotoxicology and Environmental Safety https://doi.org/10.1016/j.ecoenv.2020.110812.

Sharma, A.K., Thornberg, D., Andersen, H.R., 2013b. Application of waterworks sludge in wastewater treatment plants. Int. J. Environ. Sci. Technol. 10, 1157–1166. https://doi.org/10.1007/s13762-013-0191-6.

Shawabkeh, R.A., Al-Khashman, O.A., Al-Omari, H.S., Shawabkeh, A.F., 2007. Cobalt and zinc removal from aqueous solution by chemically treated bentonite. Environmentalist 27, 357–363. https://doi.org/10.1007/s10669-007-9048-1.

Sheta, A.S., Falatah, A.M., Al-Sewailem, M.S., Khaled, E.M., Sallam, A.S.H., 2003. Sorption characteristics of zinc and iron by natural zeolite and bentonite. Microporous and Mesoporous Materials 61, 127–136. https://doi.org/10.1016/S1387-1811(03)00360-3.

Shiraishi, Y., Saito, N., Hirai, T., 2005. Adsorption-driven photocatalytic activity of mesoporous titanium dioxide. Journal of the American Chemical Society 127, 12820–12822. https://doi.org/10.1021/ja053265s.

Shu, K., Xu, L., Wu, H., Wang, Z., Xu, Y., Fang, S., 2019. Influence of ultrasound pretreatment on ilmenite surface chemical properties and collectors' adsorption behaviour. Ultrasonics Sonochemistry 57, 98–107. https://doi.org/10.1016/j.ultsonch.2019.05.017.

Sibley, D.F., Gregg, J.M., 1987. Classification of dolomite rock textures. Journal of Sedimentary Petrology 57, 967–975. https://doi.org/10.1306/212f8cba-2b24-11d7-8648000102c1865d.

Silva, A., Martinho, S., Stawiński, W., Węgrzyn, A., Figueiredo, S., Santos, L.H.M.L.M., Freitas, O., 2018. Application of vermiculite-derived sustainable adsorbents for removal of venlafaxine. Environmental Science and Pollution Research 25, 17066–17076. https://doi.org/10.1007/s11356-018-1869-6.

Simsek, E.B., Özdemir, E., Beker, U., 2013. Process optimization for arsenic adsorption onto natural zeolite incorporating metal oxides by response surface methodology. Water, Air, and Soil Pollution 224, 1–14. https://doi.org/10.1007/s11270-013-1614-1.

Şimşek, S., Ulusoy, U., 2004. UO_2^{2+}, Tl^{+}, Pb^{2+}, Ra^{2+}, Bi^{3+} and Ac^{3+} adsorption onto polyacrylamide-zeolite composite and its modified composition by phytic acid. Journal of Radioanalytical and Nuclear Chemistry 261, 79–86. https://doi.org/10.1023/B:JRNC.0000030938.98515.82.

Singhal, A., Gangwar, B.P., Gayathry, J.M., 2017. CTAB modified large surface area nanoporous geopolymer with high adsorption capacity for copper ion removal. Applied Clay Science 150, 106–114. https://doi.org/10.1016/j.clay.2017.09.013.

Siyal, A.A., Shamsuddin, M.R., Khan, M.I., Rabat, N.E., Zulfiqar, M., Man, Z., Siame, J., Azizli, K.A., 2018. A review on geopolymers as emerging materials for the adsorption of heavy metals and dyes. Journal of Environmental Management 224, 327–339. https://doi.org/10.1016/j.jenvman.2018.07.046.

Soltermann, D., Fernandes, M.M., Baeyens, B., Dähn, R., Miehé-Brendlé, J., Wehrli, B., Bradbury, M.H., 2013. Fe(II) sorption on a synthetic montmorillonite A combined macroscopic and spectroscopic study. Environmental Science & Technology 47, 6978–6986. https://doi.org/10.1021/es304270c.

Somasundaran, P., Agar, G.E., 1967. The zero point of charge of calcite. Journal of Colloid and Interface Science 24, 433–440. https://doi.org/10.1016/0021-9797(67)90241-X.

Song, K., Kim, W., Ryu, T., Ryu, K.-W., Bang, J.-H., Jang, Y.-N., 2011. Adsorption of Cd(II) on Waste Calcite Produced by the Carbonation of Flue Gas Desulfurization (FGD) Gypsum. Materials Transactions 52, 224–228. https://doi.org/10.2320/matertrans.M2010344.

Sorwat, J., Mellage, A., Kappler, A., Byrne, J.M., 2020. Immobilizing magnetite onto quartz sand for chromium remediation. Journal of Hazardous Materials 400, 123139. https://doi.org/10.1016/j.jhazmat.2020.123139.

Sprynskyy, M., Buszewski, B., Terzyk, A.P., Namieśnik, J., 2006. Study of the selection mechanism of heavy metal (Pb^{2+}, Cu^{2+}, Ni^{2+}, and Cd^{2+}) adsorption on clinoptilolite. Journal of Colloid and Interface Science 304, 21–28. https://doi.org/10.1016/j.jcis.2006.07.068.

Stathi, P., Litina, K., Gournis, D., Giannopoulos, T.S., Deligiannakis, Y., 2007. Physicochemical study of novel organoclays as heavy metal ion adsorbents for environmental remediation. Journal of Colloid and Interface Science 316, 298–309. https://doi.org/10.1016/j.jcis.2007.07.078.

Stefaniak, E., Biliński, B., Dobrowolski, R., Staszczuk, P., Wójcik, J., 2002. The influence of preparation conditions on adsorption properties and porosity of dolomite-based sorbents. Colloids and Surfaces A: Physicochemical and Engineering Aspects. Elsevier, pp. 337–345 https://doi.org/10.1016/S0927-7757(02)00160-7.

Stefaniak, E., Dobrowolski, R., Staszczuk, P., 2000. On the adsorption of chromium(VI) Ions on dolomite and 'dolomitic sorbents'. Adsorption Science and Technology 18, 107–115. https://doi.org/10.1260/0263617001493323.

Styszko, K., Nosek, K., Motak, M., Bester, K., 2015. Preliminary selection of clay minerals for the removal of pharmaceuticals, bisphenol a and triclosan in acidic and neutral aqueous solutions. Comptes Rendus Chimie 18, 1134–1142. https://doi.org/10.1016/j.crci.2015.05.015.

Suciu, N.A., Capri, E., 2009. Adsorption of chlorpyrifos, penconazole and metalaxyl from aqueous solution by modified clays. J. Environ. Sci. Heal. Part B 44, 525–532. https://doi.org/10.1080/03601230902997543.

Suliestyah Hartami, P.N., Tuheteru, E.J., 2020. Effect of weight and contact time adsorption of activated carbon from coal as adsorbent of Cu(II) and Fe(II) in liquid solutions. AIP Conference Proceedings. American Institute of Physics Inc., p. 070025 https://doi.org/10.1063/5.0007891.

Sun, B., Li, Q., Zheng, M., Su, G., Lin, S., Wu, M., Li, C., Wang, Q., Tao, Y., Dai, L., Qin, Y., Meng, B., 2020. Recent advances in the removal of persistent organic pollutants (POPs) using multifunctional materials:a review. Environmental Pollution https://doi.org/10.1016/j.envpol.2020.114908.

Suzuki, Y., Morgan, P.E.D., Ohji, T., 2004. New Uniformly Porous $CaZrO_3$/MgO Composites with Three-Dimensional Network Structure from Natural Dolomite. Journal of the American Ceramic Society 83, 2091–2093. https://doi.org/10.1111/j.1151-2916.2000.tb01519.x.

Tabak, A., Baltas, N., Afsin, B., Emirik, M., Caglar, B., Eren, E., 2010. Adsorption of Reactive Red 120 from aqueous solutions by cetylpyridinium-bentonite. Journal of Chemical Technology and Biotechnology 85, 1199–1207. https://doi.org/10.1002/jctb.2416.

Tahergorabi, M., Esrafili, A., Kermani, M., Shirzad-Siboni, M., 2016. Application of thiol-functionalized mesoporous silica-coated magnetite nanoparticles for the adsorption of heavy metals. Desalination and Water Treatment 57, 19834–19845. https://doi.org/10.1080/19443994.2015.1106351.

Talebzadeh, F., Sobhanardakani, S., Zandipak, R., 2017. Effective adsorption of as(V) and V (V) ions from water samples using 2,4-dinitrophenylhydrazine functionalized sodium dodecyl sulfate-coated magnetite nanoparticles. Separation Science and Technology 52, 622–633. https://doi.org/10.1080/01496395.2016.1262873.

Taylor, S.R., McLennan, S.M., 1985. The Continental Crust: Its Composition and Evolution: An Examination of the Geochemical Record Preserved in Sedimentary Rocks.

Teymouri, E., Mousavi, S.F., Karami, H., Farzin, S., Kheirabad, M.H., 2020a. Reducing Urban Runoff Pollution using Porous Concrete Containing Mineral Adsorbents. J. Environ. Treat. Tech. 8, 429–436.

Teymouri, E., Mousavi, S.F., Karami, H., Farzin, S., Kheirabad, M.H., 2020b. Municipal Wastewater pretreatment using porous concrete containing fine-grained mineral adsorbents. J. Water Process Eng. 36, 101346. https://doi.org/10.1016/j.jwpe.2020.101346.

Thiebault, T., Boussafir, M., 2019. Adsorption Mechanisms of Psychoactive Drugs onto Montmorillonite. Colloids Interface Sci. Commun. 30, 100183. https://doi.org/10.1016/j.colcom.2019.100183.

Tóth, J., 1995. Uniform interpretation of gas/solid adsorption. Advances in Colloid and Interface Science 55, 1–239. https://doi.org/10.1016/0001-8686(94)00226-3.

Tsai, W.T., Lai, C.W., Su, T.Y., 2006. Adsorption of bisphenol-a from aqueous solution onto minerals and carbon adsorbents. Journal of Hazardous Materials 134, 169–175. https://doi.org/10.1016/j.jhazmat.2005.10.055.

Uddin, M.K., 2017. A review on the adsorption of heavy metals by clay minerals, with special focus on the past decade. Chemical Engineering Journal https://doi.org/10.1016/j.cej.2016.09.029.

Udovic, T.J., Dumesic, J.A., 1984. Adsorptive properties of magnetite surfaces as studied by temperature-programmed desorption: Studies of O_2, NO, CO_2, and CO adsorption. Journal of Catalysis 89, 314–326. https://doi.org/10.1016/0021-9517(84)90308-7.

Ulmanu, M., Marañón, E., Fernández, Y., Castrillón, L., Anger, I., Dumitriu, D., 2003. Removal of copper and cadmium ions from diluted aqueous solutions by low cost and waste material adsorbents. Water, Air, and Soil Pollution https://doi.org/10.1023/A:1022084721990.

Unuabonah, E.I., Adebowale, K.O., 2009. Optimization of kinetic data for two-stage batch adsorption of Pb(II) ions onto tripolyphosphate-modified kaolinite clay. Journal of Chemical Technology and Biotechnology 84, 1726–1735. https://doi.org/10.1002/jctb.2238.

Unuabonah, E.I., Adebowale, K.O., Dawodu, F.A., 2008a. Equilibrium, kinetic and sorber design studies on the adsorption of Aniline blue dye by sodium tetraborate-modified Kaolinite clay adsorbent. Journal of Hazardous Materials 157, 397–409. https://doi.org/10.1016/j.jhazmat.2008.01.047.

Unuabonah, E.I., Adebowale, K.O., Dawodu, F.A., 2008b. Equilibrium, kinetic and sorber design studies on the adsorption of Aniline blue dye by sodium tetraborate-modified Kaolinite clay adsorbent. Journal of Hazardous Materials 157, 397–409. https://doi.org/10.1016/j.jhazmat.2008.01.047.

Van, H.T., Nguyen, L.H., Nguyen, V.D., Nguyen, X.H., Nguyen, T.H., Nguyen, T.V., Vigneswaran, S., Rinklebe, J., Tran, H.N., 2019. Characteristics and mechanisms of cadmium adsorption onto biogenic aragonite shells-derived biosorbent: batch and column studies. Journal of Environmental Management 241, 535–548. https://doi.org/10.1016/j.jenvman.2018.09.079.

Velazquez-Jimenez, L.H., Vences-Alvarez, E., Flores-Arciniega, J.L., Flores-Zuñiga, H., Rangel-Mendez, J.R., 2015. Water defluoridation with special emphasis on adsorbents-containing metal oxides and/or hydroxides: a review. Separation and Purification Technology https://doi.org/10.1016/j.seppur.2015.07.006.

Velde, B., 1995. Composition and Mineralogy of Clay Minerals, in: Origin and Mineralogy of Clays. Springer, Berlin Heidelberg, pp. 8–42 https://doi.org/10.1007/978-3-662-12648-6_2.

Venkata Ramana, D.K., Kumar Reddy, D.H., Kumar, B.N., Seshaiah, K., Chandra Rao, G.P., Lu, C., 2013. Adsorption of Pb(II) from Aqueous Solutions by Chemically Modified Zeolite supported Carbon Nanotubes: Equilibrium, Kinetic, and Thermodynamic Studies. Separation Science and Technology 48, 403–412. https://doi.org/10.1080/01496395.2012.690638.

Vieira, Y., Silvestri, S., Leichtweis, J., Jahn, S.L., Flores, É.M., Dotto, G.L., Foletto, E.L., 2020. New insights into the mechanism of heterogeneous activation of nano–magnetite by microwave irradiation for use as Fenton catalyst. Journal of Environmental Chemical Engineering 8, 103787. https://doi.org/10.1016/j.jece.2020.103787.

Viglašová, E., Daňo, M., Galamboš, M., Krajňák, A., Rosskopfová, O., Rajec, P., 2017. Investigation of Cu(II) adsorption on Slovak bentonites and illite/smectite for agricultural applications. Journal of Radioanalytical and Nuclear Chemistry 314, 2425–2435. https://doi.org/10.1007/s10967-017-5610-6.

Vinuth, M., Bhojya Naik, H.S., Manjanna, J., 2015. Remediation of hexavalent chromium from aqueous solution using clay mineral Fe(II)-montmorillonite: Encompassing anion exclusion impact. Applied Surface Science 357, 1244–1250. https://doi.org/10.1016/j.apsusc.2015.09.167.

Waanders, F.B., Steyn, F.W., Fosso-Kankeu, E., 2016. Removal of Cr(VI) and Zn(II) from an aqueous solution using an organic-inorganic composite of bentonite-biochar-hematite. Desalination and Water Treatment 59, 144–153. https://doi.org/10.5004/dwt.2016.0059.

Walker, G.M., Hansen, L., Hanna, J.A., Allen, S.J., 2003. Kinetics of a reactive dye adsorption onto dolomitic sorbents. Water Research 37, 2081–2089. https://doi.org/10.1016/S0043-1354(02)00540-7.

Wan Ngah, W.S., Hanafiah, M.A.K.M., 2008. Removal of heavy metal ions from wastewater by chemically modified plant wastes as adsorbents: a review. Bioresource Technology https://doi.org/10.1016/j.biortech.2007.06.011.

Wang, D., Li, H., Yao, Q., Hui, S., Niu, Y., 2020a. Assisting effect of Al_2O_3 on MnO for NO catalytic oxidation. Green Energy Environ https://doi.org/10.1016/j.gee.2020.07.005.

Wang, Y., Reardon, E.J., 2001. A siderite/limestone reactor to remove arsenic and cadmium from wastewaters. Applied Geochemistry 16, 1241–1249. https://doi.org/10.1016/S0883-2927(01)00023-3.

Wang, A., Si, Y., Yin, H., Chen, J., Huo, J., 2019a. Synthesis of Na-, Fe-, and Mg-containing titanate nanocomposites starting from ilmenite and NaOH and adsorption kinetics, isotherms, and thermodynamics of Cu(II), Cd(II), and Pb(II) cations. Materials Science & Engineering, B 249. https://doi.org/10.1016/j.mseb.2019.114411.

Wang, Y., Wang, X., Li, J., Li, Y., Xia, S., Zhao, J., Minale, T.M., Gu, Z., 2019b. Coadsorption of tetracycline and copper(II) onto struvite loaded zeolite – An environmentally friendly product recovered from swine biogas slurry. Chem. Eng. J. 371, 366–377. https://doi.org/10.1016/j.cej.2019.04.058.

Wang, X., Zhang, Q., 2020. Role of surface roughness in the wettability, surface energy and flotation kinetics of calcite. Powder Technology 371, 55–63. https://doi.org/10.1016/j.powtec.2020.05.081.

Wang, Q., Zhang, J., Zheng, Y., Wang, A., 2014. Adsorption and release of ofloxacin from acid- and heat-treated halloysite. Colloids and Surfaces. B, Biointerfaces 113, 51–58. https://doi.org/10.1016/j.colsurfb.2013.08.036.

Warren, J., 2000. Dolomite: Occurence, evolution and economically important associations. Earth-Science Reviews 52, 1–81. https://doi.org/10.1016/S0012-8252(00)00022-2.

Wasewar, K.L., Kumar, P., Chand, S., Padmini, B.N., Teng, T.T., 2010. Adsorption of cadmium ions from aqueous solution using granular activated carbon and activated Clay. Clean-Soil Air Water 38, 649–656. https://doi.org/10.1002/clen.201000004.

Wei, C., Xu, Z., Han, F., Xu, W., Gu, J., Ou, M., Xu, X., 2018. Preparation and characterization of poly(acrylic acid-co-acrylamide)/montmorillonite composite and its application for methylene blue adsorption. Colloid & Polymer Science 296, 653–667. https://doi.org/10.1007/s00396-018-4277-z.

Weir, A., Westerhoff, P., Fabricius, L., Hristovski, K., Von Goetz, N., 2012. Titanium dioxide nanoparticles in food and personal care products. Environmental Science & Technology 46, 2242–2250. doi.https://doi.org/10.1021/es204168d.

Wen, J., Dong, H., Zeng, G., 2018. Application of zeolite in removing salinity/sodicity from wastewater: a review of mechanisms, challenges and opportunities. Journal of Cleaner Production 197, 1435–1446. https://doi.org/10.1016/j.jclepro.2018.06.270.

Wick, S., Baeyens, B., Marques Fernandes, M., Voegelin, A., 2018. Thallium Adsorption onto Illite. Environmental Science & Technology 52, 571–580. https://doi.org/10.1021/acs.est.7b04485.

Wingenfelder, U., Nowack, B., Furrer, G., Schulin, R., 2005. Adsorption of Pb and Cd by amine-modified zeolite. Water Research 39, 3287–3297. https://doi.org/10.1016/j.watres.2005.05.017.

Wongrueng, A., Sookwong, B., Rakruam, P., Wattanachira, S., 2016. Kinetic adsorption of fluoride from an aqueous solution onto a dolomite sorbent. English Journal 20, 1–9. https://doi.org/10.4186/ej.2016.20.3.1.

Wood, B.J., Fleming, R.H., Wise, H., 1984. Reactive intermediate in the alkali-carbonate-catalysed gasification of coal char. Fuel 63, 1600–1603. https://doi.org/10.1016/0016-2361(84)90234-5.

Wray, J.L., Daniels, F., 1957. Precipitation of Calcite and Aragonite. Journal of the American Chemical Society 79, 2031–2034. https://doi.org/10.1021/ja01566a001.

Wu, P., Zhang, Q., Dai, Y., Zhu, N., Dang, Z., Li, P., Wu, J., Wang, X., 2011. Adsorption of Cu (II), Cd(II) and Cr(III) ions from aqueous solutions on humic acid modified Ca-montmorillonite. Geoderma 164, 215–219. https://doi.org/10.1016/j.geoderma.2011.06.012.

Xu, L., Tian, J., Wu, H., Lu, Z., Yang, Y., Sun, W., Hu, Y., 2017. Effect of Pb^{2+} ions on ilmenite flotation and adsorption of benzohydroxamic acid as a collector. Applied Surface Science 425, 796–802. https://doi.org/10.1016/j.apsusc.2017.07.123.

Xu, W., Yang, B., Jia, F., Chen, T., Yang, L., Song, S., 2018. Removal of As(V) from aqueous solution by using cement-porous hematite composite granules as adsorbent. Results Phys. 11, 23–29. https://doi.org/10.1016/j.rinp.2018.08.031.

Xu, P., Zeng, G.M., Huang, D.L., Feng, C.L., Hu, S., Zhao, M.H., Lai, C., Wei, Z., Huang, C., Xie, G.X., Liu, Z.F., 2012. Use of iron oxide nanomaterials in wastewater treatment: a reviewSci. Total Environ 424, 1–10.

Xu, D., Zhou, X., Wang, X., 2008. Adsorption and desorption of Ni^{2+} on Na-montmorillonite: effect of pH, ionic strength, fulvic acid, humic acid and addition sequences. Applied Clay Science 39, 133–141. https://doi.org/10.1016/j.clay.2007.05.006.

Yakout, S.M., Borai, E.H., 2014. Adsorption behavior of cadmium onto natural chabazite: batch and column investigations. Desalination and Water Treatment 52, 4212–4222. https://doi.org/10.1080/19443994.2013.803938.

Yan, X., Shao, J., Wen, Q., Shen, J., 2020. Stabilization of soil arsenic by natural limonite after mechanical activation and the associated mechanisms. Sci. Total Environ. 708, 135118. https://doi.org/10.1016/j.scitotenv.2019.135118.

Yan, S., Wang, Q., Liu, J., Huo, W., Yang, J., Huang, Y., 2019. Synthesis, characterization and adsorption properties of low-cost porous calcined dolomite microspheres for removal of dyes. J. Wuhan Univ. Technol. Mater. Sci. Ed. 34, 507–515. https://doi.org/10.1007/s11595-019-2080-4.

Yang, S., Li, J., Shao, D., Hu, J., Wang, X., 2009. Adsorption of Ni(II) on oxidized multi-walled carbon nanotubes: effect of contact time, pH, foreign ions and PAA. Journal of Hazardous Materials 166, 109–116. https://doi.org/10.1016/j.jhazmat.2008.11.003.

Yang, Y., Qin, Z., Qian, Y., Guo, H., Ji, S., 2018. Adsorption of Cd(II) Ion on Aragonite Calcium Carbonate Crystals. , pp. 759–766 https://doi.org/10.1007/978-981-13-0158-2_77.

Yariv, S., Ghosh, D.K., Hepler, L.G., 1991. Metachromasy in clay-mineral systems: Adsorption of cationic dyes crystal violet and ethyl violet by kaolinite from aqueous and organic solutions. Journal of the Chemical Society, Faraday Transactions 87, 1201–1207. https://doi.org/10.1039/FT9918701201.

Yazdani, M., Bahrami, H., Arami, M., 2014. Preparation and characterization of chitosan/feldspar biohybrid as an adsorbent: Optimization of adsorption process via response surface modeling. Scientific World Journal 2014. https://doi.org/10.1155/2014/370260.

Yazdani, M., Mohammad Mahmoodi, N., Arami, M., Bahrami, H., 2012. Isotherm, Kinetic, and Thermodynamic of Cationic Dye Removal from Binary System by Feldspar. Separation Science and Technology 47, 1660–1672. https://doi.org/10.1080/01496395.2011.654169.

Yazdani, M.R., Tuutijärvi, T., Bhatnagar, A., Vahala, R., 2016. Adsorptive removal of arsenic (V) from aqueous phase by feldspars: Kinetics, mechanism, and thermodynamic aspects of adsorption. Journal of Molecular Liquids 214, 149–156. https://doi.org/10.1016/j.molliq.2015.12.002.

Yean, S., Cong, L., Yavuz, C.T., Mayo, J.T., Yu, W.W., Kan, A.T., Colvin, V.L., Tomson, M.B., 2005. Effect of magnetite particle size on adsorption and desorption of arsenite and arsenate. Journal of Materials Research 20, 3255–3264. https://doi.org/10.1557/jmr.2005.0403.

Yin, H., Zhu, J., 2016. In situ remediation of metal contaminated lake sediment using naturally occurring, calcium-rich clay mineral-based low-cost amendment. Chemical Engineering Journal 285, 112–120. https://doi.org/10.1016/j.cej.2015.09.108.

Yousef, L.A., 2017. Uranium Adsorption using Iron-Titanium mixed Oxides Separated from Ilmenite Mineral, Black Sands, Rosetta. Egypt. Arab J. Nucl. Sci. Appl. 50, 43–57.

Yu, D.Y., Song, W.H., Zhou, B., Li, W.F., 2009. Assessment of Cu (II)-bearing montmorillonite on Cd adsorption. Biological Trace Element Research 130, 185–192. https://doi.org/10.1007/s12011-009-8327-8.

Yu, R., Wang, S., Wang, D., Ke, J., Xing, X., Kumada, N., Kinomura, N., 2008. Removal of Cd^{2+} from aqueous solution with carbon modified aluminum-pillared montmorillonite. Catalysis Today 139, 135–139. https://doi.org/10.1016/j.cattod.2008.08.015.

Zeng, Y., Woo, H., Lee, G., Park, J., 2010. Adsorption of Cr(VI) on hexadecylpyridinium bromide (HDPB) modified natural zeolites. Microporous and Mesoporous Materials 130, 83–91. https://doi.org/10.1016/j.micromeso.2009.10.016.

Zhan, Y., Lin, J., Li, J., 2013. Preparation and characterization of surfactant-modified hydroxyapatite/zeolite composite and its adsorption behavior toward humic acid and copper(II). Environmental Science and Pollution Research 20, 2512–2526. https://doi.org/10.1007/s11356-012-1136-1.

Zhang, S.Q., Cui, M., Chen, J., Ding, Z., Wang, X., Mu, Y., Meng, C., 2019a. Modification of synthetic zeolite X by thiourea and its adsorption for Cd (II). Mater. Lett. 236, 233–235. https://doi.org/10.1016/j.matlet.2018.10.100.

Zhang, X., Gao, J., Zhao, S., Lei, Y., Yuan, Y., He, C., Gao, C., Deng, L., 2019b. Hexavalent chromium removal from aqueous solution by adsorption on modified zeolites coated with Mg-layered double hydroxides. Environ. Sci. Pollut. Res. 26, 32928–32941. https://doi.org/10.1007/s11356-019-06410-5.

Zhang, Z.L., Hong, H.S., Zhou, J.L., Huang, J., Yu, G., 2003. Fate and assessment of persistent organic pollutants in water and sediment from Minjiang River Estuary, Southeast China. Chemosphere 52, 1423–1430. https://doi.org/10.1016/S0045-6535(03)00478-8.

Zhang, Q., Jing, R., Zhao, S., Wu, M., Liu, X., Shao, Y., Lv, F., Liu, A., Meng, Z., 2019c. Adsorption of cationic and anionic dyes on montmorillonite in single and mixed wastewater. J. Porous Mat. 26, 1861–1867. https://doi.org/10.1007/s10934-019-00782-2.

Zhang, N., Nguyen, A.V., Zhou, C., 2018. A review of the surface features and properties, surfactant adsorption and floatability of four key minerals of diasporic bauxite resources. Advances in Colloid and Interface Science https://doi.org/10.1016/j.cis.2018.03.005.

Zhang, H.X., Wang, X.Y., Liang, H.H., Tan, T.S., Wu, W.S., 2016. Adsorption behavior of Th (IV) onto illite: effect of contact time, pH value, ionic strength, humic acid and temperature. Appl. Clay Sci. 127–128, 35–43. https://doi.org/10.1016/j.clay.2016.03.038.

Zhang, S., Wen, S., Xian, Y., Zhao, L., Feng, Q., Bai, S., Han, G., Lang, J., 2019e. Lead ion modification and its enhancement for xanthate adsorption on smithsonite surface. Appl. Surf. Sci. 498, 143801. https://doi.org/10.1016/j.apsusc.2019.143801.

Zhang, X., Xue, Y., Gao, J., He, C., Ji, Y., Dou, Y., 2020. Comparison of adsorption mechanisms for cadmium removal by modified zeolites and sands coated with Zn-layered double hydroxides. Chemical Engineering Journal 380, 122578. https://doi.org/10.1016/j.cej.2019.122578.

Zhang, B., Zhang, T., Zhang, Z., Xie, M., 2019f. Hydrothermal synthesis of a graphene/magnetite/montmorillonite nanocomposite and its ultrasonically assisted methylene blue adsorption. J. Mater. Sci. 54, 11037–11055. https://doi.org/10.1007/s10853-019-03659-6.

Zhao, K., Guo, H., 2014. Behavior and mechanism of arsenate adsorption on activated natural siderite: Evidences from FTIR and XANES analysis. Environmental Science and Pollution Research 21, 1944–1953. https://doi.org/10.1007/s11356-013-2097-8.

Zhu, S., Dong, G., Yu, Y., Yang, J., Yang, W., Fan, W., Zhou, D., Liu, J., Zhang, L., Huo, M., Wang, Y., 2018. Hydrothermal synthesis of a magnetic adsorbent from wasted iron mud for effective removal of heavy metals from smelting wastewater. Environmental Science and Pollution Research 25, 22710–22724. https://doi.org/10.1007/s11356-018-2378-3.

Zhu, X., Han, Y., Sun, Y., Li, Y., Wang, H., 2020. Siderite as a novel reductant for clean utilization of refractory iron ore. Journal of Cleaner Production 245, 118704. https://doi.org/10.1016/j.jclepro.2019.118704.

Zhu, S., Lin, X., Dong, G., Yu, Y., Yu, H., Bian, D., Zhang, L., Yang, J., Wang, X., Huo, M., 2019. Valorization of manganese-containing groundwater treatment sludge by preparing magnetic adsorbent for Cu(II) adsorption. Journal of Environmental Management 236, 446–454. https://doi.org/10.1016/j.jenvman.2019.01.117.

Ziane, S., Bessaha, F., Marouf-Khelifa, K., Khelifa, A., 2018. Single and binary adsorption of reactive black 5 and Congo red on modified dolomite: Performance and mechanism. Journal of Molecular Liquids 249, 1245–1253. https://doi.org/10.1016/j.molliq.2017.11.130.

Zuo, Q., Gao, X., Yang, J., Zhang, P., Chen, G., Li, Y., Shi, K., Wu, W., 2017. Investigation on the thermal activation of montmorillonite and its application for the removal of U (VI) in aqueous solution. J. Taiwan Inst. Chem. Eng. 80, 754–760. https://doi.org/10.1016/j.jtice.2017.09.016.